Identification of Glutathione *S*-Transferase Inhibiting Natural Products From *Matricaria chamomilla* and Biotransformation Studies on Oxymatrine and Harmine

By

Chad Douglas Iverson

A thesis submitted to the Faculty of Graduate Studies of

The University of Manitoba

in partial fulfilment of the requirements of the degree of

MASTER OF SCIENCE

Department of Chemistry
University of Manitoba
Winnipeg, Manitoba,
Canada

THE UNIVERSITY OF MANITOBA

FACULTY OF GRADUATE STUDIES
****
COPYRIGHT PERMISSION

Identification of Glutathione *S*-Transferase Inhibiting Natural Products From *Matricaria chamomilla* and Biotransformation Studies on Oxymatrine and Harmine

By

Chad Douglas Iverson

A thesis submitted to the Faculty of Graduate Studies of The University of Manitoba in partial fulfillment of the requirement of the degree

MASTER OF SCIENCE

Abstract

This thesis describes the results obtained from the phytochemical analysis of *Matricaria chamomilla*, and the microbial transformation of oxymatrine (**85**) and harmine (**87**), as summarized below.

1. Chemical investigation of the crude methanolic extract of *Matricaria chamomilla* resulted in the isolation of a new natural product, matriisobenzofuran (**72**), along with four known compounds: apigenin (**73**), apigenin-7-*O*-β-glucopyranoside (**74**), scopoletin (**75**), and fraxidin (**76**). The structures of compounds **72-76** were elucidated with the aid of extensive NMR and mass spectroscopic studies. All of the aforementioned compounds showed moderate to good inhibitory activities against glutathione *S*-transferase, an enzyme which has been implicated in the resistance of cancer cells to chemotherapeutic agents. These compounds were also evaluated for antioxidant activity and displayed moderate to good free radical scavenging activity. Additionally, compounds **72-76** were screened for anti-leishmanial activity. Compounds **75** and **76** were significantly active in this assay, while the remaining compounds were weakly active. In the antibacterial and antifungal assays, compounds **72-76** were not active.
2. The second part of this thesis deals with the biotransformation studies on oxymatrine (**85**) and harmine (**87**). Oxymatrine (**85**) was metabolized to the deoxy analogue, matrine (**84**) by *Penicillum chrysogeneum* (ATCC 9480), *Cunninghamella bainieri* (ATCC 9244), *Cunninghamella blakesleena* (ATCC 9245 and 8688A), *Curvularia lunata* (ATCC 12017), and *Fusarium sp.* In the time-based analysis of this transformation, the metabolism of oxymatrine (**85**) could be detected after 48 hours of

incubation. Additionally, incubation of harmine (**87**) with *Mucor plumbeus* (ATCC 4740) resulted in the isolation of harmine-*N*-oxide (**94**). The biotransformed products (**84** and **94**) were identified using IR, UV, NMR, and mass spectroscopic techniques. Compound **94** was evaluated for its ability to inhibit the enzyme acetylcholinestrase, whose overexpression has been linked to Alzheimer's disease, and was found to possess weaker activity than harmine (**87**).

Acknowledgements

First of all, I wish to thank my graduate supervisor, Dr. Athar Ata. He has helped me to acquire a wealth of knowledge and has been an excellent mentor to me these last few years. I thank my family, friends, and colleagues for supporting me throughout my graduate program. I extend my gratitude to Ursula Hrysio and Yimeng Li; two brilliant scientists whom I had the distinct pleasure of working with and who helped me over the course of my studies. I thank Peter Balagus, Ramin Vakili, and Ed Segstro for their technical assistance. I thank Dr. Paul Holloway and Brenda van Dekerkhove in the University of Winnipeg Biology department for their assistance with microbiological work. I thank Dr. Randy Whittal of the University of Alberta for his assistance with the high resolution mass spectrometry. I thank Dr. Ilkay Orhan of Gazi University for her assistance with some of the biological assays. The graduate scholarships received from the National Science and Engineering Research Council of Canada (NSERC), as well as the Department of Chemistry, the Faculty of Science, and the Faculty of Graduate Studies of the University of Manitoba are gratefully acknowledged. Last but not least, I am indebted to all my past and present teachers who have made positive contributions to my academic pursuit.

"*Half of the modern drugs could well be thrown out of the window, except that the birds might eat them*" –Martin Henry Fischer.

TABLE OF CONTENTS

	Page
Abstract	iv
Acknowledgements	vi
List of Tables	xi
List of Figures	xii
List of Schemes	xiii
List of Abbreviations	xiv
CHAPTER 1: Natural Products Chemistry	
1.1 Brief History of Plants as Pharmaceuticals	1
1.2 Natural Products	4
1.3 The Role of Natural Products in Drug Discovery	6
1.3.1 Natural Products as Anti-Cancer Agents	6
1.3.2 Natural Products as Anti-Infective Agents	9
1.3.3 Natural Products in the Treatment of Other Diseases and Disorders	17
1.4 Combinatorial Chemistry: Both Friend and Foe	19
1.5 Biological Targets of Interest	20
1.5.1 GST Inhibitors	22
1.5.2 Acetylcholinesterase Inhibitors	24
1.5.3 Compounds With Antioxidant Activity	26
1.5.4 Anti-Infective Agents	26
1.6 Summary	27

1.7 References 28

CHAPTER 2: Phytochemical Studies on *Matricaria chamomilla*

2.1 Introduction 33

2.1.1 Previously Reported Compounds From the Genus *Matricaria* 34

2.2 Results and Discussion

2.2.1 Structure Elucidation of Compounds **72-76** 38

2.2.1.1 Matriisobenzofuran (**72**) 38

2.2.1.2 Apigenin (**73**) 43

2.2.1.3 Apigenin-7-*O*-β-glucopyranoside (**74**) 46

2.2.1.4 Scopoletin (**75**) 50

2.2.1.5 Fraxidin (**76**) 54

2.2.2 Biological Activity of Compounds **72-76** 56

2.2.2.1 GST Inhibitory Activity 56

2.2.2.2 Antioxidant Activity 57

2.2.2.3 Anti-Leishmanial Activity 57

2.2.2.4 Antimicrobial Activity 58

2.3 Experimental 60

2.4 References 68

CHAPTER 3: Biotransformation Studies on Oxymatrine and Harmine

3.1 Introduction 71

3.1.1 The Role of Biotransformations in the Modeling of Drug Metabolism 73

3.1.2 Matrine (**84**) and Oxymatrine (**85**) 76

3.1.3 Harmine (**87**) and Related *Harmala* Alkaloids 79

3.2 Results and Discussion

3.2.1 Biotransformation of Matrine (**84**) and Oxymatrine (**85**) 82

3.2.1.1 Time-Based Analysis of the Biotransformation of Oxymatrine (**85**) 84

3.2.1.2 Importance of Findings 85

3.2.2 Biotransformation of Harmine (**87**) 85

3.2.2.1 Acetylcholinesterase Inhibitory Assay 88

3.3 Experimental 89

3.4 References 95

Conclusions 99

Appendix 101

LIST OF TABLES **Page**

Table 2.1. ^{1}H (400 MHZ) and ^{13}C (100 MHZ) NMR data for **72** and ^{1}H/^{13}C one-bond shift correlations as determined by HSQC ($CDCl_3$). 42

Table 2.2. ^{1}H (400 MHZ) and ^{13}C (100 MHZ) NMR data for **73** and ^{1}H/^{13}C one-bond shift correlations as determined by HSQC (acetone-d_6). 45

Table 2.3. ^{1}H (400 MHZ) and ^{13}C (100 MHZ) NMR data for **74** and ^{1}H/^{13}C one-bond shift correlations as determined by HSQC (DMSO-d_6). 50

Table 2.4. ^{1}H (400 MHZ) and ^{13}C (100 MHZ) NMR data for **75** and ^{1}H/^{13}C one-bond shift correlations as determined by HSQC ($CDCl_3$). 53

Table 2.5. ^{1}H (400 MHZ) and ^{13}C (100 MHZ) NMR data for **76** and ^{1}H/^{13}C one-bond shift correlations as determined by HSQC ($CDCl_3$). 56

Table 2.6. Anti-GST, antioxidant, and anti-leishmanial activities of compounds **72-76**. 58

Table 3.1. ^{1}H (400 MHZ) and ^{13}C (100 MHZ) NMR data for **84** and **85** (CDCl3). 84

Table 3.2. ^{1}H (400 MHZ) and ^{13}C (100 MHZ) NMR data for **94** and ^{1}H/^{13}C one-bond shift correlations as determined by HSQC (DMSO-d_6). 88

LIST OF FIGURES **Page**

Figure 2.1. Important HMBC interactions in **72**. 42

Figure 2.2. Important HMBC interactions in **73**. 45

Figure 2.3. ROESY interactions observed in **74**. 47

Figure 2.4. Important HMBC interactions in **74**. 49

Figure 2.5. ROESY interactions observed in **75**. 52

Figure 2.6. Important HMBC interactions in **75**. 53

Figure 2.7. NOESY interactions observed in **76**. 54

Figure 2.8. Important HMBC interactions in **76**. 56

Figure 3.1. Important HMBC interactions in **94**. 87

LIST OF SCHEMES **Page**

Scheme 1.1. General reaction catalyzed by GST; X^+ = electrophilic substance. 22

Scheme 1.2. Enzymatic hydrolysis of acetylcholine by AChE. 25

Scheme 3.1. General oxygenation mechanism of drugs by cytochrome P_{450}. 75

LIST OF ABBREVIATIONS

°C	Degrees Celsius
µg	Micrograms
µg/mL	Micrograms per milliliter
µL	Microlitre
µM	Micromolar
µm	Micrometer
^{13}C-NMR	Carbon-13 nuclear magnetic resonance
1D-NMR	One-dimensional nuclear magnetic resonance
^{1}H-NMR	Proton nuclear magnetic resonance
2D-NMR	Two-dimensonal nuclear magnetic resonance
Å	Angstrom
AChE	Acetylcholinesterase
ADHD	Attention-deficit hyperactivity disorder
ATCC	American Type Culture Collection
ATP	Adenosine triphosphate
$CDCl_3$	Deuterated chloroform
CDNB	1-Chloro-2,4-dinitrobenzene
$CHCl_3$	Chloroform
COSY	Correlation spectroscopy
d	Doublet
dd	Double-doublet

DEPT	Distortionless enhancement by polarization transfer
DMSO	Dimethylsulfoxide
DNA	Deoxyribonucleic acid
DPPH	2,2-Diphenyl-1-picrahydrazyl
DTNB	5-5'-Dithiobis(2-nitrobenzoic acid)
e^-	Electron
EC_{50}	Dose at which half of the maximal effect of a drug is achieved
EI-MS	Electron impact mass spectrum
EtOAc	Ethyl acetate
g	Grams
GC-MS	Gas chromatography-mass spectrum
GSH	Glutathione
GST	Glutathione *S*-transferase
h	Hour
H_20	Water
HIV	Human immunodeficiency virus
HMBC	Heteronuclear multiple bond connectivity
HMG-CoA	3-Hydroxy-3-methylglutaryl-coenzyme A
HPLC	High pressure liquid chromatography
HR-EI-MS	High-resolution electron impact mass spectrometry
HSQC	Heteronuclear single quantum coherence
Hz	Hertz
IC_{50}	Concentration of inhibitor required to inhibit a target by 50%

IL-6	Interleukin 6
IR	Infrared
J	Coupling constant
kg	Kilograms
m	Multiplet
M	Molar
m/z	Mass to charge ratio
MeOH	Methanol
mg	Milligrams
MHz	Mega hertz
MIC	Minimum inhibitory concentration
min	Minutes
mL	Milliliter
mL/min	Milliliters per minute
mm	Millimeters
mRNA	Messenger ribonucleic acid
MRSA	Methicillin resistant *Staphylococcus aureus*
MS	Mass spectrometry
NCCLS	National Committee for Clinical Laboratory Standards
ng/mL	Nanograms per milliliter
nM	Nanomolar
nm	Nanometers
NMR	Nuclear magnetic resonance

NOE	Nuclear Overhauser effect
NOESY	Nuclear Overhauser effect spectroscopy
PCI-MS	Positive chemical ionization mass spectrometry
prep. TLC	Preparative thin-layer chromatography
R_f	Retention factor
ROESY	Rotating-frame Overhauser effect spectroscopy
S.E.M	Standard error of the mean
TLC	Thin-layer chromatography
TNF-α	Tumor necrosis factor α
U/mL	Enzyme units per milliliter
UV	Ultraviolet
VRE	Vancomycin resistant enterococci
δ	Chemical shift value

CHAPTER 1

Natural Products Chemistry

1.1 BRIEF HISTORY OF PLANTS AS PHARMACEUTICALS

Since as early as the Neanderthal era, nature-based medicines have been utilized in the treatment of a wide variety of diseases and disorders[1]. One of the earliest and best known written records of early nature-based medicine is the Ebers Papyrus, which contains over 700 prescriptions, dating back approximately to 1500 BCE[2]. During this period, plants or crude plant extracts were used to treat various ailments. The extract of opium, for instance, was used to relieve pain and fever[2]. Other medicinal plants/plant extracts included myrrh, frankincense, fennel, cassia, senna, thyme, henna, juniper, linseed, aloe, castor oil, and garlic[1,2]. With the development of chemical sciences, modern pharmaceuticals were introduced in the late 1700's AD[2]. At this time, a movement began in France and Germany to abolish polypharmacy: the use of crude extracts in the practice of medicine[2]. Using newly discovered solvent-solvent extraction and chromatographic techniques, scientists attempted to isolate pure compounds responsible for the medicinal actions present in the preparations used in previous pharmaceutical treatments[2]. The first pure compound, narcotine (**1**), was isolated in 1803 by the French apothecary Jean François Derosne[2]. Other bioactive compounds isolated during this period include the anti-tachycardic digitalis (**2**), and the analgesic, morphine (**3**)[1]. In 1897, Arthur Eichengrun and Felix Hoffmann at Bayer[3] synthesized the first pure plant-derived analgesic, aspirin (**4**). Today, natural products continue to play a significant role in medicine: both in the use of the extracts of traditional medicinal plants for the treatment

of various ailments, and in the isolation of bioactive compounds for the discovery of new pharmaceuticals.

In a number of second and third world countries where many families cannot afford to use modern pharmaceuticals, the extracts of traditional medicinal plants are still used to treat disease. As much as 60% of the world's population relies on medicinal plants for their primary healthcare[4]. Many of these traditional plants are quite effective in treating various diseases and disorders. For instance, administration of the alcoholic extract of the Indian Anjani tree (*Memecylon umbellatum*) has been shown to be useful in the treatment of diabetes mellitus, having a significant hypoglycemic effect with little toxicity[4]. In Russia, extracts of the greater celandine tree (*Chelidonium majus*) are used to treat cancer patients[5]. *In vitro* studies have shown a significant reduction in cancer cell proliferation (29% of control) at a dose of 10 μg/ml and complete inhibition of cell proliferation at higher doses[5]. In the Msambweni district of Kenya, extracts of the Neem tree (*Azadirachta indca*) are used regularly for the treatment of malaria, one of the most prevalent diseases in Africa today[6]. Other examples are the members of the genus *Desmos*, which are commonly used in traditional Chinese medicine to treat infectious diseases of varying origin[7].

In more developed countries, the focus in the area of natural products research is the isolation of the bioactive constituents found in these medicinal plants for the development of new pharmaceuticals. For instance, investigation of *A. indca* resulted in the isolation of the limonoid, gedunin[8] (**5**), which exhibited strong anti-malarial activity (IC_{50} = 0.14 μM) *in vitro*[9]. Phytochemical investigation of *Desmos sp.* yielded the

chalcone, 2-methoxy-3-methyl-4,6-dihydroxy-5-(3'-hydroxy)cinnamoylbenzaldehyde (**6**), which demonstrated potent anti-HIV activity with an IC_{50} of 0.022 µg/mL[7].

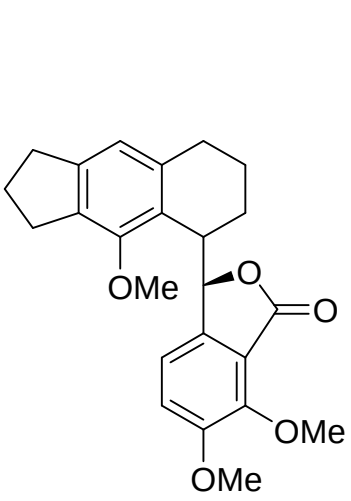

1

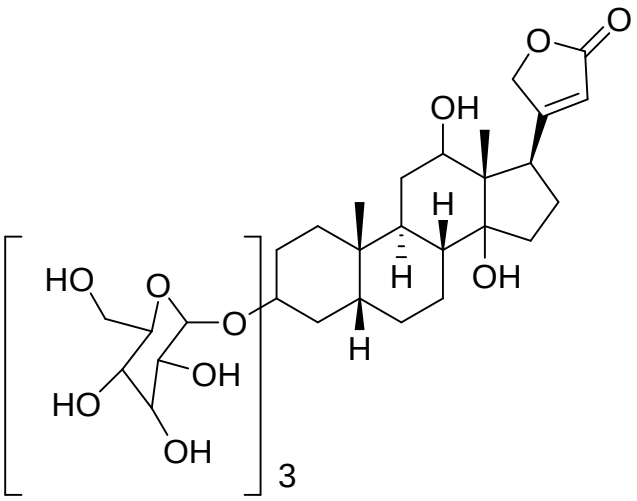

2

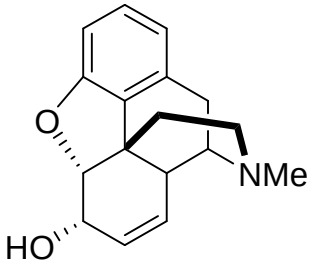

3

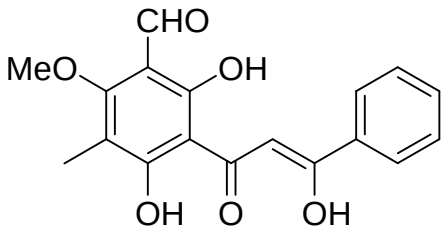

4

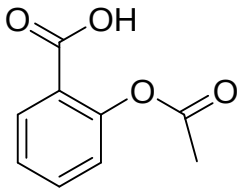

5

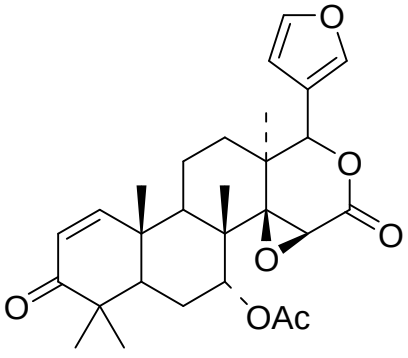

6

It is well documented in the literature that over 25 million flowering plants are present in the world[1]. Only 3% of these plants have been explored for pharmaceutical applications and structural diversity to obtain new chemical entities[1].

1.2 NATURAL PRODUCTS

As part of normal cellular functions, an organism will synthesize and metabolize two classes of organic compounds: primary and secondary metabolites[10]. Primary metabolites are normally simpler compounds which are common to all organisms and are essential for life[10]. These compounds are generally involved in energy metabolism and form the starting materials for the biosynthesis of more complex molecules[10]. The primary metabolites include: carbohydrates, amino acids, fatty acids, and nucleic acids[10].

Secondary metabolites, on the other hand, are not ubiquitous to all organisms. That is, all living organisms produce secondary metabolites of some type, but many specific secondary metabolites are only produced by a particular species or genus[10]. These secondary metabolites are also known as natural products. These compounds are often more complex and are produced in response to the presence of primary metabolites or lack thereof[10]. Thus, these secondary metabolites play an ecologically important role in how an organism interacts with its surroundings and will often serve to provide the producing organism an advantage in its survival[11]. For instance, when the mold *Penicillum chrysogeneum* reaches the stationary phase of its growth (a phase in which the organism stops dividing and energy sources become limited) it will synthesize the compound penicillin (**7**) to reduce the number of competing organisms, specifically bacteria, in its nearby surroundings and thereby conserve available nutrients for its own

survival. Furthermore, many of these compounds may be used in pharmaceutical practice. Returning to the above example, penicillin and penicillin derivatives are still some of the most widely prescribed classes of antibiotics.

Traditionally, natural product chemists have focused on plants as a source of bioactive compounds[10-12]. More recently, there has been an increased interest in other sources of natural products including insects, microorganisms[11], and most notably, marine organisms which have yielded structurally diverse compounds with significant biological activity[13,14]. Examples include the β-carboline alkaloid, hyrtiocarboline (**8**), which was isolated from the marine sponge *Hyrtios reticulates* and showed selective anti-proliferative activity against several cancer cell lines[15]; and the anti-cancer agent, ecteinacidin-743 (**9**), which was isolated from the Caribbean tunicate, *Ecteinascidia turbinata* and is currently marketed under the trade name Yondelis[14]. Nearly 50% of drugs available on the market are of natural product origin[1]. Twenty-five percent of these prescribed drugs are derived from plants[1]. This thesis focuses on plant-derived natural products.

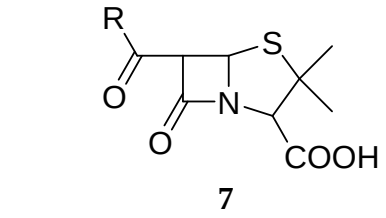

7

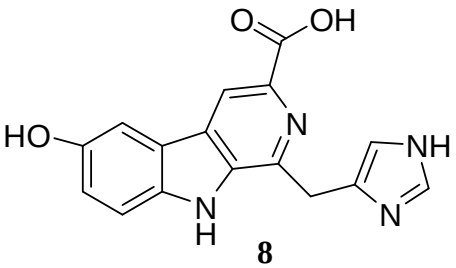

8

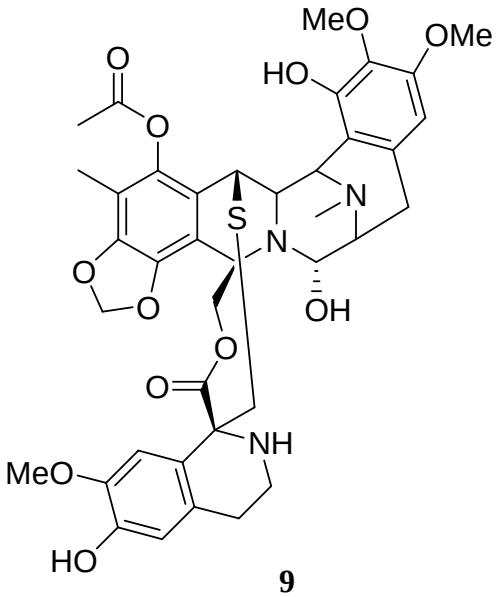

9

1.3 THE ROLE OF NATURAL PRODUCTS IN DRUG DISCOVERY

Natural product chemistry is considered to be one of the major providers of lead drug molecules[16,17]. Of the 1184 new chemical entities filed between 1981 and 2006, approximately 52% of them were either natural products, their semisynthetic analogues, or synthetic products based on natural products[1,3,16-18]. Between 2000 and 2006, 26 plant-based drugs were approved for marketing worldwide[1]. Between 2005 and 2007 alone, 13 natural product-related drugs were approved for marketing worldwide[18,19]. As of 2008, there were over 100 natural product-derived compounds in clinical trials and at least 100 in preclinical development[18]. Moreover, approximately half of these had origins from plant sources[18]. Altogether, it has been estimated that the global market for natural product-derived drugs is well over $20 billion[1]. Much of the focus in natural product-based pharmaceuticals has been in the areas of cancer and infectious diseases[19]. Natural products, however, have also played a role in the treatment of neurological, cardiovascular, and inflammatory diseases[19]. In the remainder of this section, the role of natural products in each of these areas will be described.

1.3.1 Natural Products as Anti-Cancer Agents

As of December 2007, there were 191 anti-cancer drugs on the market[20]. Of these, 123 (64%) were either a natural product, derived from a natural product, or natural product mimic[20]. Generally, anti-cancer agents fall into two broad classes: those that target the tumor at the cellular level and those that target the tumor at the gene level. Compounds that target cancer at the cellular level work by preventing cell growth, metabolism, and replication. One such example of a natural product belonging to this

class is Taxol (**10**), originally isolated from the bark of the pacific yew tree (*Taxus brevifolia*)[20,21]. Taxol (**10**) arrests the division of cancer cells by binding to tubulin heterodimers and stabilizing the microtubule assembly, thereby suppressing the dynamic changes in microtubule functions[21]. Taxol (**10**) is effective against breast and ovarian cancers and is still used today[21].One other example is the apoptosis-inducing compound, β-lapachone (**11**), isolated from the lapacho tree, *Tabebuia avellanedae*[22]. It is believed that this compound induces apoptosis in cancer cells via the activation of caspase-3, inhibition of NFκB, and subsequent downregulation of *bcl*-2[23]. Currently, this compound is in phase II clinical trials against advanced solid tumors and has shown good activity against a number of multi-drug resistant tumors[22].

The other broad class of anti-cancer compounds targets the tumor at the gene level, mostly affecting genome replication processes and the regulation of these processes. One subclass of gene-level anti-cancer agents, for instance, is the DNA topoisomerase inhibitors. DNA topoisomerase is a well known target in oncology which is ubiquitous in the treatment of a number of different cancers[20,24]. This enzyme is responsible for several cellular functions, including the control of DNA topology, the interaction with proteins associated with DNA repair, and the phosphorylation/activation of mRNA splicing proteins[24]. The first function has long been targeted by compounds based on the natural product, campothecin (**12**), isolated from the Chinese tree, *Campotheca acuminate*[20,24]. Most of these compounds inhibit the unwinding of DNA by forming a covalent complex with the enzyme[24]. More recently, newer drugs have been developed which can target the other functions of DNA topoisomerase such as the glycosylated indolcarbazole derivative, NB-506 (**13**), derived from the streptomycete

metabolite, BE-13793C (**14**)[25]. In addition to inhibiting DNA topoisomerase's DNA relaxing activity, it is also a potent inhibitor of the enzyme's kinase activity, modulating pre-mRNA splicing through the inhibition of the phosphoryation of the SF2/ASF splicing factors[25].

Another subclass of gene-level anti-cancer agents targets the histone deacetylases, which are involved in the regulation of gene expression and the transformation of oncogenes. Inhibition of these processes can exert a significant role in the suppression of the mutations that promote tumor growth[20]. Most histone deacetylase inhibitors are described as a tripartite: containing an enzyme binding group, a hydrophobic spacer, and an inhibitor group[26-28]. One example of such a compound is trichostatin A (**15**), isolated from a broth culture of *Streptomyces platensis*. This compound demonstrated potent inhibitory activity (K_i = 3.4 nM) both *in vitro* and *in vivo* against the histone deacetylases[29]. More recently, derivatives of this compound have been prepared. In 2006, the trichostatin A analogue, Varinostat (**16**), was approved for cancer treatment. In addition, Varinostat is still in over 40 clinical trials as either a single agent or as part of a combination therapy against a variety of solid and leukemic tumors[20].

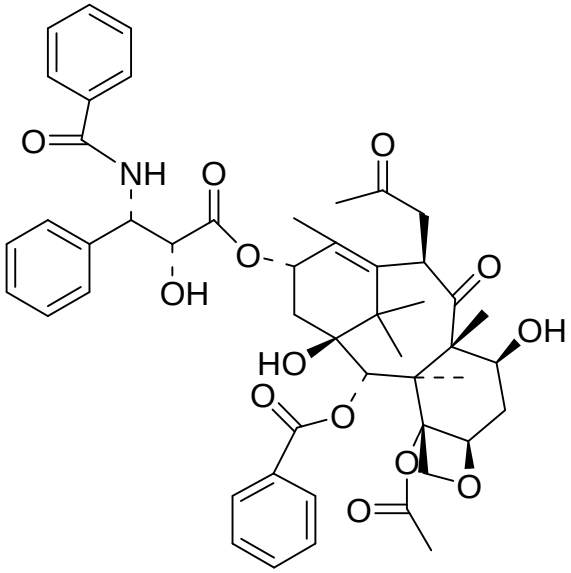

10

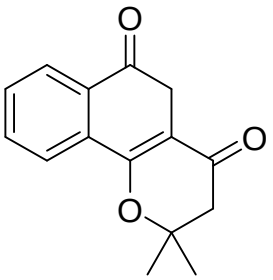

11

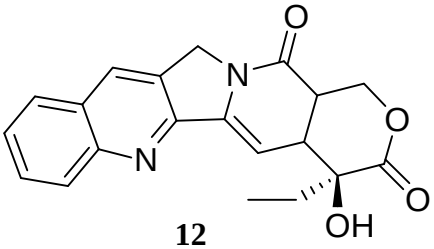

12

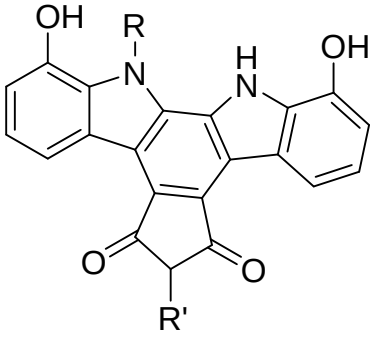

13 R= glucose R' = NHCHO
14 R = H, R' = H

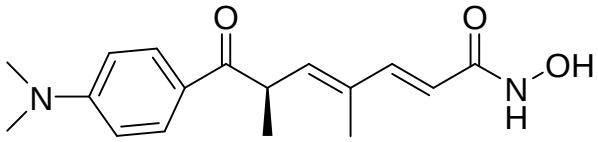

15

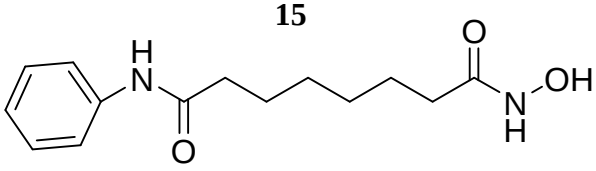

16

1.3.2 Natural Products as Anti-Infective Agents

As in the treatment of cancer, the statistics show that natural products have played a significant role in the treatment of infectious diseases of bacterial, fungal, viral, and parasitic origin. Of the 230 anti-infective agents marketed between 1981 and 2006, 124 (54%) had some sort of natural product origin as described before[16].

Naturally, the greatest focus has been on antibacterial agents where natural

products have traditionally been a source of potent antibiotics. Some of the most recognized antibiotics include penicillin (**7**); cephalosporin antibiotics such as cephalosporin C (**17**), isolated from *Acremonium chrysogeneum*; and macrolide antibiotics such as erythromycin (**18**), produced by cultures of *Saccharopolyspora sp.*[30]. Antibiotics such as these have been long used to treat a variety of Gram positive and Gram negative bacterial infections[30].

Unfortunately, over time, antibiotic resistant strains have emerged which are of concern: most notably some of the nosocomial infections present in our hospitals today such as methicillin resistant *Staphylococcus aureus* (MRSA), vancomycin resistant enterococci (VRE), and *Clostridium difficile*[25,26]. In addition, multi-drug resistant *Mycobacterium tuberculosis* also provides cause for concern[31,32]. Fortunately, natural products or natural product-derived compounds have shown promise in combating some of these infections. Hyperforin (**19**) for instance, isolated from St. John's wort (*Hypericum perforatum*), has shown minimal inhibitory concentration (MIC) values in the range of 0.1-1 μg/mL against MRSA and penicillin-resistant organisms[33,34]. Compound **20**, isolated from *Evodia rutaecarpa*, has shown excellent activity against several *Mycobacterium* species[31]. PTK-0796 (**21**), a synthetic tetracycline derivative, is currently in phase II clinical trials and has shown broad spectrum activity against a number of different bacteria, including MRSA and VRE[35]. Ceftobiprole medocaril (**22**), a fourth generation cephalosporin, has shown potent MRSA bacteriocidal activity[36]. It is in the final stages of clinical trials prior to approval[36-38]. Lastly, the actinomycete derived macrolactone, tiacumicin B (**23**), isolated from *Dactylsporangium aurantiacum*, is

currently in several phase III clinical trials for the treatment of hospital-acquired *C. difficile* associated diarrhea[39,40].

As of late, the increase in the population of immunocompromised individuals has led to an increase in fungal infections[41]. As fungi are eukaryotes there are relatively few drug targets that can be exploited without causing unnecessary toxicity to the infected host, thus making fungal infections more difficult to treat[41]. Furthermore, the appearance of resistant strains requires the development of new antifungals, and natural products have provided good leads in this area. For example, derivatives of zofimarin (**24**), isolated from *Zopfiella marina*, have shown potent antifungal activity against several species of *Candida*[42]. Semisynthetic derivatives of sesquiterpenes produced by fermentation of *Paecilomyces inflatus* have shown strong antifungal activity in the low micromolar range against the systemic pathogen, *Trichosporum cutaneum*[43]. As one other example, a semisynthetic derivative (**25**) of the cyclic depsipeptide, patricin A (**26**), is currently in phase II clinical trials for the treatment of systemic mycoses caused by *Candida* and *Aspergillus* species[19]. This compound has similar activity to amphoterocin B but with better biovailability and less toxicity[19].

Natural products or their derivatives have also been used in or show promise in the treatment of viral infections; most notably the human immunodeficiency virus (HIV), which has affected an untold number of people for over 20 years[44]; and hepatitis B and C, the causative agents of liver diseases which combined have afflicted over a half billion people worldwide[45]. Examples of compounds with anti-HIV activity include triptonine B (**27**), calanolide A (**28**), and betulinic acid (**29**). The sequiterpene alkaloid, triptonine B (**27**), extracted from the root bark of *Tripterygium hypoglacum*, inhibited HIV replication

with an IC_{50} of less than 0.1 µg/mL[46]. Further, this compound has low toxicity with a therapeutic index of over 1000[46]. Currently calanolide A (**28**), isolated from *Calophyllum lanigerum*, is undergoing clinical trials as a new anti-HIV agent. It has shown potent anti-HIV activity (EC_{50} = 0.1 µM) against both wild type and resistant strains[44,47,48]. In 1994, the triterpene, betulinic acid (**29**), was isolated from the leaves of *Syzigium claviforum* by Fujioka *et al*[49]. Subsequent investigations showed that this compound was also present in the bark of *Platanus acerifolia*[50]. *In vitro* studies of **29** demonstrated potent anti-HIV activity with an IC_{50} of 1.4 µM[49]. Currently, the ester derivative 3-*O*-(3',3'-dimethylsuccinyl)betulinic acid (**30**) is in phase III clinical trials for the treatment of HIV as a combination therapy with other pharmaceuticals[50].

Examples of compounds with anti-hepatitis activity include celegosivir (**31**) and wogonin (**32**). Celegosivir (**31**), a potent anti-hepatitis agent with low side effects that is currently in clinical trials, is a prodrug of castanospermine (**33**), derived from *Castanospermum australe*[51]. Wogonin (**32**), a monoflavonoid isolated from the Chinese medicinal herb, *Scutellarial radix,* has shown significant anti-hepatitis B activity with an IC_{50} of 4 µg/mL[52]. It is currently in the early stages of drug development[52].

One other area of interest in anti-infective agents is the treatment of parasitic diseases such as malaria and leishmaniasis. Malaria, caused by several members of the protozoan genus *Plasmodium*, is still one of the most important diseases in the developing world, accounting for an estimated 1.1 to 2.7 million deaths per year[53]. Thus, there is a great need for antimalarial compounds and there are numerous examples of natural products with potent anti-malarial activity in the literature. Some of these include the indolquinoline, cryptolepine (**34**) (IC_{50} = < 0.5 µM), isolated from the West African

herb *Cryptolepsis sanguinolenta*[54]; the quasinoid orinocide **35**, recently isolated from *Gimian orinocensis* which showed high potency (IC_{50} = < 9 ng/mL) and low toxicity[55]; and the sesquiterpene lactone **36**, isolated from the leaves of *Vernopsis caudata*, which demonstrated potent activities (IC_{50} = 190 nM) against drug-resistant strains of *P. falciparium*[56]. Unfortunately, the high cytotoxicity of this compound prevented further clinical development but it could serve as a good lead for other anti-malarial compounds[56].

Leishmaniasis, caused by members of the parasitic genus *Leishmania*, is one other important disease in the developing world. According to the World Health Organization, the disease threatens about 350 million men, women, and children in 88 countries around the world with about 2 million affected annually, accounting for an untold number of fatalities[57-59]. As with malaria, there are numerous examples of natural products with anti-leishmanial activity such as the isoquinoline alkaloid, cryptodorine (**37**), purified from the young leaves of *Guatteria dumetorum*, which effectively reduced the parasite burden at a concentration of 3 µM[60]; the steroidal alkaloid, holamine (**38**), obtained from the leaves of *Holarrhena curtisii*, which exhibited antileishmanial activity against promastigotes of *L. donovani* at a concentration range of $1.56>IC_{50}>0.39$ µg/mL[61]; the monoterpene, linalool (**39**), extracted from *Croton cajucara*, which showed strong activity (IC_{50} = 28 nM) against *L. amazoneninsis*[62]; and the flavonoid, luteolin (**40**), isolated from *Vitex negundo*, which exhibited anti-leishmanial activity against *L. donovani* intracellular amastigotes at an IC_{50} of 12.5 µM[63].

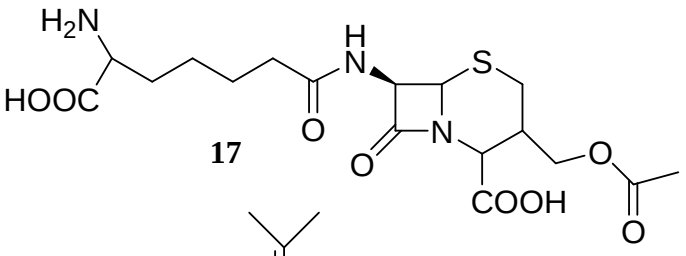

17

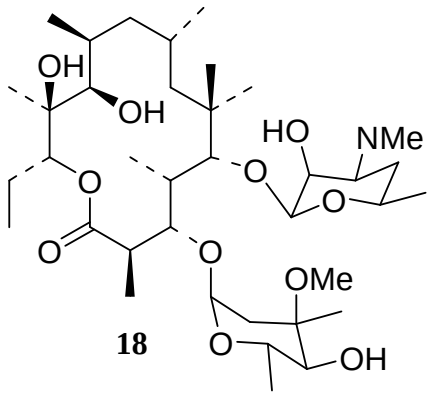

18

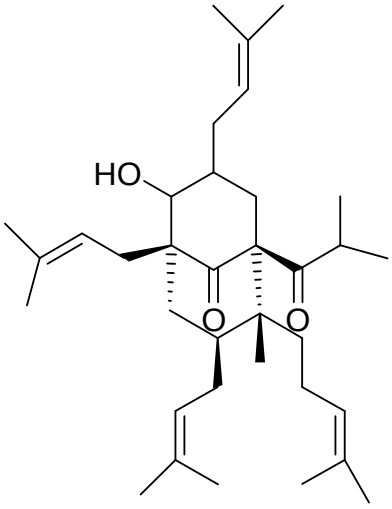

19

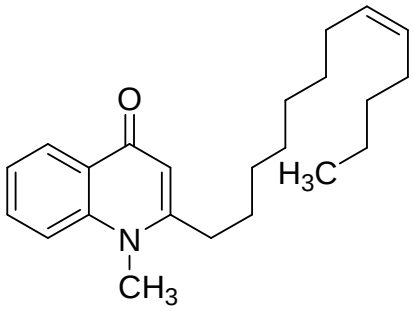

20

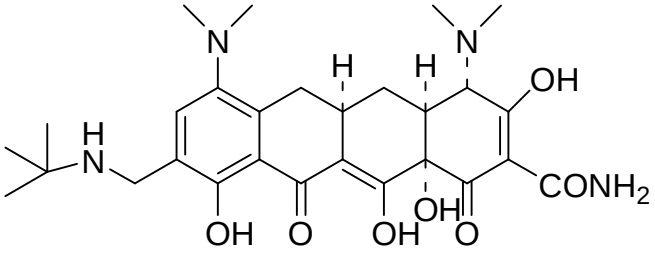

21

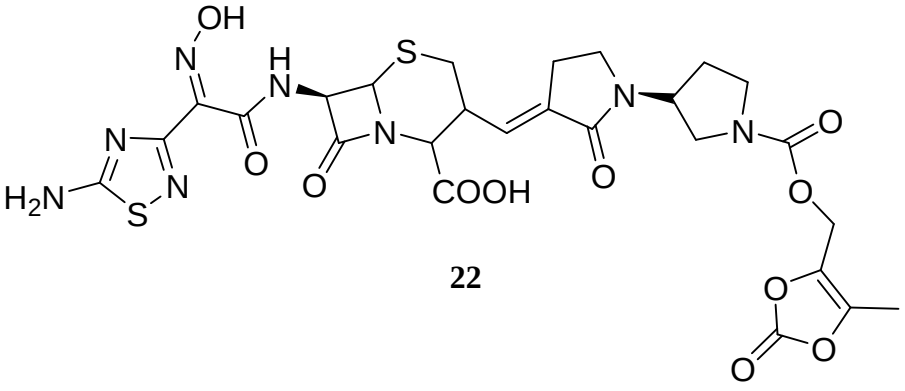

22

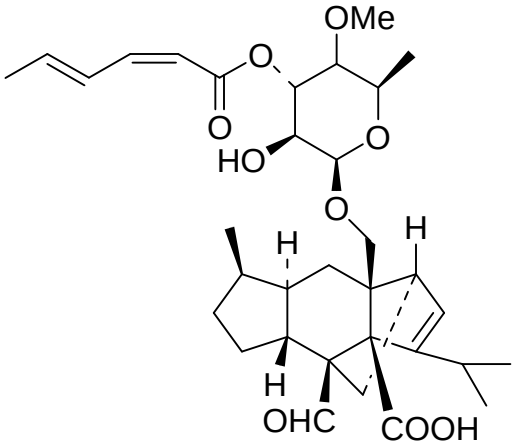

23

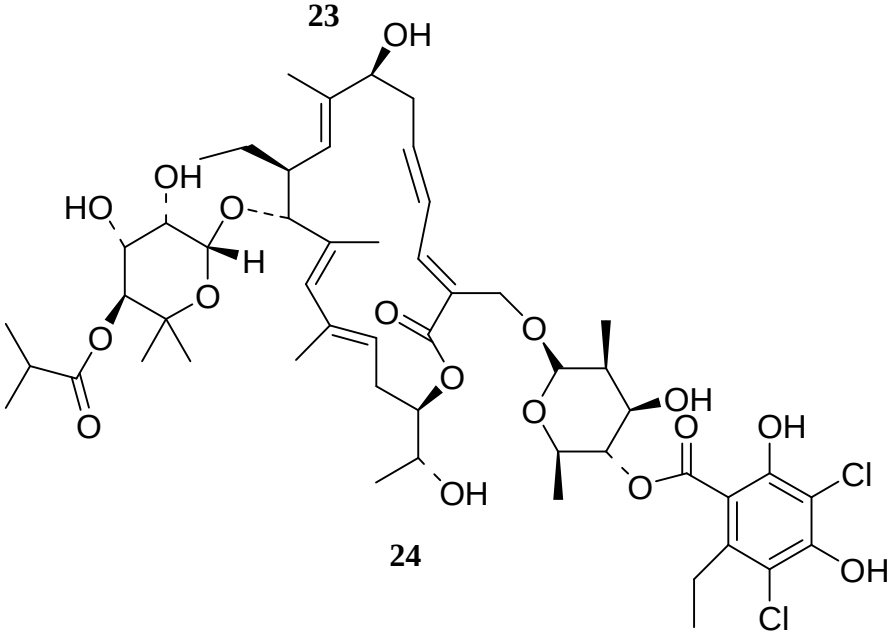

24

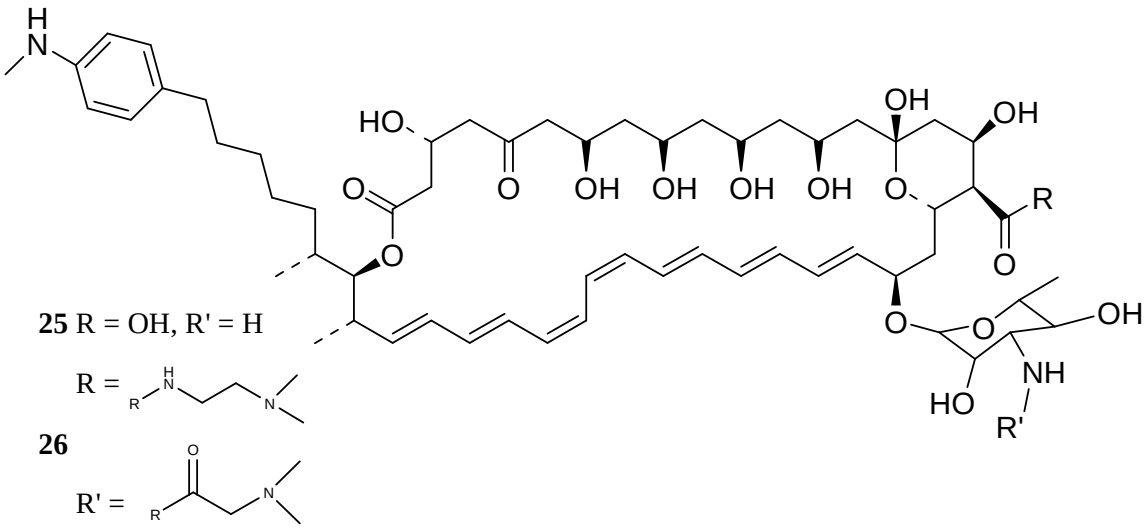

25 R = OH, R' = H

R =

26

R' =

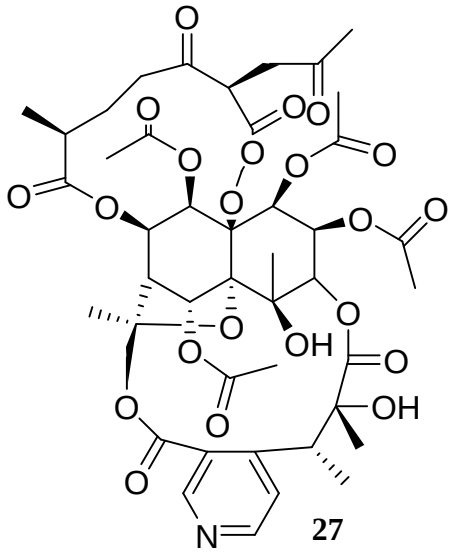

27

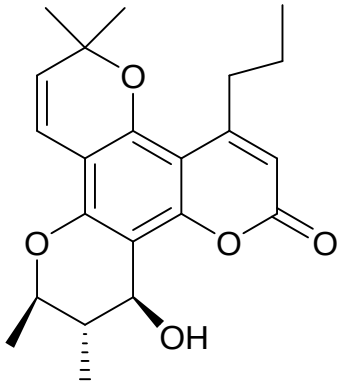

28

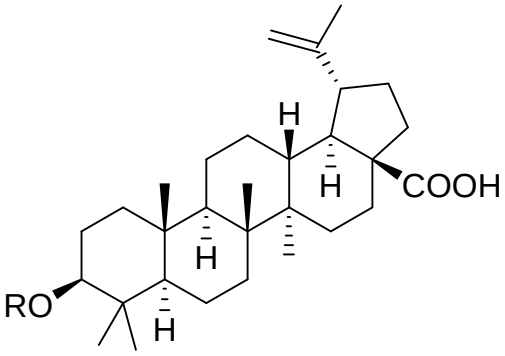

29 R = H

30 R = 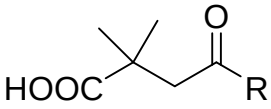

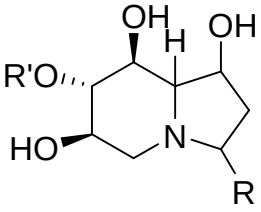

31 R = H, R’ = H
33 R = OH,
R’ = $CO(CH_2)_2CH_3$

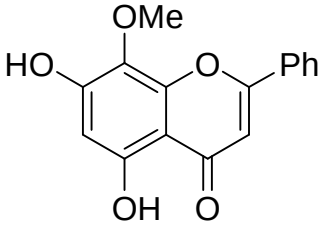

32

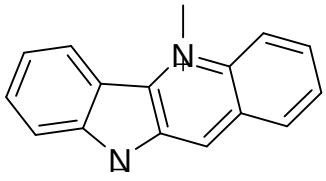

34

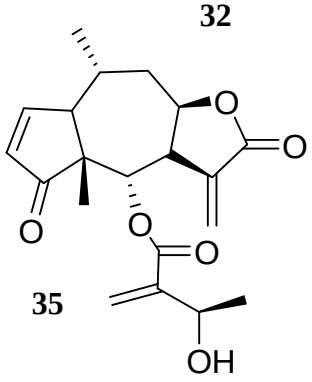

35

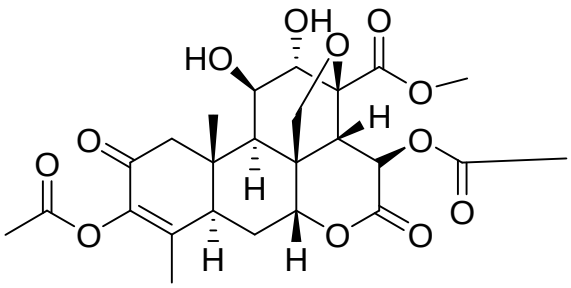

36

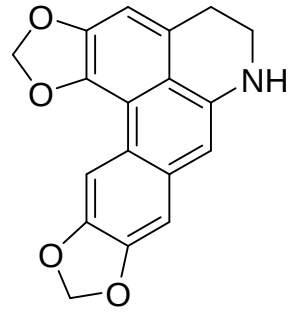

37

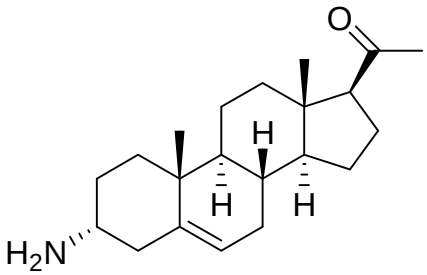

38

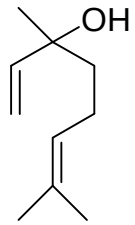

39

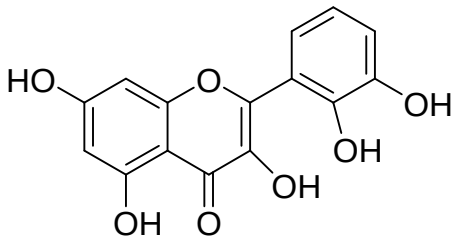

40

1.3.3 Natural Products in the Treatment of Other Diseases and Disorders.

In addition to natural products being an effective tool in the battle against cancer and infectious diseases, they have been utilized in some form to treat a variety of other diseases such as Alzheimer's disease, cardiovascular disease, diabetes, and various immunological and inflammatory diseases. The natural product, huperzine (**41**), is a potent acetylcholinesterase inhibitor that is marketed as a herbal remedy for the treatment

of Alzheimer's disease[64]. A synthetic prodrug analogue (**42**) of this compound is in ongoing clinical trials with promising results[19]. Lovastatin (Mevastatin) (**43**) is a cholesterol lowering drug. It functions by inhibiting HMG-CoA reductase, an enzyme involved in the biosynthesis of cholesterol[30]. An analogue (**44**) of the natural product, staurosporine (**45**), is in the latter stages of clinical trials for the treatment of diabetic retinopathy. Its mode of action is as a competitive inhibitor of the binding of ATP to protein kinase C[65]. Lastly, the analogue (**46**) of the flavone, eupatilin (**47**), a major component of *Artemisia argyi*, is in phase II clinical trials for the treatment of ulcerative colitis[19].

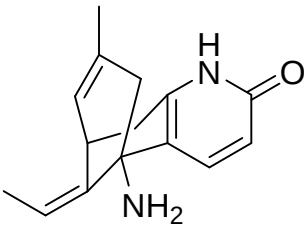

41

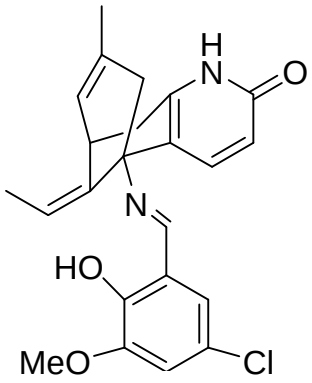

42

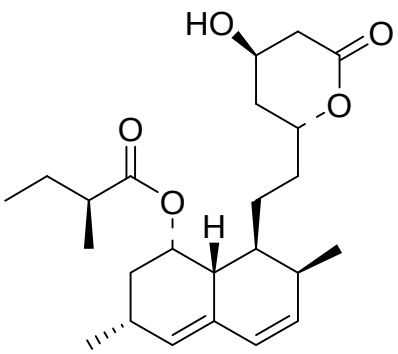

43

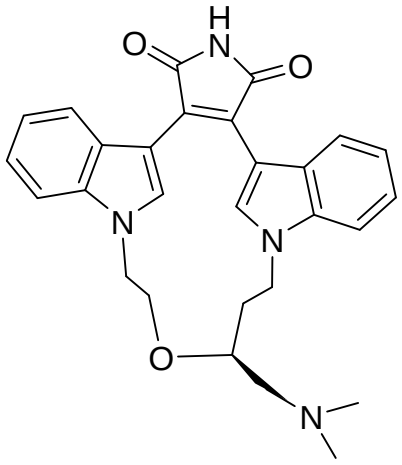

44

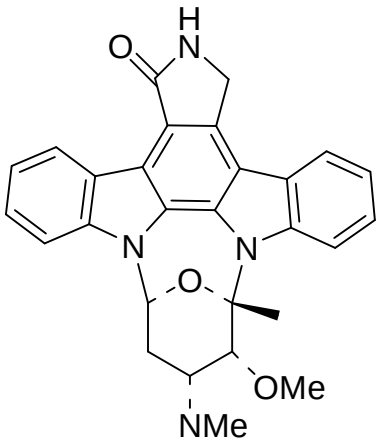

45

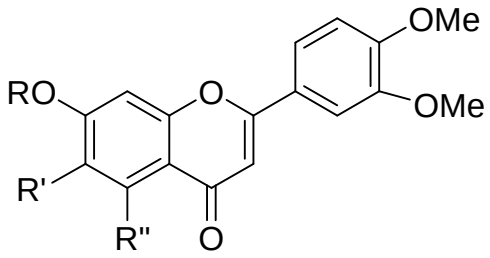

46 R = H, R' = OMe, R" = H
47 R = CH_2COOH, R' =H, R" = OMe

1.4 COMBINATORIAL CHEMISTRY: BOTH FRIEND AND FOE

Despite all of the structural diversity and biological and medicinal potential of natural products, many pharmaceutical companies have greatly scaled back their programs on the isolation of natural products for the generation of lead structures in favor of the use of libraries generated by combinatorial synthesis and screened by automated high throughput processes [3,66,67]. Much of this is due to the perceived cost efficiency of the latter and the disadvantages of natural products[66,67]. Specifically, the isolation of natural products can often be a slow, tedious, inefficient process involving complex mixtures in which apparent biological activities are frequently the result of a synergetic effect rather than being attributed to a single compound, thereby making it not cost-effective[66,67]. Further, the sourcing of natural products can be an issue as many sources of natural products are rare and identification records are not well kept[67]. Difficulties can arise in obtaining an authentic sample when one wishes to verify the results in the early stages of commercialization[67]. However, even with the advances in combinatorial

synthesis, combinatorial chemistry cannot generate the structural diversity found in nature[66,67]. To date, only one approved pharmaceutical (Sorafenexib) has been generated *de novo* from traditional combinatorial synthesis[16].

Nevertheless, natural products and combinatorial chemistry can comingle to work towards the discovery of new pharmaceuticals. While natural products have previously been regarded as not amenable to high throughput screening (mostly because of the issues of working with complex mixtures) newer methods have allowed for the high throughput screening of crude extracts as well as individual natural products for drug discovery[68]. Furthermore, when starting from diverse natural products as lead structures, or designing combinatorial syntheses based on natural product scaffolds, combinatorial chemistry can be useful in drug discovery[69]. One area where it is especially useful is the derivatization of a biologically active natural product to improve its pharmacokinetic properties and decrease toxicity[69]. Lastly, advances in molecular biology have brought about combinatorial biosynthesis whereby genetic modifications are made in organisms to influence biosynthetic pathways, such as the synthesis of polyketides and non-ribosomal peptides, to generate new natural products with medicinal potential[70].

1.5 BIOLOGICAL TARGETS OF INTEREST

Overall, there is great potential in natural products for the treatment of the diseases and disorders that currently afflict humans, and until cures are found this research must continue. This section will describe the biological targets that this thesis will focus on: specifically, the discovery of compounds which possess the ability to inhibit the medicinally important enzymes, acetylcholinesterase (AChE) and

glutathione-*S*-transferase (GST), as well as compounds with antioxidant and/or anti-infective activities.

In order to screen for the above activities, a number of different biological assays will be utilized. In general, these assays can be grouped into two types: cell-based assays, and enzymatic and chemical-based assays. As the name implies, cell-based assays utilize cultured cell lines of different origins to screen for different biological activities[12]. Most commonly, this type of assay is used in the screening of anticancer agents where one can observe the effect of the compound in question on a particular tumor cell line, and in the screening of anti-infective agents where the effect of the compound is observed on the pathogen of interest[12]. While the results obtained from these assays are very useful, there are several disadvantages to cell-based assays. Specifically, these assays often require more time to complete and require more specialized facilities and equipment for the maintenance of the cell lines and to run the assays[12].

Enzyme and chemical based assays, in contrast, target the activity of a particular enzyme. Most often the aim is to inhibit the activity of a particular enzyme to hinder cell growth or to dampen the rate of activity of an overexpressed enzyme such as GST or AChE, which are described below. Unlike cell-based assays, this type of assay does not require specialized facilities or equipment and can often be quickly performed right on the bench[12]. Of course, the design of an enzyme-based assay to target a specific ailment requires knowledge of the specific target responsible for that ailment.

1.5.1 GST Inhibitors

The GSTs are a large family of phase II detoxification enzymes, being comprised of at least 20 isozymes[71,72]. These isozymes all exist as either heterodimers or homodimers and have been classified into three broad groups on the basis of their isoelectric points: acidic, near-neutral, and basic[71,72]. The diversity of these GST enzymes allows for a broad range of substrate specificities. Overall, they aid in the excretion of mutagens, carcinogens, and other noxious chemical substances through the conjugation of glutathione (γ-glutamylcysteinylglycine) to electrophilic groups on the substance to be eliminated, making it more water soluble and easier to extract from the blood and tissues for excretion[71,72]. A typical reaction is shown in Scheme 1.1.

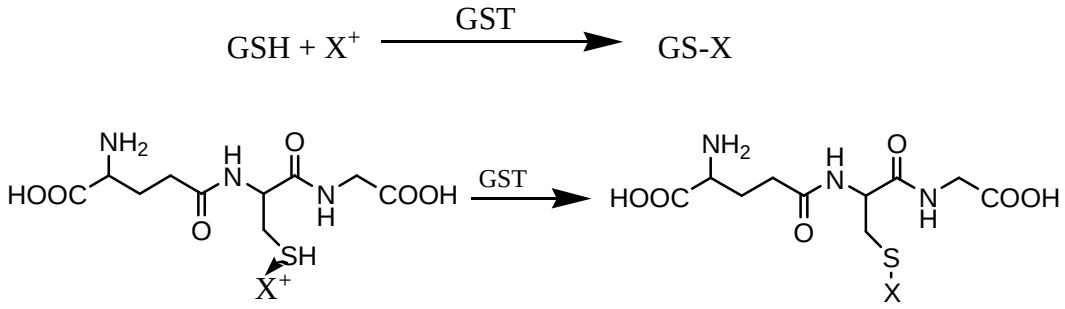

Scheme 1.1. General reaction catalyzed by GST; X^+ = electrophilic substance

As discussed earlier in this chapter, one area of concern in human health is the increasing occurrence of multidrug resistant tumors; that is, during the treatment of many cancers, there is often development of drug resistance in tumors that were originally sensitive to chemotherapeutic treatment[73]. There are a number of mechanisms by which multi-drug resistance can arise and these include: alterations in drug transport resulting in impaired entry or enhanced efflux of the drug from the tumor cell, enhanced DNA repair,

alterations in target proteins, and alterations in drug metabolism[73]. Focusing on the last mechanism, it has been shown that the GST enzymes are often overexpressed in drug resistant cancer cell lines[73]. This leads to hypermetabolism of the chemotherapeutic agents, hindering them from effecting their functions[73].

In order to overcome this mechanism of resistance there are two possible solutions. The first is to discover new pharmaceuticals which are resistant to this hyperactive metabolism. As shown previously, efforts are being made to do such that but the progress is quite slow. The alternative is to develop agents which can be given to modulate the anti-cancer drug resistance by inhibiting the overexpressed GST enzymes. Given in conjunction with current anti-cancer agents, these inhibitors may once again restore the effectiveness of these anti-cancer agents.

There are currently a number of examples of natural products which have exhibited potent GST inhibitory activity such as the α,β-carbonyl derivative, ethacrynic acid (**48**)[74]; the flavonoid, quercetin (**49**)[75]; the homoisofavonoid, caesalpinianone (**50**)[76]; the phenylethanoid glycoside, barlerinoside (**51**)[77]; and the iridoid glycoside, *p*-coumaroyl-8-*O*-acetylshanzhiside methyl ester (**52**)[77]. There is still a need, however, for the discovery of new GST-inhibiting natural products with lower toxicity and higher potency.

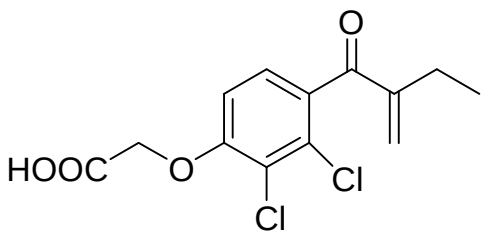

48

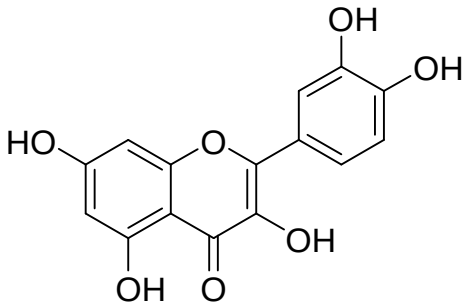

49

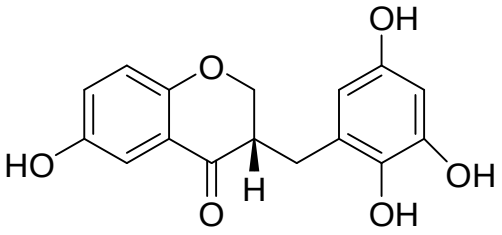

50

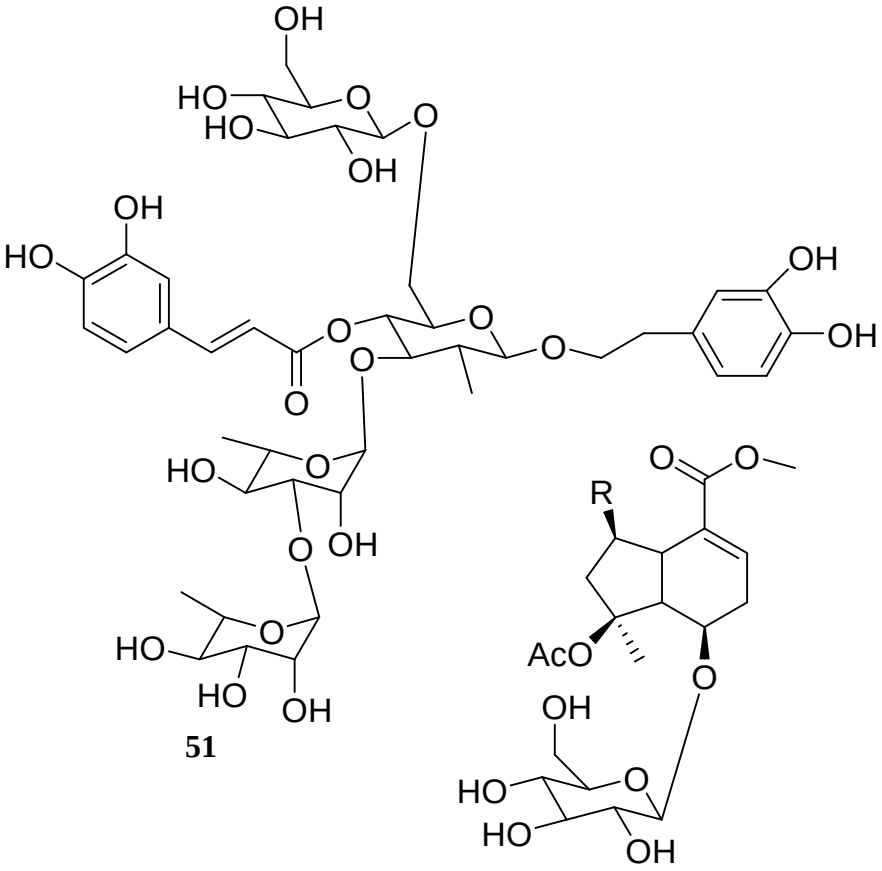

51

52 R= *O*-*trans*-p-coumaroyl group

1.5.2 Acetylcholinesterase Inhibitors

According to Alzheimer's Disease International[78], an estimated 35.6 million people will be living with dementia worldwide in 2010. Alzheimer's disease is a progressive degenerative neurological disorder that results from a deficiency of cholinergic function in the brain. This is due to an overexpression of the enzyme

acetylcholinesterase, which causes the hydrolysis of the neurotransmitter acetylcholine at a faster rate than normal[79,80] (The reaction scheme for the hydrolysis of acetylcholine is shown in Scheme 1.2). Currently, the inhibition of AChE is believed to be one of the most promising approaches for treating Alzheimer's disease[79,80]. In addition, the inhibition of AChE has also been shown to produce a neuroprotective effect, mainly through the inhibition of the formation of β-amyaloid plaques which have been associated with neuronal death, contributing to the neurodegeneration in Alzheimer's disease[80,81]. AChE inhibitors have also been shown to cause an upregulation in the level of nicotinic AChE receptors, which has been shown to provide further neuroprotective effects and lessen the progression of Alzheimer's disease[81].

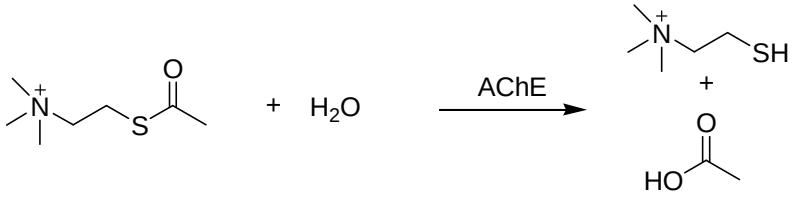

Scheme 1.2. Enzymatic hydrolysis of acetylcholine by AChE.

While there are several AChE inhibitors currently on the market [such as huperazine[64] (**41**), Donepezil[80] (**53**) and galantamine[80] (**54**)], it is valuable to discover more to find ones with higher potency, lower toxicity, and to be proactive in dealing with potential future tolerance issues.

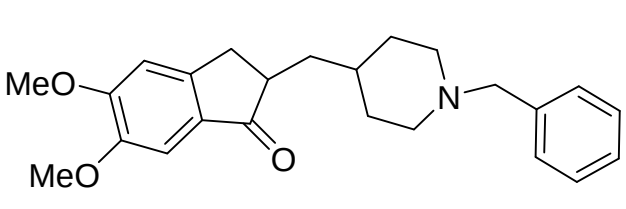

53

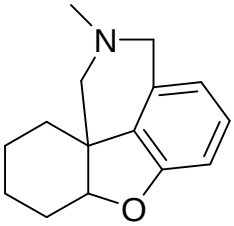

54

1.5.3 Compounds with Antioxidant activity

As part of normal cellular functions, free radicals are produced on a continual basis. There is a large amount of circumstantial evidence that implicates excess reactive oxygen radicals (species) such as superoxide ($O_2^{\cdot -}$), perhydroxyl radicals ($O_2H^{\cdot}$), and hydroxyl radicals in the pathophysiology of a number of common diseases including hemorrhagic shock, cancer, pulmonary emphysema, atherosclerosis, cardiac/brain infarction, chronic renal failure, diabetes, diabetic complications, and autoimmune diseases[82]. They have also been implicated in the failure of surgical interventions including transplant graft rejection and coronary bypass[82]. Furthermore, these reactive oxygen species have been linked with damage to the brain on the cellular level, causing age associated memory loss and more serious neurological conditions such as Alzheimer's, Parkinson' s and Huntington's diseases[82]. To reduce the oxidative stress responsible for the above diseases, disorders, and conditions, compounds with antioxidative properties that promote free-radical decomposition and reduce the concentration of reactive oxygen species can be administered. There have been many compounds, especially those with aromatic functionalities (such as flavonoids) that have been reported to possess significant antioxidant activities[82-84]. There is still, however, a need to find compounds that have low toxicity, high potency, and good pharmacokinetic properties.

1.5.4 Anti-infective Agents

While there have been great strides made in the discovery and development of anti-infective agents, the emergence of new and resistant infectious diseases of various

origins dictates the need for further work to discover new compounds with anti-infective properties.

1.6 SUMMARY

The examples presented in this chapter have shown that a vast array of diverse structures can be obtained from nature. Many of these compounds possess significant biological activities and hold promise in treating the diseases and disorders which currently affect the human race, such as those presented in this chapter. Until treatments and/or cures are found for those ailments, efforts must continue to isolate novel compounds from nature and to evaluate their biological activities.

Based on the aforementioned importance of natural products in drug discovery, the present project was undertaken to isolate natural products from *Matricaria chamomilla* and evaluate them for glutathione *S*-transferase inhibitory, anti-leishmanial, antibacterial, and antifungal bioactivities. Additionally, efforts to biocatalytically modify the structures of two alkaloids, oxymatrine (**85**) and harmine (**87**), were also made. These findings have been discussed in Chapters 2 and 3.

1.7 REFERENCES

1. Saklani, A.; Kutty, S. K. *Drug Discov. Today* **2008**, *13*, 161-171.

2. Wermuth, C. G., Ed. *The Practice of Medicinal Chemistry*, 2nd ed.; Associated Press: San Diego, CA, 2003.

3. Schmidt, B.; Ribnicky, D. M.; Poulev, A.; Logendra, S.; Cefalu, W. T.; Raskin, I. *Metabolism: clinical and experimental* **2008**, *57* (Supp 3), S3-S9.

4. Grover, J. K.; Yadav, S.; Vats, V. *J. Ethnopharmacol.* **2002**, *81*, 81-100.

5. Nguta, J. M.; Mbaria, J. M.; Gakuya, D. W.; Gathumbi, P. K.; Kiama, S. G. *J. Ethnopharmacol.* **2010**, *128*, 424-432.

6. Spiridonov, N. A.; Konovalov, D. A.; Arkhipov, V. V. *Phytother. Res.* **2005**, *19*, 428-432.

7. Wu, JH; Wang, XH; Yi, YH; Lee, KH *Bioorg. Med. Chem. Lett.* **2003**, *13*, 1813-1815.

8. Bray, D. H.; Warhurst, D. C.; Connoly, J. D.; O'Neill, M. J.; Philipson, J. D. *Phytother. Res.* **1990**, *4*, 29-35.

9. Lee, SE.; Kim, MR.; Kim, JH.; Takeoka, G. R.; Kim, TW.; Park, BS. *Phytomedicine* **2008**, *15*, 533-535.

10. Stanniforttth, S. *Natural Product Chemistry at a Glance*; Blackwell Publishing: Oxford, UK, 2006.

11. Bhat, S.V.; Nagasampagi, B. A.; Meenakshi, S. *Natural Products: Chemistry and Applications*; Alpha Science: Oxford, UK, 2009.

12. Cseke, L. J.; Kirakosyan, A.; Kaufmann, P. B.; Warber, S. L.; Duke, J. A.; Brielman, H. L., Eds. *Natural Products from Plants*, 2nd ed.; CRC Taylor and Francis: Boca Raton, FL, 2006.

13. Molinski, T. F.; Dalisay, D. D.; Lievens, S. L.; Saludes, J. P. *Nat. Rev.* **2009**, *8*, 69-85.

14. Glaser, K. B.; Mayer, A. M. S. *Biochem. Pharmacol.* **2009**, *78*, 440-448.

15. Inman, W. D.; Bray, W. M.; Gassner, N. C.; Lokey, R. S.; Tenney, K.; Shen, Y. Y.; TenDyke, K.; Suh, T.; Crews, P. *J. Nat. Prod.* **2010**, *73*, 255-257.

16. Newman, D. J.; Cragg, G. M. *J. Nat. Prod.* **2007**, *70*, 461-477.

17. Newman, D. J. *J. Med. Chem.* **2008**, *51*, 2589-2599.

18. Harvey, A. L. *Drug Discov. Today* **2008**, *13*, 894-901.

19. Butler, M. S. *Nat. Prod. Rep.* **2008**, *25*, 475-516.

20. Cragg, G. M.; Grothaus, P. G.; Newman, D. J. *Chem. Rev.* **2009**, *109*, 3012-3043.

21. Coseri, S. *Mini Rev. Med. Chem.* **2009**, *9*, 560-571.

22. Bailly, C. *Biochem. Pharmacol.* **2009**, *77*, 1447-1457.

23. Sattely, E. S.; Fischbach, M. A.; Walsh, C. T. *Nat. Prod. Rep.* **2008**, *25*, 757-793.

24. Yoshida, M.; Furumai, R.; Nishiyama, M.; Komatsu, Y.; Nishino, N.; Horinouchi, S. *Cancer Chemother. Pharmacol.* **2001**, *73* (Suppl 1), S20-S26.

25. Remiszewski, S. W. *Curr. Opin. Drug Discovery Dev.* **2002**, *5*, 487-499.

26. Yoshida, M.; Matsuyama, A; Komatsu, Y; Nishino, N. *Curr. Med. Chem.* **2003**, *10*, 2351-2358.

27. Vanhaecke, T.; Papeleu, P.; Elaut, G.; Rogiers, V. *Curr. Med. Chem.* **2004**, *11*, 1629-1643.

28. Ravelo, A. G.; Estevez-Braun, A.; Chavez-Orellana, H.; Perez-Sacau, E.; Mesa-Siverio, D. *Curr. Top. Med. Chem.* **2004**, *4*, 241-265.

29. Choi, B. T.; Cheong, J.; Choi, Y. H. *Anticancer Drugs* **2003**, *14*, 845-850.

30. Dewick, P. M. *Medicinal Natural Products: A Biosynthetic Approach*, 3rd ed.; Wiley: Chirchester, UK, 2009.

31. Gibbons, S. *Planta Medica.* **2008**, *74*, 594-602.

32. Fishbach, M. A.; Walsh, C. T. *Science* **2009**, *325*, 1089-1093.

33. Gurevich, A. L.; Dobrynin, V. N.; Kolosov, M. N.; Popravko, S. A.; Riabova, I. D. *Antibiotiki* **1971**, *16*, 510-513.

34. Schempp, C. M.; Pelz, K.; Wittmer, A.; Schopf, E.; Simon, J. C. *Lancet* **1999**, *353*, 2129.

35. Paratek Pharmaceuticals. www.paratekpharmaceuticals.com (accessed April 20, 2010).

36. Hebeisen, P.; Heinze-Kraus, I.; Angehrn, P.; Hohl, P.; Page, G. P.; Then, R. L. *Antimicrob. Agents. Chemother.* **2001**, *45*, 825-836.

37. Noel, G. J., Bush, K.; Bagchi, P.; Ianus, J.; Strauss, R. S. *Clin. Infect. Dis.* **2008**, *46*, 647-655.

38. Bush, K.; Heep, M.; Macielag, M. J.; Noel, G. J. *Expert Opin. Invest. Drugs* **2007**, *16*, 419-429.

39. Johnson, A. P. *Curr. Opin. Invest. Drugs* **2007**, *8*, 168-173.

40. Shue, Y. K.; Sears, P. S.; Walsh, R. B.; Lee, C.; Gorbach S. L.; Okumu, F.; Preston, R. A. *Antimicrob. Agents. Chemother.* **2008**, *52*, 1391-1395.

41. Di Santo, R. *Expert Opin. Ther. Patents.* **2008**, *18*, 275-292.

42. Basilio, A.; Justice, Harris, G.; Bills, G.; Collado, J.; de la Cruz, M.; Diez, M. T.; Hernandez, P.; Liberator, P.; Nielsen kahn, J.; Pelaez, F.; Platas, G.; Schmatz, D.; Shastry, M.; Tormo, J. R.; Andersen, G. R.; Vicente, F. *Bioorg. Med. Chem.* **2006**, *14*, 560-566.

43. Banyu Pharmaceutical, International PatentWO0008010, 2000.

44. Mehellou, Y.; De Clercq, E. *J. Med. Chem.* **2010**, *53*, 521-538.

45. Wohlfarth, C.; Efferth, T. *Acta. Pharmacol. Sin.* **2009**, *30*, 25-30.

46. Lee, N. H.; Ho, J. W. *Anti Infect. Agent. Med. Chem.* **2008**, *7*, 97-100.

47. Kashman, Y.; Gustafson, K. R.; Fuller, R. W.; Cardellina, J. H.; McMahon, J. B.; Currens, M. J.; Buckheit, R. W.; Hughes, S. H.; Cragg, G. M.; Boyd, M. R. *J. Med. Chem.* **1992**, *35*, 2735-2743.

48. Flavin, M. T.; Rizzo, J. D.; Khilevich, A.; Kucherenko, A.; Sheinkman, A. K.; Vilaychack, V.; Lin, L.; Chen, W.: Greenwood, E. M.; Pengsuparp, T.; Pezzuto, J. M.; Hughes, S. H.; Flavin, T. M.; Boulanger, W. A.; Shone, R. L.; Xu, Z. Q. *J. Pharmacol. Exp. Ther.* **1996**, *279*, 645-651.

49. Fujioka, T.; Kashiwada, Y.; Kilkuskie, R. E.; Cosentino, L. M.; Ballas, L. M.; Jiang, J. B.; Janzen, W. P.; Chen, I. S.; Lee, K. H.; *J. Nat. Prod.* **1994**, *57*, 243-247.

50. Lee, KH. *J. Nat. Prod.* **2010**, *73*, 500-516.

51. Sorbera, L. A.; Castaner, J.; Garcia-Capdevila, L. *Drugs Fut.* **2005**, *30*, 545-552.

52. Guo, Q.; Zhao, L.; You, Q.; Yang, Y.; Gu, H.; Song, G.; Lu, N.; Xin, J. *Antivir. Res.* **2007**, *74*, 16-24.

53. Turschner, S.; Efferth, T. *Mini Rev. Med. Chem.* **2009**, *9*, 206-214.

54. Wright, C. W.; Addae, Kyereme, J.; Breen, A. G.; Brown, J. E.; Cox, M. F.; Croft, S. L.; Gokcek, Y.; Kendrick, H.; Phillips, R. M.; Pollet, P. L. *J. Med. Chem.* **2001**, *44*, 3187-3194.

55. Rafatro, H.; Ramanitrahasimbola, D.; Rasoanaivo, P; Ratsimamanga-Urveg, S.; Rakoto-Ratsimamanga, A.; Frappier, F.; *Biochem. Pharmacol.* **2000**, *59*, 1053-1061.

56. Rasoanaivo, P.; Ramanitrahasimbola, D.; Rafatro, H.; Robijaona, B.; Rakotozafty, A.; Ratsimamanga-Urveg, S.; Labaied, M.; Grellier, P.; Allorge, L.; Mambu, L.; Frappier, F. *Phytother. Res.* **2004**, *18*, 742-747.

57. Rocha, L. G.; Almeida, J. R. G. S.; Macedo, R. O.; Barbosa-Filho, J. M. *Phytomedicine* **2005**, *12*, 514-535.

58. Mishra, B. B.; Kale, R. R.; Singh, R. K.; Tiwari, V. K. *Fitoterapia* **2009**, *80*, 81-90.

59. Polonio, T.; Efferth, T. *Int. J. Mol. Med.* **2008**, *22*, 277-286.

60. Correa, J. E.; Rios, C. H.; del Rosario, C. A.; Romero, L. I.; Ortega-Barria, E.; Coley, P. D.; Kursar, T. A.; Heller, M. V.; Gerwick, W. H.; Rios L. C. *Planta Medica* **2006**, *72*, 270-272.

61. Kam, T.; Sim, K.; Koyano, T.; Toyoshima, M. Hayashi, M.; Komiyama, K. *J. Nat. Prod.* **1998**, *61*, 1332-1336.

62. Do Socorro, S. R. M. S.; Mendonca-Filho, R. R.; Bizo, H. R.; de Almeida, R. I.; Soares, R. M. A.; Souto-Padron, T.; Alviano, C. S.; Lopes, A. H. C. S. *Antimicrob. Agents Chemother.* **2003**, *47*, 1895-1901.

63. Mittra, B.; Saha, A.; Chowdhary, A. R.; Pal, C.; Mandal, S.; Mukhopadhyay, S.; Bandyopadhyay, S.; Majumder, H. K. *Mol. Med.* **2000**, *6*, 527-541.

64. Ma, X.; Gang, D. R. *Nat. Prod. Rep.* **2004**, *21*, 752-772.

65. Yasuzawa, T.; Iida, T.; Yoshida, M.; Hirayama, N. Takahashi, M.; Shirahata, K.; San, H. *J. Antibot.* **1986**, *39*, 1072-1078.

66. McChesney, J. D.; Venkataraman, S. K.; Henri, J. T. *Phytochemistry* **2007**, *68*, 2015-2022.

67. Li, J. W. H.; Vederas, J. C. *Science* **2009**, *325*, 161-165.

68. Mishra, K. P.; Ganju, L.; Sairam, M.; Banerjee, P. K.; Sawhney, R. C. *Biomed. Pharmacother.* **2008**, *62*, 94-98.

69. Grabowski, K.; Baringhaus, K-H.; Schneider, G. *Nat. Prod. Rep.* **2008**, *25*, 892-904.

70. Zhang, W.; Tang, Y. *J. Med. Chem.* **2008**, *51*, 26929-26933.

71. Mannervik, B.; Danielson, U. H. *Crit. Rev. Biochem. Mol. Bio.* **1988**, *23*, 283-337.

72. Ionescu, C.; Caira, M. R., Eds. *Drug Metabolism: Current Concepts*; Springer: Dordrecht, The Netherlands, 2005.

73. Hayeshi, R.; Mutingwende, I.; Mavengere, W.; Masiyanise, V.; Mukanganyama, S. *Food Chem. Toxicol.* **2007**, *45*, 286-295.

74. Zhao, G.; Yu, T.; Wang, R.; Wang, X.; Jing, Y. *Bioorg. Med. Chem.* **2005**, *26*, 91-104.

75. Zanden van, J. J.; Hamman, O. B.; Iersel Van, M. L. P. S.; Boeren, S.; Cnubben, N. H. P.; Lo Bello. M.; Vervoort, J.; Bladeren van, P. J.; Rietgens, I. M. C. M. *Chem. Biol. Interact.* **2003**, *145*, 139-148.

76. Ata, A.; Gale, E. M.; Samarasekera, R. *Phytochem. Lett.* **2009**, *2*, 106-109.

77. Ata, A.; Kalhari, K. S.; Samarasekera, R. *Phytochem. Lett.* **2009**, *2*, 37-40.

78. Prince, M.; Jackson, J. World Alzheimer Report 2009: Executive Summary; Alzheimer's Disease International, 2010.

79. Babar, Z. H.; Ata, A.; Meshkatalsadat, M. H. *Steroids* **2006**, *71*, 1045-1051.

80. Loizzo, M. R.; Tundis, R.; Menichini, F.; Menichini, F. *Curr. Med. Chem.* **2008**, *15*, 1209-1228.

81. Takada-takatori, Y.; Kume, T. Izumi, Y.; Ohgi, Y.; Niidome, T.; Fujii, T.; Sugimoto, H.; Akaike, A. *Biol. Pharm. Bull.* **2009**, *32*, 318-324.

82. Ma, A.; Qi, S.; Chen, H. *Cardiovasc. Hematol. Agents Med. Chem.* **2008**, *6*, 20-43.

83. Slemmer, J. E.; Shacka, J. J.; Sweeny, M. I.; Weber, J. T. *Curr. Med. Chem.* **2008**, *15*, 404-414.

84. Pietta, PG. *J. Nat. Prod.* **2000**, *63*, 1035-1042.

CHAPTER 2

Phytochemical Studies on *Matricaria chamomilla*

2.1 INTRODUCTION

Matricaria chamomilla (*Asteraceae),* commonly known as German chamomile, is a flowering plant which is native to Europe, but was more recently introduced to North America[1]. For centuries extracts of this plant have been utilized by folk healers to treat wounds, ulcers, eczema, gout, skin irritations, neuralgia, rheumatic pain, chicken pox, fevers, gastrointestinal upset, and a vast number of other ailments[2-4]. Recent *in vitro* studies of the essential oil of *M. chamomilla* have verified the efficacy of chamomile in some of the above mentioned ethnomedical applications. For instance, when chamomile extract was applied to shaved male albino rats that had suffered full thickness burns to 20% of their bodies, it was found that the wounds resulting from these injuries healed approximately 20% faster as compared to a control group that did not receive the chamomile extract[5]. Additionally, a recent observational study has demonstrated that *M. chamomilla* may improve the symptoms of attention-deficit hyperactivity disorder (ADHD)[6].

Recent phytochemical studies on this plant have shown that the majority of the demonstrated effects of chamomile may be attributed to the high content of terpenes and flavonoids found within this plant[4]. These compounds have been shown to possess antioxidant, antibacterial, antifungal, anti-inflammatory, anti-cancer, anti-allergic, antipyretic, and antispasmodic activities, as well as mild sedative properties[4].

2.1.1 Previously Reported Compounds From the Genus *Matricaria*

In addition to German chamomile, the genus *Matricaria* contains two other members: *M. aurea* (syn. *M. matricarioides*—pineapple weed)[7,8] and *M. perforata*[9] (scentless chamomile). Phytochemical studies on these plants have resulted in the isolation of over 120 compounds[2,7-9].

Among these three plants *M. chamomilla* is perhaps most famous for the major constituents of its essential oil, the terpenes α-bisabolol (**55**) and α-bisabolol oxide A (**56**)[10], and the biological activities they impart. For instance, when α-bisabolol was screened for antimicrobial activity, it showed weak antibacterial activity and moderate antifungal activity against *Candida albicans* (MIC = 36 mM)[11]. This compound has also demonstrated its potential as an anti-inflammatory agent, showing IC_{50} values ranging between 10 and 30 µg/mL in the 5-lipoxygenase assay[12]. Similarly, when administered to the gastric tissue of mice, α-bisabolol reduced the occurrence of gastric mucosal lesions[13].

While α-bisabolol oxide, for the most part, possesses similar biological activities as α-bisabolol[10], it is also known for its anti-cancer activities. Specifically, α-bisabolol oxide has been shown to be a potent caspase activator, thereby inducing apoptosis[14].

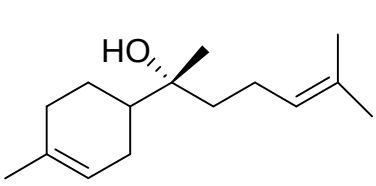

55

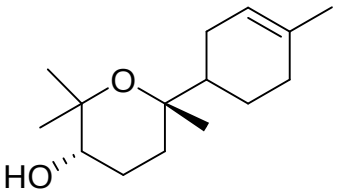

56

In addition to the above two compounds, a number of other chemical constituents have been identified in *M. chamomilla*. GC-MS analysis of *M. chamomilla* essential oil by Szoke *et al*[15], Sashidhara *et al*[16], and most recently Tolouee *et al*[17] have identified a

large number of terpenes. Some of the major terpene constituents include (Z,Z)-farnesol (**57**), (E)-β-farnesene (**58**), α-cubebene (**59**), matricin (**60**), and the matricin artifact, chamazulene (**61**), which is formed during the steam distillation of the oil.

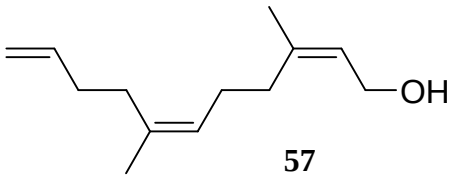

57

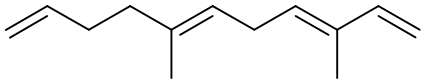

58

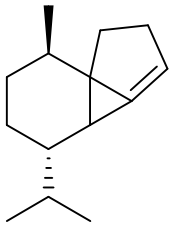

59

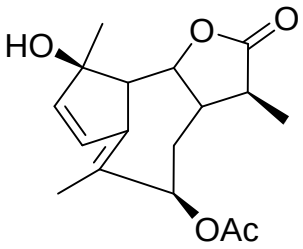

60

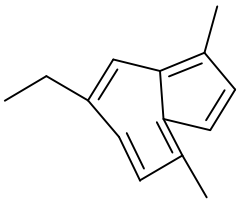

61

HPLC studies on the oil have identified flavonoids such as quercetin (**49**) and luteolin (**40**), and their glycosides[18,19], as well as the coumarins, umbelliferone (**62**) and herniarin (**63**)[20].

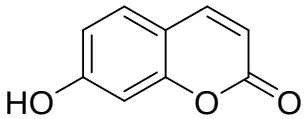

62

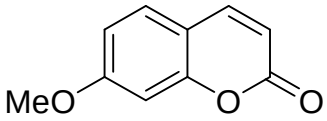

63

Phytochemical studies on the aqueous-alcoholic extracts of the aerial parts of *M. chamomilla* have yielded terpenoids and steroids, including anthecotulide (**64**)[21], matricolone (**65**), dihidrooridentin (**66**), 2α-hydroxyyarborescin (**67**)[22], stigmasterol (**68**), oleanolic acid (**69**), β-sitosterol (**70**), and β-sitosterol glucoside (**71**)[1].

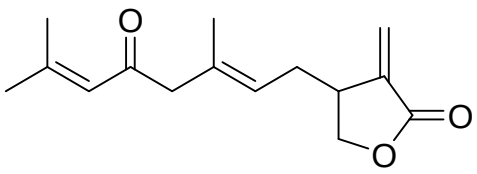

64

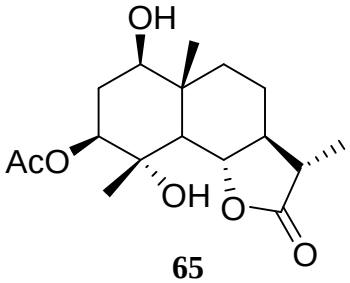

65

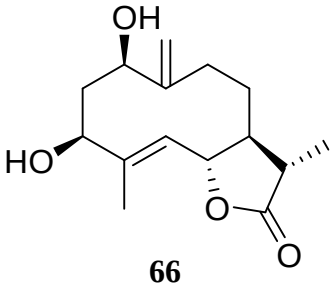

66

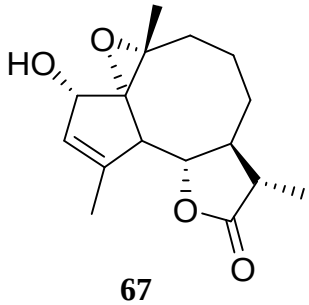

67

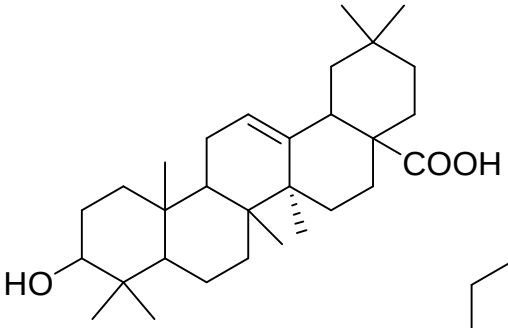

68

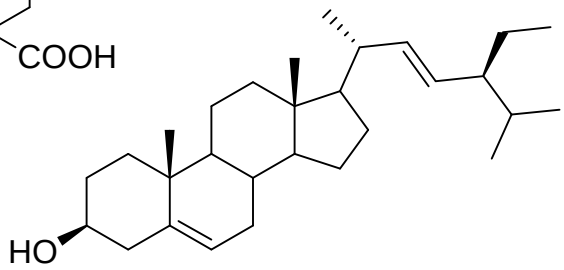

69

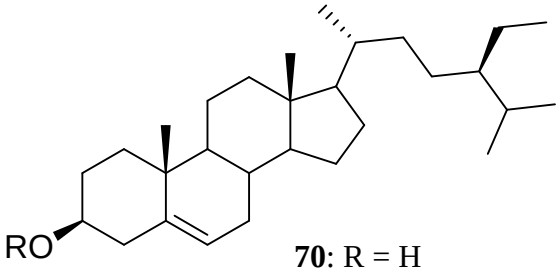

70: R = H
71: R = glucose

Although, as described above, there has been significant investigation of the biological activity of the essential oil of *M. chamomilla*, there have been relatively few investigations of the biological activity of the individual chemical constituents beyond

the major components. Thus, given the wide range of biological activities reported for this plant a project was designed to perform a detailed chemical analysis on the methanolic extract of *M. chamomilla* and evaluate the resulting pure natural products for anti-GST, antioxidant, anti-leishmanial, and antibacterial and antifungal activities. These studies yielded one new natural product, matriisobenzofuran (**72**), as well as four known compounds: apigenin (**73**), apigenin-7-O-β-glucopyranoside (**74**), scopoletin (**75**), and fraxidin (**76**). Structures of all of these natural products were elucidated with the aid of UV, IR, mass, 1D-NMR (^{1}H, ^{13}C, DEPT) and 2D-NMR (COSY, NOESY, ROESY, HSQC, and HMBC) spectroscopic methods. In this chapter, the isolation and structure elucidation of compounds **72-76**, as well as their bioactivity data have been discussed.

2.2 RESULTS AND DISCUSSION

M. chamomilla, collected from outside Selkirk, Manitoba was dried and cut into small pieces. The coarsely mulched plant material (4 kg) was extracted with methanol at room temperature. The solvent was evaporated under reduced pressure to yield a dark brown to blackish gum (204 g). The gummy extract was fractionated by solvent-solvent partitioning and the resulting fractions were subjected to chromatographic techniques including column chromatography and thin-layer chromatography (TLC) to isolate five compounds (**72-76**; for detailed purification methods see section 2.3). In this section, the structure elucidation of compounds **72-76** and their biological activity data are described.

2.2.1 Structure Elucidation of Compounds 72-76

*2.2.1.1 Matriisobenzofuran (**72**)*

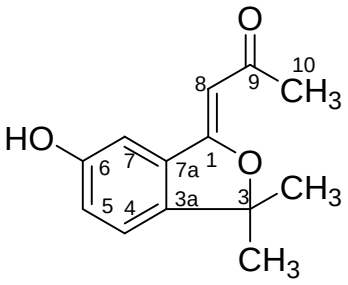

72

Compound **72** was isolated as a pale yellow amorphous solid. The high-resolution electron-impact mass spectrum (HR-EI-MS) of **72** showed the molecular ion peak at *m/z* 218.0939, which was in agreement with the molecular formula $C_{13}H_{14}O_3$ (calcd. 218.0943) and indicated the presence of seven degrees of unsaturation in this compound. Five of them were accounted for by an isobenzofuran moiety and two were due to the α, β-unsaturated carbonyl group. The peak at *m/z* 203.0703 ($C_{12}H_{11}O_3$, calcd. 203.0708) was

due to the loss of a methyl group from the molecular ion. In addition to these peaks, the low resolution electron-impact mass spectrum (EI-MS) showed a base peak at *m/z* 43, indicating the presence of an acetyl group in **72**. The UV spectrum of **72** showed a maximum absorption at 234 nm, indicating the presence of an α, β-unsaturated carbonyl functionality in **72**[23]. The IR spectrum of **72** displayed intense absorption bands at 3427 (OH) and 1677 (C=O) cm^{-1}.

The ^{1}H-NMR spectrum ($CDCl_3$, 400 MHz) of **72** exhibited an ABX spin system at δ 7.50 (d, *J* = 8.5 Hz), 7.94 (dd, *J* = 8.5, 1.7 Hz), and 8.19 (d, *J* = 1.7 Hz), suggesting the presence of a tri-substituted benzene functionality in **72**. These signals were assigned to H-4, H-5 and H-7, respectively. A singlet, integrating for one proton, resonated at δ 6.69 and was ascribed to an olefinic C-8 methine proton. A three-proton singlet at δ 2.67 was assigned to the C-10 methyl protons. The downfield chemical shift value of this signal indicated the presence of a geminal carbonyl functionality. Another six-proton singlet at δ 1.70 was due to the protons of two geminal methyl groups, substituted at C-3.

The COSY spectrum of **72** provided information about ^{1}H-^{1}H spin correlations that helped to establish partial structures **72a-72c**. The presence of an ABX spin system was also inferred in the COSY spectrum, which showed cross-peaks between H-4 and H-5. The latter in turn showed *meta*-coupling with H-7. These COSY data helped to establish the partial structure **72a**. H-8 did not show any significant coupling in the COSY spectrum but the UV spectrum indicated the presence of an α, β-unsaturated carbonyl group. Additionally, the ^{1}H-NMR spectrum showed the presence of an acetyl methyl group in this compound. These spectral data led to the drawing of another partial structure, **72b**. The ^{1}H-NMR spectrum further displayed signals for two geminal dimethyl

groups, and the ^{13}C-NMR spectrum showed the resonances of a quaternary carbon (C-3, δ 69.7) and two chemically equivalent methyl groups (C-3/$(CH_3)_2$, δ 28.7). These spectral data suggested the presence of partial structure **72c**.

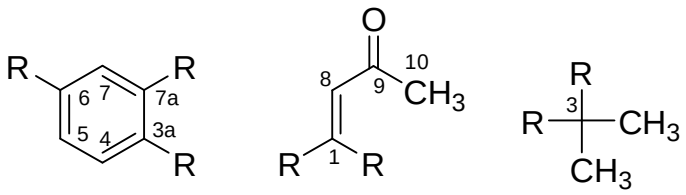

72a **72b** **72c**

The ^{13}C-NMR spectrum ($CDCl_3$, 100 MHz) of **72** displayed resonances of all thirteen carbons, with the two geminal methyl groups (δ 28.7), bonded to C-3, appearing as one resonance. DEPT experiments were also performed in order to establish the multiplicity of each carbon signal. These spectra revealed the presence of three methyl and four methine carbons in **72**. Subtraction of the DEPT spectral data from the broadband ^{13}C-NMR spectrum indicated the presence of six quaternary carbons in this compound. These signals were due to C-1, C-3, C-3a, C-6, C-7a, and C-9. The C-9 carbonyl carbon resonated at δ 197.7 while C-1 appeared at δ 164.7. The other downfield signal at δ 157.3 was assigned to the hydroxyl-bearing C-6. The remaining three quaternary carbons, C-3, C-3a, and C-7a, resonated at δ 69.7, 132.7, and 128.4, respectively. The four methine signals in the DEPT spectrum that resonated at δ 111.2, 124.9, 122.3, and 101.0 were ascribed to C-4, C-5, C-7, and C-8, respectively. The C-10 methyl carbon resonated at δ 26.8.

The heteronuclear single quantum coherence (HSQC) spectrum of **72** aided in assigning the ^{1}H/^{13}C one-bond shift correlations of **72**. This spectrum, for instance, showed ^{1}H/^{13}C one-bond coupling of H-4 (δ 7.50) with C-4 (δ 111.2), H-5 (δ 7.94) with

C-5 (δ 124.9), and H-7 (δ 8.19) with C-7 (δ 122.3). The C-10 methyl protons (δ 2.67) were correlated to the carbon resonating at δ 26.8 while the C-3 geminal methyl protons (δ 1.70) were ascribed to the carbon signal at δ 28.7. Complete ^{1}H- and ^{13}C-NMR chemical shift assignments for **72**, and ^{1}H/^{13}C one-bond shift correlations of protonated carbons, as determined from the HSQC spectrum, are shown in Table 2.1.

The heteronuclear multiple bond correlation (HMBC) spectrum of **72** was useful in the chemical shift assignment of the quaternary carbons and in connecting partial structures **72a-c** to build structure **72**. H-8 (δ 6.67) showed cross-peaks with C-1 (δ 164.7) and C-7a (δ 128.4), suggesting a bond between C-1 and C-7a. The C-3 geminal methyl protons (δ 1.70) exhibited cross-peaks with C-3 (δ 69.7) and C-1 (δ 164.7). The HMBC interaction between the C-3 geminal methyl protons and C-1 represents J_4 coupling. This J_4 coupling is occasionally observed in the HMBC spectrum[24]. These HMBC spectral data led to the connection of partial structures **72a-c** as shown in **72d**. As previously stated the molecular formula $C_{13}H_{14}O_3$ indicated seven degrees of unsaturation. To satisfy these degrees of unsaturation, a bond between C-3 and C-3a was made. The observed HMBC interactions in **72** are shown in Figure 2.1.

Once the structure of **72** was carefully determined, the *Z*-geometry of the double bond between C-1 (δ 164.7) and C-8 (δ 101.0) was established on the basis of a NOESY interaction between H-7 (δ 8.19) and H-8 (δ 6.67). Additionally, the absence of NOE interactions between H-8 and the other aromatic protons confirmed the substitution of the hydroxyl group at C-6 (δ 157.3)[*].

[*] The NOESY data presented in this paragraph was inserted after submission of the thesis to the examining committee but was presented during the oral defense.

A combination of IR, UV, mass and NMR spectral data helped to propose structure **72** for this new compound, which was named matriisobenzofuran.

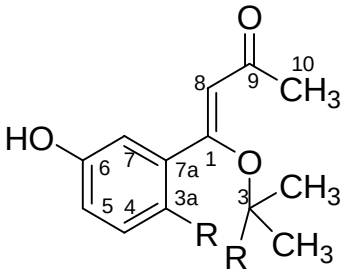

72d

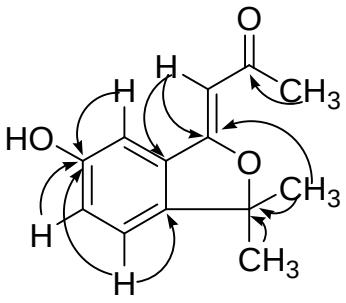

Figure 2.1. Important HMBC interactions in **72**.

Table 2.1. ^{1}H (400 MHz) and ^{13}C (100 MHz) NMR data for **72** and $^{1}H/^{13}C$ one-bond shift correlations as determined by HSQC ($CDCl_3$).

Position	δH (J in Hz)	δC (multiplicity[a])
1	-	164.7 (-C-)
2	-	-
3	-	69.7 (-C-)
3a	-	132.7 (-C-)
4	7.50 d, (8.5)	111.2 (-CH-)
5	7.94, dd, (8.5, 1.7)	124.9 (-CH-)
6	-	157.3 (-C-)
7	8.19, d, (1.7)	122.3 (-CH-)
7a		128.4 (-C-)
8	6.67, s	101.0 (-CH-)
9	-	197.7 (-C-)
10	2.67, s	26.8 ($-CH_3-$)
C-3/$(CH_3)_2$	1.70, s	28.7 ($-CH_3-$)

[a]Multiplicity determined using DEPT.

*2.2.1.2 Apigenin (**73**)*

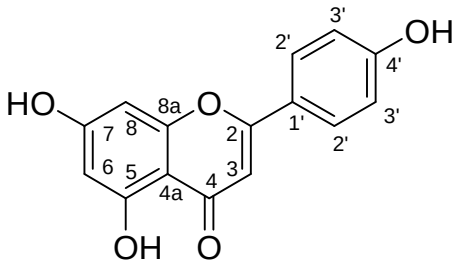

73

Compound **73** was isolated as a yellow amorphous solid. The UV spectrum of **73** displayed maximum absorptions at 268 and 336 nm, indicative the presence of a flavonoid-type skeleton[25]. The IR spectrum of **73** displayed intense absorption bands at 3413 (OH) and 1702 (C=O) cm^{-1}.

The ^{1}H-NMR spectrum (acetone-d_6, 400 MHz) of **73** displayed downfield signals at δ 6.65, 6.26, and 6.55 which were assigned to H-3, H-6, and H-8, respectively. The two doublets observed at δ 7.96 (J = 9.0 Hz) and 7.04 (J = 9.0 Hz), integrating for two protons each, were due to the two pairs of chemically equivalent methine protons at H-2' and H-3', respectively.

The COSY spectrum of **73** displayed two sets of cross peaks. The first was between H-2' and H-3'. Given that each of these signals were integrating for two protons in the ^{1}H-NMR spectrum, the presence of partial structure **73a** within the molecule was indicated. In the second set of cross peaks, *meta* coupling was observed between H-6 and H-8, giving the second partial structure, **73b**.

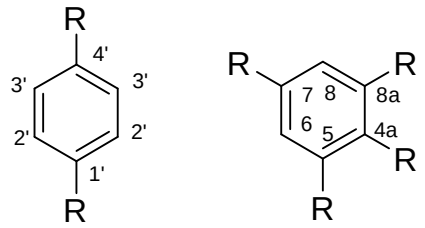

73a **73b**

The ^{13}C-NMR spectrum (acetone-d_6, 100 MHz) of **73** displayed the resonances of all fifteen carbons, with the pairs of chemically equivalent carbons at C-2' (δ 128.4) and C-3' (δ 115.9) each appearing as one resonance. The signal at δ 182.2 was assigned to C-4 while C-2 was assigned to the resonance at δ 163.5. The other downfield resonances at δ 164.2, 162.5, 157.9, and 161.0 were ascribed to C-5, C-7, C-8a, and C-4', respectively. Their downfield chemical shift values were indicative of the presence of geminal oxygen moieties. C-4a resonated at δ 104.4.

The HSQC spectrum of **73** showed the ^{1}H/^{13}C one-bond coupling of H-3 (δ 6.65) with C-3 (δ 103.2), H-6 (δ 6.26) with C-6 (δ 98.8), H-8 (δ 6.55) with C-8 (δ 93.8), H-2' (δ 7.96) with C-2' (δ 128.4), and H-3' (δ 7.04) with C-3' (δ 115.9). Complete ^{1}H- and ^{13}C-NMR chemical shift assignments for **73**, and ^{1}H/^{13}C one-bond shift correlations of protonated carbons, as determined from the HSQC spectrum, are shown in Table 2.2.

The HMBC spectrum of **73** showed long-range ^{1}H/^{13}C couplings of H-3' (δ 7.04) with C-1' (δ 122.4) and C-4' (δ 161.0). H-2' (δ 7.96) showed couplings with C-4' and C-2 (δ 163.9). H-3 (δ 6.65) also displayed coupling with C-2, as well as C-4 (δ 182.2) and C-4a (δ 104.4). H-6 (δ 6.26) also showed a cross-peak with C-4a and with C-7 (δ 162.5). The chemical shift of C-8a (δ 157.9) was assigned on the basis of a long range

coupling with H-8 (δ 6.55). These HMBC data helped to connect partial structures **73a** and **73b** to build structure **72**. Important HMBC interactions are displayed in Figure 2.2.

The UV, IR, and ^{1}H- and ^{13}C-NMR spectral data of **73** were similar to those of apigenin, reported in the literature[25]. This known compound is a major constituent of *M. chamomilla*[18] and has been purified from a large number of other plants such as: *Isodon oresbius*[26], *Ajuga decumbens*[27], *Chrysanthemum morifolium*[28], *and Tecucrium polium L*[29].

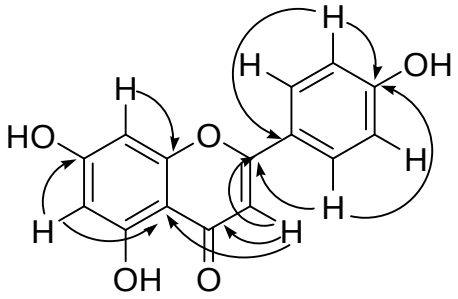

Figure 2.2. Important HMBC interactions in **73**.

Table 2.2. ^{1}H (400 MHz) and ^{13}C (100 MHz) NMR data for **73** and ^{1}H/^{13}C one-bond shift correlations as determined by HSQC (acetone-d_6).

Position	δH (J in Hz)	δC (multiplicity[a])
1	-	-
2	-	163.9 (-C-)
3	6.65, s	103.2 (-CH-)
4	-	182.2 (-C-)
4a	-	104.4 (-C-)
5	-	164.2 (-C-)
6	6.26, d, (2.1)	98.8 (-CH-)
7	-	162.5 (-C-)
8	6.55, d, (2.1)	93.8 (-CH-)
8a	-	157.9 (-C-)
1’	-	122.4 (-C-)
2’	7.96, d, (9.0)	128.4 (-CH-)
3’	7.04, d, (9.0)	115.9 (-CH-)
4’	-	161.0 (-C-)

[a]Multiplicity was determined with the help of the HSQC spectrum.

*2.2.1.3 Apigenin-7-O-β-glucopyranoside (**74**)*

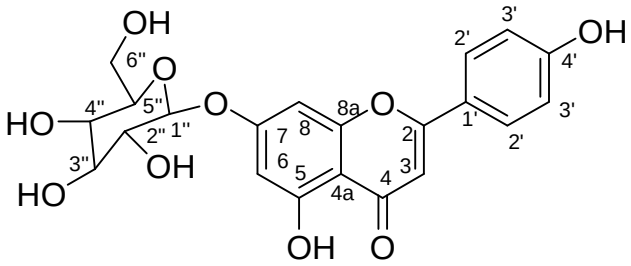

74

Compound **74** was isolated as a yellow amorphous solid. The UV spectrum of **74** showed absorption maxima at 268 and 333 nm, and indicated the presence of the same chromophores as those present in **73**[25,30]. The IR spectrum showed intense absorptions at 3411 (OH) and 1657 (C=O) cm^{-1}.

The ^{1}H-NMR spectrum (DMSO-d_6, 400 MHz) of **74** was similar to compound **73**, displaying downfield signals at δ 6.81, 6.43, and 6.82, corresponding to H-3, H-6, and H-8, respectively. As in compound **73**, two doublets, integrating for two protons each, were observed at δ 6.90 (H-3'; J = 8.8 Hz) and 7.92 (H-2'; J = 8.8 Hz), once again indicating the presence of a *para*-disubstituted benzene. The anomeric proton (H-1") resonated as a doublet at δ 5.06 (J = 7.0 Hz). These ^{1}H-NMR data indicated that compound **74** was the apigenin aglycone of **73**[30]. The remaining protons of glucose appeared as an overlapped multiplet, and resonated at δ 3.25-3.75.

The COSY spectrum of **74** showed vicinal coupling between H-2' and H-3'. Additionally, vicinal coupling between the anomeric proton (H-1") and H-2" (δ 3.27) was observed. The cross peaks for the remaining glycoside protons were difficult to observe as this region of the spectrum was overlapped.

The rotating-frame Overhauser effect spectroscopy (ROESY) spectrum, which shows spatial couplings by measuring NOE's in the rotating frame of reference, was quite helpful in unambiguously determining the exact position of the sugar moiety. Here, the anomeric proton showed spatial coupling with both H-6 and H-8. These ROESY data suggested the presence of a glucose moiety at C-7 (δ 162.9). The ROESY spectrum of **74** also showed couplings between H-3' and H-2'. The latter showed a NOE with H-3. These ROESY couplings are shown in Figure 2.3.

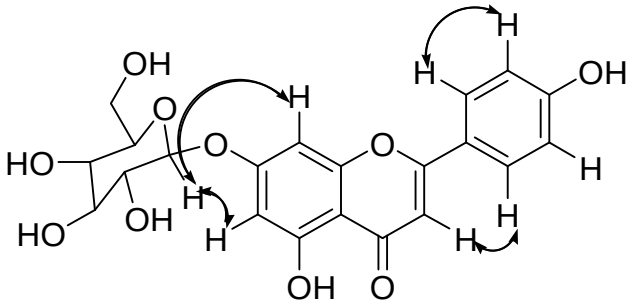

Figure 2.3. ROESY interactions observed in **74**.

The ^{13}C-NMR spectrum (DMSO-d_6, 100 MHz) of **74** displayed resonances for all twenty-one carbons, with the pairs of chemically equivalent carbons at C-2' (δ 128.5) and C-3' (δ 116.3) each appearing as one resonance. A combination of ^{13}C broadband and DEPT spectra indicated the presence of one methylene, twelve methine, and eight quaternary carbons in **74**. As in **73** the C-4 carbonyl carbon resonated downfield at δ 181.8, while C-2 and C-3 were found at δ 164.5 and 102.5, respectively. The remaining downfield carbons, C-5, C-7, C-8a, and C-4', resonated at δ 161.1, 162.9, 156.9, and 163.0, respectively. The signal at δ 105.2 was assigned to the other ring-junction carbon, C-4a. Further, the observation of five signals at δ 60.6 (C-6"), 69.5 (C-4"), 73.1 (C-2"), 76.4 (C-3"), and 77.2 (C-5"), along with the anomeric carbon (C-1") at δ 99.9 suggested

that the sugar moiety was glucose as all of these signals has the same chemical shift values as those of glucose reported in the literature[30,31].

In the HSQC spectrum of **74**, $^{1}H/^{13}C$ one-bond coupling between H-3 (δ 6.81) and C-3 (δ 102.5), H-6 (δ 6.43) and C-6 (δ 99.5), H-8 (δ 6.82) and C-8 (δ 94.7), H-2' (δ 7.92) and C-2' (δ 128.5), and between H-3' (δ 6.90) and C-3' (δ 116.3) were observed. Further, the HSQC spectrum of **74** was especially useful in assigning the $^{1}H/^{13}C$ one-bond shift correlations for the glucose moiety. For instance, the anomeric proton (H-1", δ 5.06) showed connectivity with the carbon at δ 99.9 (C-1"). Complete ^{1}H- and ^{13}C-NMR chemical shift assignments for **74**, and $^{1}H/^{13}C$ one-bond shift correlations of all hydrogen-bearing carbons, as determined from the HSQC spectrum, are shown in Table 2.3.

The HMBC spectrum of **74** provided further confirmation as to the position of the glucose moiety, in addition to providing confirmation of the overall structure and aiding in chemical shift assignments. In this spectrum, HMBC interactions between H-1" and C-7 (δ 162.9) were observed. Other important HMBC interactions within the glucose moiety include H-2" (δ 3.27) and H-4" (δ 3.19) coupling with C-3" (δ 76.4), H-5" (δ 3.44) coupling with C-4" (δ 69.5), and the C-6" methylene protons (δ 3.72, 3.49) coupling with C-5" (δ 77.2). These HMBC interactions confirmed the presence of a glucose moiety at C-7. Within the rest of the molecule, similar HMBC interactions were observed as in compound **73**. For instance, H-3 (δ 6.81) showed coupling with C-1' (δ 120.0), C-4 (δ 181.8) and C-4a (δ 105.2). H-6 (δ 6.43) displayed HMBC interactions with C-5 (δ 105.2), and C-7. H-8 (δ 6.82) also showed interactions with C-7 as well as with C-8a (δ 156.9). Lastly, both H-2' (δ 7.92) and H-3' (δ 6.90) had long-range $^{1}H/^{13}C$

couplings with C-4' (δ 163.0), while H-2' also showed coupling with C-2 (δ 164.5). These HMBC interactions are shown in Figure 2.4.

After the careful determination of the structure of **74**, the β-orientation of the glycosidic linkage was ascertained on the basis of the large coupling constant (J = 7.4 Hz) between H-1" (δ 5.06) and H-2" (δ 3.27), which indicated that these two protons were *diaxially* oriented with respect to each other[30].

These spectral data led to the identification of compound **74** as apigenin-7-*O*-β-glucopyranoside. The UV, IR, and ^{1}H- and ^{13}C-NMR spectral data of **74** were similar to those of apigenin-7-*O*-β-glucopyranoside reported in the literature[31]. Based on this, compound **74** was identified as the known flavonoid glycoside, apigenin-7-*O*-β-glucopyranoside. This compound is also a major constituent of *M. chamomilla*[32] and has been purified from a large number of other sources. Examples of other sources of this compound include: *Crataegus sp.*[33], *Itoa orientalis*[34], *Saussurea medusa*[35], and *Salvia patens*[30].

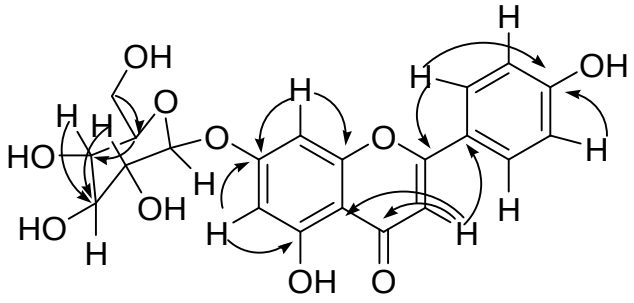

Figure 2.4. Important HMBC interactions in **74**.

Table 2.3. ^{1}H (400 MHz) and ^{13}C (100 MHz) NMR data for **74** and $^{1}H/^{13}C$ one-bond shift correlations as determined by HSQC (DMSO-d_6).

Position	δH (J in Hz)	δC (multiplicity[a])
1	-	-
2	-	164.5 (-C-)
3	6.81, m	102.5[b] (-CH-)
4	-	181.8 (-C-)
4a	-	105.2 (-C-)
5	-	161.1 (-C-)
6	6.43, d, (2.1)	99.5 (-CH-)
7	-	162.9 (-C-)
8	6.82, m	94.7[b] (-CH-)
8a	-	156.9 (-C-)
1’	-	120.0 (-C-)
2’	7.92, d, (8.8)	128.5 (-CH-)
3’	6.90, d, (8.8)	116.3 (-CH-)
4’	-	163.0 (-C-)
1”	5.06, d, (7.4)	99.9 (-CH-)
2”	3.27, m	73.1 (-CH-)
3”	3.31, m	76.4 (-CH-)
4”	3.19, m	69.5 (-CH-)
5”	3.44, m	77.2 (-CH-)
6”	α 3.72[c], m	60.6 ($-CH_2-$)
	β 3.49[c], m	

[a]Multiplicity determined using DEPT
[b]These carbon assignments may be interchangeable
[c]These proton assignments may be interchangeable

*2.2.1.4 Scopoletin (**75**)*

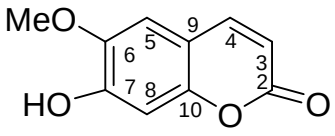

75

Compound **75** was isolated as a white amorphus solid. The UV spectrum of **75** displayed absorption maxima at 229, 255, 296, and 344 nm, indicating a coumarin-type chromophore in **75**[36]. The IR Spectrum showed intense absorptions at 3335 (OH) and 1708 (COOR) cm^{-1}.

The ^{1}H-NMR spectrum ($CDCl_3$, 400 MHz) of **75** also displayed a spectral pattern that was consistent with a coumarin-type structure[36]. The two singlets at δ 6.86 (H-5) and 6.93 (H-8), integrating for one proton each, suggested the presence of an *ortho, meta*-tetrasubstituted benzene in this compound. Two doublets at δ 6.27 (J = 9.5 Hz) and 7.62 (J = 9.5 Hz) were ascribed to H-3 and H-4, respectively. The three-proton singlet at δ 3.96 was due to the protons of a methoxy group.

The COSY spectrum of **75** displayed two spin systems. The first spin system corresponded to the vicinal coupling of H-3 to H-4. The downfield chemical shift value of H-4 indicated the presence of an α, β-unsaturated carbonyl group. These COSY data provided fragment **75a**. The second spin system corresponded to *para*- coupling between H-5 and H-8, providing additional evidence of the presence of an *ortho, meta*-tetrasubstituted benzene (**75b**) in **75**.

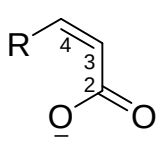

75a

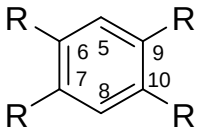

75b

The ROESY spectrum of **75** was utilized to unequivocally determine the position of the methoxy group, thereby distinguishing compound **75** from its structural isomer, isoscopoletin (**75c**). Previously, these two compounds were distinguished by their melting points[37], which can be unreliable. In the ROESY spectrum of **75**, the methoxy protons displayed spatial coupling with H-5, which was coupled to H-4, which showed further coupling with H-3. These ROESY data permitted the substitution of the methoxy group at C-6. These aforementioned ROESY interactions are shown in Figure 2.5.

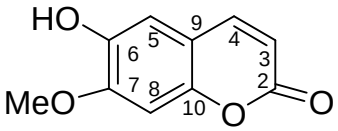

75c

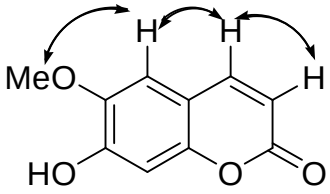

Figure 2.5. ROESY interactions observed in **75**.

The ^{13}C-NMR spectrum ($CDCl_3$, 100 MHz) of **75** displayed resonances of all ten carbons. The signal at δ 162.4 was ascribed to C-2. The other three oxygen-bearing quaternary carbons, C-6, C-7, and C-9, resonated at δ 145.2, 150.8, and 150.0, respectively. Another downfield signal was observed at δ 144.1, and was assigned to C-4. The remaining quaternary resonance (δ 111.1) was assigned to C-9. The methoxy carbon appeared at δ 56.2.

The HSQC spectrum of **75** showed the connectivities of H-3 (δ 6.27), H-4 (δ 7.62), H-5 (δ 6.86), and H-8 (δ 6.93) with C-3 (δ 112.3), C-4 (δ 144.1), C-5 (δ 103.2), and C-8 (δ 108.0), respectively. Complete ^{1}H- and ^{13}C-NMR chemical shift assignments for **75**, and ^{1}H/^{13}C one-bond shift correlations of protonated carbons, as determined from the HSQC spectrum, are shown in Table 2.4.

The HMBC spectrum of **75** displayed long range couplings between the methoxy protons (δ 3.96) and C-6 (δ 145.2). H-4 (δ 7.62) showed interactions with C-10 (δ 150.0) and C-2 (δ 162.4). H-5 (δ 6.86) also displayed interactions with C-10, as well as with C-6

and C-7 (δ 150.8). Lastly, H- 3 (δ 6.27) showed coupling with C-9 (δ 111.1) and C-2. These HMBC data helped to connect partial structures **75a** and **75b** to give structure **75**. The HMBC interactions of **75** are shown in Figure 2.6.

These spectral data led to the characterization of compound **75** as scopoletin. The UV, IR, and ^{1}H- and ^{13}C-NMR spectral data of **75** were found to be identical to those of scopoletin, reported in the literature[37]. This is the first report of the isolation of this compound from *M. chamomilla*. Previously, this compound has also been purified from other plants, including: *Anthemis nobilis*[38], *Sophora mollis*[39], *Sinomonium acutum*[40], *Clausensa excavata*[41], and *Manihot esculenata*[36].

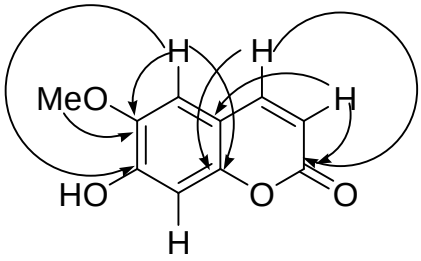

Figure 2.6. Important HMBC interactions in **75**.

Table 2.4. ^{1}H (400 MHz) and ^{13}C (100 MHz) NMR data for **75** and ^{1}H/^{13}C one-bond shift correlations as determined by HSQC ($CDCl_3$).

Position	δH (J in Hz)	δC (multiplicity[a])
1	-	-
2	-	162.4 (-C-)
3	6.27, d, (9.5)	112.3 (-CH-)
4	7.62, d, (9.5)	144.1 (-CH-)
5	6.86, s	103.2 (-CH-)
6	-	145.2 (-C-)
7	-	150.8 (-C-)
8	6.93, s	108.0 (-CH-)
9	-	111.1 (-C-)
10	-	150.0 (-C-)
-OMe	3.96, s	56.2 (-CH_3-)

[a]Multiplicity was determined with the help of the HSQC spectrum.

*2.2.1.5 Fraxidin (**76**)*

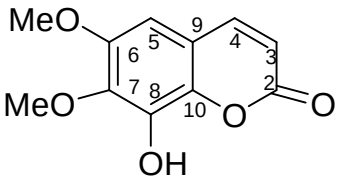

76

Compound **76** was isolated in a relatively minor quantity as a white amorphous solid. The ^{1}H-NMR spectrum ($CDCl_3$, 400 MHz) of **76** was similar to that of compound **75**, displaying two doublets, integrating for one proton each, at δ 6.29 (*J* = 9.5 Hz) and 7.60 (*J* = 9.5 Hz), corresponding to the olefinic H-3 and H-4, respectively. A singlet at δ 6.66 (H-5) indicated the presence of a pentasubstituted benzene. Two singlets, each integrating for three protons and resonating at δ 3.94 and 4.10, indicated the presence of two methoxy groups within the compound.

The nuclear Overhauser effect spectroscopy (NOESY) spectrum was utilized to determine the substitution pattern of **76**. In this spectrum, an NOE was observed between the two methoxy groups. The methoxy protons resonating at δ 3.94 showed cross-peaks with H-5. The latter exhibited an NOE with H-4. H-4 showed further cross peaks with H-3. These NOESY data suggested that the methoxy groups were substituted at C-6 and C-7. These NOESY interactions are shown in Figure 2.7.

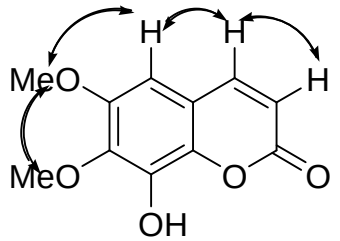

Figure 2.7. NOESY interactions observed in **76**.

The ^{13}C-NMR spectrum ($CDCl_3$, 100 MHz) of **76** displayed resonances for all eleven carbons. The downfield resonance at δ 160.6 was assigned to C-2. The other downfield signals resonating at δ 143.8, 144.6, 134.5, 142.6, and 143.0 were ascribed to the deshielded C-4, and the oxygen-bearing C-6, C-7, C-8, and C-10, respectively. The signal at δ 111.2 was assigned to C-9. The C-6 and C-7 methoxy carbons resonated at δ 56.5 and 61.7, respectively.

The HSQC spectrum of **76** showed the one-bond connectivity of H-3 (δ 6.29) with C-3 (δ 113.6), H-4 (δ 7.60) with C-4 (δ 143.8), and H-5 (δ 6.66) with C-5 (δ 103.2). The C-6 methoxy protons were found to be coupled with the carbon resonating at δ 56.5, and the C-7 methoxy protons were coupled with the carbon signal at δ 61.7. Complete ^{1}H- and ^{13}C-NMR chemical shift assignments for **76**, and ^{1}H/^{13}C one-bond shift correlations of all hydrogen-bearing carbons, as determined from the HSQC spectrum, are shown in Table 2.5.

The HMBC spectrum of **76** demonstrated long range ^{1}H/^{13}C couplings between the C-6 methoxy protons (δ 3.94) and C-6 (δ 144.6), and the C-7 (δ 4.10) methoxy protons and C-7 (δ 134.5). H-3 (δ 6.29) showed interactions with C-2 (δ 160.6) and C-9 (δ 111.2). H-4 (δ 7.60) also showed coupling with C-2, as well as with C-8 (δ 142.6) and C-10 (δ 143.0). H-5 (δ 6.66) showed coupling to both C-8 and C-10, as well as C-6. These HMBC interactions are shown in Figure 2.8.

These NMR spectral data helped to identify compound **76** as fraxidin. The ^{1}H- and ^{13}C-NMR spectral data of **76** were similar to those of fraxidin, reported in the literature[42]. This is the first report of the isolation of fraxidin (**76**) from *M. chamomilla*.

Compound **76** has been previously isolated from several sources such as *Fraxinus ornus*[43] and *Nectandra gardneri*[44].

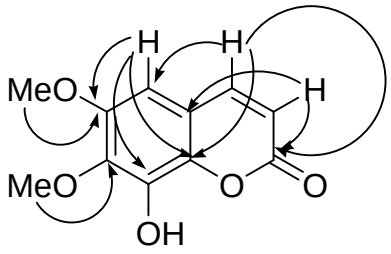

76

Figure 2.8. Important HMBC interactions in **76**.

Table 2.5. ^{1}H (400 MHz) and ^{13}C (100 MHz) NMR data for **76** and $^{1}H/^{13}C$ one-bond shift correlations as determined by HSQC ($CDCl_3$).

Position	δH (J in Hz)	δC (multiplicity[a])
1	-	-
2	-	160.6 (-C-)
3	6.29, d, (9.5)	113.6 (-CH-)
4	7.60, d, (9.5)	143.8 (-CH-)
5	6.66, s	103.2 (-CH-)
6	-	144.6 (-C-)
7	-	134.5 (-C-)
8	-	142.6 (-C-)
9	-	111.2 (-C-)
10	-	143.0 (-C-)
C-6/-OMe	3.94, s	56.5 ($-CH_3$-)
C-7/-OMe	4.10, s	61.7 ($-CH_3$-)

[a]Multiplicity was determined with the help of the HSQC spectrum.

2.2.2 Biological Activity of Compounds 72-76

2.2.2.1 GST Inhibitory Activity

In the GST inhibitory assay, all compounds exhibited different levels of activity with IC_{50} values ranging from 20-57 µM. Ethacrynic acid (**48**) was used as a

positive control and was active in this bioassay with an IC_{50} value of 15 µM. The bioactivity data of compound **72** (IC_{50} = 20 µM) was close to that of ethacrynic acid. The results of all the GST assays are shown in Table 2.6. A careful examination of structures **72-76** revealed that all of these compounds have an α, β-unsaturated carbonyl functionality in their structures. The GST inhibitory activities of these compounds might result from this common functional group. All of these compounds might make adducts with glutathione via Michael reactions, thereby decreasing the reactivity of glutathione[45]. Further structure-activity relationship studies on these compounds are warranted in order to confirm this hypothesis and to determine the active pharmacophore required for GST inhibition.

2.2.2.2 Antioxidant Activity

Compounds **72-76** were also screened for antioxidant activity by using the 2,2-diphenyl-1-picrylhydrazyl (DPPH) assay. Compound **72** had the highest free radical scavenging activity with an IC_{50} value of 26 µg/mL. The rest of the compounds showed varying activities with IC_{50} values ranging from 40-80 µg/mL. Quercetin (**49**) was used as a positive control and was active in this assay with an IC_{50} value of 17 µg/mL. The free radical scavenging activity data of compounds **72-76** are shown in Table 2.6.

2.2.2.3 Anti-Leishmanial Activity

Compounds **72-76** were next screened for anti-leishmanial activity. Both compounds **75** and **76** showed significant activity with IC_{50} values of 10 and 12 µg/mL, respectively. In comparison to the positive control, miltefosine (**77**; IC_{50} = 0.4 µg/mL),

however, the activity was moderate. The rest of the compounds were found to be weakly active in this assay. Anti-leishmanial activity data of all the isolates are shown in Table 2.6.

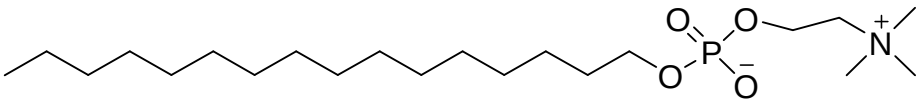

77

Table 2.6. Anti-GST, antioxidant, and anti-leishmanial activities of compounds **72-76**.

Compounds	GST IC_{50} (µM)*	Anti-oxidant IC_{50} (µg/mL)	Anti-leishmanial IC_{50} (µg/mL)
72	20.3±4.0	25.8±0.5	50.0
73	56.8±2.0	80.4±1.0	50.0
74	52.0±5.0	70.7±0.7	43.0
75	24.2±2.0	45.0±0.5	10.0
76	25.0±1.0	40.2±1.5	12.0
Ethacrynic acid	15.0±1.0	-	-
Miltefosine	-	-	0.4
Quercetin	-	17.3±0.2	-

*IC_{50} value represents the concentration of compounds required to inhibit 50% of the activity of GST. ± represents the standard error of the mean; ethacrynic acid, milteofsine, and quercetin were used as positive controls.

2.2.2.4 Antimicrobial Activity

Given that extracts of *M. chamomilla* have shown antimicrobial activity[2], compounds **72-76** were tested for antibacterial and antifungal activity against *Staphylococcus aureus, Escherichia coli, Pseudomonas aeruginosa, Mycobacterium goodii, Streptococcus mitis, Streptococcus bovis, Streptococcus mutans* and *Candida albicans* using the disc-diffusion method (see experimental). Each disc was impregnated with 100 µg of the respective compound. While both the standards and the negative

controls gave the expected results, none of the isolates showed activity against the above microorganisms at this concentration.

2.3 EXPERIMENTAL

2.3.1 General Conditions

UV spectra were recorded in methanol on a Shimadzu UV-2501 PC spectrophotometer. IR spectra were acquired on a Varian 1000 FT-IR (Scimitar Series). Low resolution electron impact and chemical ionization mass spectra were recorded on a Hewlett-Packard 5989B MS. High resolution electron impact mass spectra were recorded on a Kratos Analytical MS-50G mass spectrometer at the University of Alberta. ^{1}H-NMR, ^{13}C-NMR, and 2D-NMR spectra were obtained from a Bruker Avance 400 MHz spectrometer. Column chromatography was carried out using 60 Å silica gel (230-400 mesh) as the stationary phase. Thin layer chromatography (TLC) was performed on silica gel 60 F_{254} aluminum-backed TLC plates (Machery-Nagel, Germany; Merck, Germany).TLC UV-visualization was done by using an Entela multiband (UV-254/366 nm) Model UVGL-58 Mineral light® lamp. GST inhibitory activities were measured spectrophotometrically using a Synergu HT multidetection BioTek microplate reader. Free radical scavenging activities were measured spectrophotometrically on a Unico 4802 UV-visible double beam spectrophotometer. Anti-leishmanial activities were measured spectrofluorometrically on a Spectramax Gemini XS microplate fluorometer. Glutathione (GSH), equine liver GST, and resazurin were purchased from Sigma-Aldrich. 1-chloro-2,4-dinitrobenzene (CDNB) was purchased from MP Biomedicals. The 2,2-diphenyl-1-picrylhydrazyl (DPPH) as well as all biological media (except the blood agar plates) and reagents were obtained from EMD. The blood agar plates were purchased from Oxoid Inc. All solvents were ACS reagent grade, and were purchased

from Caledon Laboratories. NMR solvents were purchased from Cambridge Isotope Laboratories.

2.3.2 Plant Material

The plant material was collected outside of Selkirk, Manitoba in the summer of 2007. This was identified by Dr. Richard Staniforth, Department of Biology, the University of Winnipeg, and a voucher specimen was deposited in the Natural Products Laboratory at the University of Winnipeg.

2.3.3 Extraction and Isolation of Compounds 72-76

The air-dried plant material of *M. chamomilla* (4 kg) was cut into small pieces and extracted twice with methanol. The extract was evaporated under reduced pressure to prepare a gum (204 g). This was dissolved in 80:20 H_2O:MeOH and partitioned with hexane to de-fat this extract. The aqueous-alcoholic layer was concentrated, redissolved in water (a small portion of this was insoluble and was kept separate) and was extracted with chloroform and butanol.

For the isolation of compounds **72**, **75**, and **76**, the chloroform fraction (2.3 g) was loaded onto a silica gel column and eluted with hexane-chloroform (0-100) and chloroform-methanol (0-100). This afforded 123 fractions which were pooled on the basis of similar R_f values into 30 fractions. Combined fraction F-6 (20:80 hexane:$CHCl_3$; 190 mg) was loaded onto a silica gel column and eluted with hexane-chloroform (15:85) and chloroform-methanol (100:0, 90:10, 0:100). This afforded 54 subfractions which were combined on the basis of TLC data into five fractions. Preparative TLC (prep. TLC)

of combined subfraction f-5 (90:10 $CHCl_3$:MeOH; 30 mg) using chloroform:acetone (80:20) afforded compounds **72** (6.0 mg) and **75** (6.0 mg). Prep. TLC of combined fraction F-8 (99:1 $CHCl_3$:MeOH; 40 mg) using chloroform:isopropanol (99:1) afforded compound **76** (2.5 mg).

For the isolation of compound **73**, the hexane-soluble extract (44 g) was loaded onto a silica gel column and eluted with hexane-ethyl acetate (0-100) and ethyl acetate-methanol (0-100). This afforded 190 fractions which were pooled on the basis of similar R_f values into 30 fractions. Combined fraction F-17 (60:40 hexane:EtOAc; 554 mg) was loaded onto a silica gel column and eluted with hexane-ethyl acetate (100:0, 35:65, 40:60, 50:50, 0:100) and ethyl acetate-methanol (100:0, 90:10, 70:30, 0:100). This afforded 63 subfractions which were combined into 15 subfractions. Prep. TLC of combined subfraction f-5 (40:60 hexane:EtOAc; 20 mg) using hexane:ethyl acetate:acetic acid (60:40:0.01) afforded compound **73** (5.0 mg).

For the isolation of compound **74**, the aqueous insoluble portion (but soluble in methanol) of the crude extract (18 g) was loaded onto a silica gel column and eluted with hexanes-ethyl acetate (0-100) and ethyl acetate-methanol (0-100). This afforded 73 fractions which were pooled on the basis of similar R_f values into 13 fractions. Prep. TLC of the crystalline portion of combined fraction F-9 (90:10 EtOAc:MeOH; 114 mg) using ethyl acetate:methanol:acetic acid (80:20:0.01) afforded **72** (10.0 mg).

Matriisobenzofuran (**72**); pale yellow amorphous solid, 6.0 mg; UV (MeOH): λ_{max} 234, 271, 300 nm; IR ($CHCl_3$): v_{max} 3427, 2928, 1677, 1599, 1445, 1274 cm^{-1}; EIMS (70 eV): *m/z* (%) = 218 (22), 203 (67), 200 (12), 43 (100); HR-EI-MS *m/*z 218.0940 (calcd. for $C_{13}H_{14}O_3$, 218.0943), 203.0703 (calcd. for $C_{12}H_{11}O_3$, 203.0708); ^{1}H-NMR ($CDCl_3$, 400 MHz) = see Table 2.1; ^{13}C-NMR ($CDCl_3$, 100 MHz) = see Table 2.1.

Apigenin (**73**); yellow amorphous solid, 5.0 mg; UV (MeOH): λ_{max} 203, 268, 336 nm; IR ($CHCl_3$): v_{max} 3414, 2927 1702, 1421, 1341, 1093 cm^{-1}; ^{1}H-NMR (acetone-d_6, 400 MHz) = see Table 2.2; ^{13}C-NMR (acetone-d_6, 100 MHz) = see Table 2.2.

Apigenin-7-*O*-β-glucopyranoside (**74**); yellow amorphous solid, 10.0 mg; UV (MeOH): λ_{max} 268, 336 nm; IR ($CHCl_3$): v_{max} 3411, 2924, 1657, 1496, 1347, 1289, 1072 cm^{-1}; ^{1}H-NMR (DMSO-d_6, 400 MHz) = see Table 2.3; ^{13}C-NMR (DMSO-d_6, 100 MHz) = see Table 2.3.

Scopoletin (**75**); white amorphous solid, 6.0 mg; UV (MeOH): λ_{max} 229, 255, 297, 344 nm; IR ($CHCl_3$): v_{max} 3334, 2922, 1708, 1565, 1437, 1293 cm^{-1}; ^{1}H-NMR ($CDCl_3$, 400 MHz) = see Table 2.4; ^{13}C-NMR ($CDCl_3$, 100 MHz) = see Table 2.4.

Fraxidin (**76**); white amorphous solid, 2.5 mg; ^{1}H-NMR ($CDCl_3$, 400 MHz) = see Table 2.5; ^{13}C-NMR ($CDCl_3$, 100 MHz) = see Table 2.5.

2.3.4 Biological Assays

2.3.4.1 GST Inhibitory Assay

Glutathione *S*-transferase inhibitory activity of compounds **72-76** was determined by using the Habig method[46] with slight modifications. In this assay specific concentrations of compound were incubated with 133 µL of phosphate buffer (pH 6.5), 2 µL of GST (with an initial effective assay activity of 0.12106 U/mL) and 25 µL of 1 mM CDNB for 25 minutes at room temperature. After this time period, 40 µL of 1 mM GSH was added and the product of conjugation was measured at 340 nm using a 96-well microplate reader as described in section 2.3.1. The inhibitory activity of GST was calculated with reference to a control assay (assay carried out under similar conditions without test compound). Ethacrynic acid was used as a positive control. The percentage inhibition was calculated with the aid of the following equation:

[(E-S) / E] x 100

where E is the activity of the enzyme without test compound and S is the activity of the enzyme with test compound. The IC_{50} values were calculated by plotting a concentration response curve. Analyses were run in triplicate and the results were expressed as average values ± S.E.M (Standard error of the mean).

2.3.4.2 DPPH Assay

The stable DPPH radical scavenging activity of compounds **72-76** was determined by Bloi's method[47]. The samples and references dissolved in ethanol (75%) were mixed with DPPH solution (1.5×10^{-4} M). After incubating in the dark for 30 minutes, the remaining DPPH amount was measured spectrophotometricaly at 520 nm. Quercetin was

employed as a reference. Inhibition of DPPH in percent (I%) was calculated as given below:

$I\% = [(A_{blank}-A_{sample}) / A_{blank}] \times 100$

where A_{blank} is the absorbance of the control reaction (containing all reagents except the test sample), and A_{sample} is the absorbance of the test compound. The IC_{50} values were calculated by plotting a concentration response curve. Analyses were run in triplicate and the results were expressed as average values ± S.E.M.

2.3.4.3 Anti-Leishmanial Assay

The anti-leishmanial activities of compounds **72-76** was determined using the method described by Kolodziej *et al*[48] with slight modifications. Amastigotes of *Leishmania donovi* strain MHOM/ET/67/L82 were grown in axenic culture at 37 °C under an atmosphere of 5% CO_2 in SM medium at pH 5.4 supplemented with 10% heat-inactivated fetal bovine serum. 100 µL of culture medium containing 10^5 amastigotes from axenic culture with or without a serial drug dilution were seeded in 96-well microtitre plates. Serial dilutions of the test compounds covering a range of 90-0.123 µg/mL were prepared. After 72 h of incubation the plates were inspected under an inverted microscope to assure growth of the controls and sterile conditions. 10 µL of Alamar Blue (12.5 mg resazurin dissolved in 100 mL distilled water) were then added to each well and the plates incubated for another 2 h. After this time, the plates were read spectrofluorometrically at an excitation wavelength of 536 nm and emission wavelength of 588 nm. Miltefosine was used as the positive control. Decrease of fluorescence (which corresponded to the amount of inhibition) was expressed as a percentage of the

fluorescence of the control cultures (assay run under similar conditions without test compound) and plotted against the concentrations of the test compounds. From the sigmoidal inhibition curves the IC_{50} values were calculated.

2.3.4.4 Antibacterial and Antifungal Assays

2.3.4.4.1 Microorganisms

Staphylococcus aureus (ATCC 25923), *Escherichia coli* (ATCC 25922), *Pseudomonas aeruginosa* (ATCC 27853), *Mycobacterium goodii* (ATCC 87709813), *Streptococcus mitis* (ATCC 9811), *Streptococcus bovis* (ATCC 9809), *Streptococcus mutans* (ATCC 25175) and *Candida albicans* (ATCC 90028 and 14054) were all obtained from the Department of Biology, the University of Winnipeg. The *S. aureus, E. coli, M. goodii, and P.aeruginosa* cultures were periodically replated onto tryptic soy agar, whereas the *C. albicans* was replated onto Sabouraud dextrose agar, and *S. mitis, S. bovis,* and *S. mutans* were replated onto blood agar to facilitate their nutrient requirements. Replating of the stock cultures was executed on a bi-weekly basis and cultures were maintained at 4 °C.

2.3.4.4.2 Bioassay Procedure

The antibacterial and antifungal activities of compounds **72-76** were screened using a disc-diffusion protocol based on the guidelines from NCCLS document M2-A5[49]. Prior to performing the assay, overnight broth cultures (in tryptic soy broth for bacteria and fungal broth for yeast) of the organisms listed above were prepared. The cultures were then diluted to optically match a McFarland 1 standard, equivalent to

3×10^8 CFU/mL. These diluted cultures were thoroughly streaked across the surface of an appropriate agar medium (Sabouraud dextrose agar for *Candida albicans,* Blood agar for the *Streptococci,* Mueller-Hinton Agar for the remaining organisms). Sample discs were prepared by impregnating 100 µg of each compound, dissolved in a suitable solvent, onto sterile BBL 6 mm blank paper disks (Beckton, Dickonson and Co., Sparks, MD) and allowing the solvent to evaporate. These discs were placed on the surface of the inoculated media, along with solvent blanks (negative control) and pre-prepared discs containing the antibiotics Ciprofloxacin and Ceftriaxone (Beckton, Dickonson and Co., Sparks, MD; standards). All bacterial plates were incubated at 37 °C for 24-48 hours. The plates inoculated with *Candida albicans* were incubated at 30 °C for 24-48 hours. After this time, all plates were examined for zones of inhibition around the discs.

2.4 REFERENCES

1. Ahmad, A.; Misra, L. N. *Pharm. Biol.* **1997**, *35*, 121-125.

2. McKay, D. L.; Blumberg, J. B. *Phytother. Res.* **2006**, *20*, 519-530.

3. Ashnagar, A.; Naseri, N.L. Alavi, S. Y. *Asian J. Chem.* **2009**, *21*, 4981-4986.

4. Srivastava, J. K.; Gupta, S. *J. Agric. Food Chem.* **2007**, *55*, 9470-9478.

5. Jarrahi, M. *Nat. Prod. Res.* **2008**, *22*, 422-427.

6. Niederhofer, H. *Phytomedicine* **2009**, *16*, 284-286.

7. Ma, CM.; Winsor, L.; Danesthalab, M. *Phytochem. Anal.* **2007**, *18*, 42-49.

8. Ahmed, A. A.; Elela, M. A. A. *Phytochemistry* **1999**, *51*, 551-554.

9. Bar, B.; Schultze, W. *Planta Medica* **1996**, *62*, 332-335.

10. Kamatou, G. P. P.; Viljoen, A. M. *J. Am. Oil. Chem. Soc.* **2010**, *81*, 1-7.

11. Van Zyl, R. L.; Seatlholo, S. T.; Van Vuuren, S. F.; Viljoen, A. M. *J. Essent. Oil Res.* **2006**, *18*, 129-133.

12. Baylac, S.; Racine, P. *Int. J. Aromather.* **2003**, *13*, 138-142.

13. Rocha, N. F. M.; Venancio, E. T.; Moura, B. A.; Silva, M. I. G.; Neto, M. R. A.; Rios, E. R. V.; de Sousa, D. P.; Vasconcelos, S. M. M.; Fonteles, M. M. F.; de Sousa, F. C. F. *Fundam. Clin. Pharmacol.* **2010**, *24*, 63-71.

14. Ogata, I.; Lawanai, T.; Hashimoto, E.; Nishimura, Y.; Oyama, Y.; Seo, H. *Arch. Toxicol.* **2010**, *84*, 45-52.

15. Szoke, E.; Maday, E.; Tyihak, E.; Kuzovkina, I. N.; Lembaekovicks, E. *J. Chromatogr. B.* **2004**, *800*, 231-238.

16. Sashidhara, K. V.; Verma, R. S.; Ram, P. *Flavour Fragr. J.* **2006**, *21*, 274-276.

17. Tolouee, M.; Alinezhad, S.; Saberi, R.; Eslamifar, A.; Zad, S. J.; Jaimand, K.; Taeb, J.; Rezaee, MB. Kawachi, M. Shams-Ghahfarokhi, M.; Razzaghi-Abyaneh, M. *Int. J. Food Microbiol.* **2010**, *141*,127-133.

18. Svehlikova, V.; Repcak, M. *Biochem. System. Ecol.* **2006**, *34*, 654-657.

19. Anonymous *Altern. Med. Rev.* **2008**, *13*, 58-62.

20. Redaeli, C.; Formentini, L.; Santaniello, E. *Planta Medica* **1981**, *43*, 412-413.

21. Yamazaki, H.; Miyakado, M. *J. Nat. Prod.* **1982**, *45*, 508.

22. Zaiter, L.; Bouheroum, M.; Benayache, S.; Benayache, F.; Leon, F.; Brouard, I.; Quintana, J.; Estevez, F.; Bermejo, J. *Biochem. System. Ecol.* **2007**, *35*, 533-538.

23. Ata, A.; Andersh, B. J. In *The Alkaloids*; Cordell, G. Ed.; Elsevier Science: Amsterdam, 2008; Vol. 66, p. 191-213.

24. ur-Rahman, A; Choudhary, M. I. *Solving Problems With NMR Spectroscopy*; Academic Press: San Diego, CA, 1996.

25. Miski, M.; Ulubelen, A.; Johansson, C.; Mabry, T. J. *J. Nat. Prod.* **1983**, *46*, 874-875.

26. Hao, H.; Handong, S.; Shouxun, Z. *Phytochemistry*, **1996**, *42*, 1247-1248.

27. Takasaki, M.; Tokuda, H.; Nishino, H.; Konoshima, T. *J. Nat. Prod.* **1999**, *62*, 972-975.

28. Miyazawa, M.; Hisama, M. *Biosci. Biotechnol. Biochem.* **2003**, *67*, 2091-2099.

29. Sharifiar, F.; Dehghn-Nudeh, G.; Mirtajaldini, M. *Food Chem.* **2009**, *112*, 885-888.

30. Oyama, K.; Kondo, T. *Tetrahedron*, **2004**, *60*, 2025-2034.

31. Guvenalp, Z.; Ozbek, H.; Kuruuzum-Uz, A.; Kazaz, C.; Demirezer, L. O. *Turkish J. Chem.* **2009**, *33*, 667-675.

32. Svehlikova, V.; Bennett, R. N.; Mellon, F. A.; Needs, P. W.; Piacente, S. Kroon, P. A.; Bao, Y. *Phytochemistry*, **2004**, *65*, 2323-2332.

33. Rayyan, S.; Fossen, T.; Nateland, H. S. Anderson, O. M. *Phytochem. Anal.* **2005**, *16*, 334-341.

34. Chai, X. Y.; Song, Y. L.; Xu, Z. R.; Shi, H. M.; Bai, C. C.; Bi, D.; Wen, J.; Li, F. F.; Tu, P. F. *J. Nat. Prod.* **2008**, *71*, 814-819.

35. Dawa, Z.; Bai, Y.; Zhou, Y.; Gesang, S.; A, P.; Ding, L. *J. Nat. Med.* **2009**, *63*, 327-330.

36. Bayoumi, S. A. L.; Rowan, M. G.; Beeching, J. R.; Blagbrough, I. S. *Phytochemistry* **2010**, *71*, 598-604.

37. Cassady, J. M.; Ojima, N.; Chang, CJ.; McLaughlin, J. L. *J. Nat. Prod.* **1979**, *42*, 274-278.

38. Herisset, A.; Chaumont, J. P.; Paris, R. *Plants Medicinales et Phytotherapie* **1974**, *8*, 306-313.

39. Zhang, GP.; Xiao, ZY.; Rafique, J.; Arfan, M.; Smith, P. J.; Lategan, C. A.; Hu, LH. *J. Nat. Prod.* **2009**, *72*, 1265-1268.

40. Shaw, CY.; Chen, CH.; Hsu, CC.; Chen, CC.; Tsai, YC. *Phytother. Res.* **2003**, *17*, 823-825.

41. Laphookhieo, S.; Sripisut, T.; Prawat, U.; Karalai, C. *Heterocycles* **2009**, *78*, 2115-2119.

42. Yasuda, T.; Fukui, M.; Nakazawa, T.; Hoshikawa, A.; Ohsawa, K. *J. Nat. Prod.* **2006**, *69*, 755-757.

43. Kostova, I. *Planta Medica* **1992**, *58*, 484.

44. Garcez, F. R.; Garcez, W. S.; Martins, M.; Cruz, A. C.; *Planta Medica* **1999**, *65*, 775.

45. Udenigwe, C. C.; Ata, A.; Samarasekera, R. *Chem. Pharm. Bull.* **2007**, *55*, 442-445.

46. Habig, W. H.; Pabst, M. J.; Jakoby, W. B. *J. Biol. Chem.* **1974**, *249*, 7130-7139.

47. Blois, M. S. *Nature* **1958**, *181*, 1199-1200.

48. Kolodziej H.; Kayser O.; Kiderlen A. F.; Ito H.; Hatano T.; Yoshida T.; Foo L. Y. *Biol. Pharm. Bull.* **2001**, *24*, 1016-1021.

49. National Committee for Clinical Laboratory Standards *Performance Standards for Antimicrobial Disc Susceptibility Tests*, 5th ed; approved standard, NCCLS document M2-A5; NCCLS: Vilanova, Pensylvania, 1993.

CHAPTER 3

Biotransformation Studies on Oxymatrine and Harmine

3.1 INTRODUCTION

Like any other living organism, microorganisms utilize enzymatic reactions in all aspects of their metabolism. Many of these reactions are increasingly being utilized as a tool in organic synthesis by both industrial and academic chemists in a process known as biocatalysis, or more commonly, a biotransformation[1]. Utilizing either whole-cell cultures or purified enzyme preparations, synthetic chemists are able to regioselectively and mostly stereospecifically perform a wide range of reactions that are often difficult to achieve by traditional synthetic chemistry[1-6]. Examples of common bioorganic reactions include hydroxylations, epoxidations, oxidations, reductions, eliminations, and a wide variety of other reactions [1-7]. In addition to high selectivity, the use of biotransformations in organic chemistry has a number of other advantages. First of all, the reaction conditions are mild, normally utilizing temperatures in the range of 20 to 40 °C and pH values in the range of 5 to 8[1-6]. As a result, the risks of compound degradation are lessened.

Second of all, biotransformations are more environmentally friendly for several reasons: 1) they do not require large amounts of energy for heating; 2) they do not use toxic solvents (in the reaction phase), other organics, or heavy metals which are hazardous to human health, detrimental to the environment, and costly to dispose of. Instead, all residual materials from the biocatalytic reaction are non-hazardous and readily broken down in the environment; and 3) the selectivity of the reactions reduces or

altogether eliminates the need for protection and deprotection steps, thereby reducing the number harmful reagents needed for the transformation[1-6].

Third of all, biotransformations are highly economical. In addition to low energy requirements, only inexpensive, readily available materials such as sugars and amino acids are required in order to maintain the microbial cultures and to run the reactions.

Lastly, the biotransformation of a starting material will often result in the conversion of a less biologically-active molecule into a more biologically-active molecule. For instance, when the ferulic acid dimer 5,5'-dehydroi-(3-(4-hydroxy-3-ethoxyphenyl) acrylic acid (**78**) was incubated with a mixed culture of human intestinal microbiota, it was converted into the hydrogenated analogue 5,5'-dehydroi-(3-(4-hydroxy-3-ethoxyphenyl) propionic acid (**79**), which showed an 11-fold increase in the inhibition of human prostanoid production[8]. This is considered to be beneficial as high levels of prostanoids have been correlated with the recurrence of colorectal cancer[8]. Another example is the biotransformation of isoseviol (**80**) by *Absidia* p*seudocylindrospora* into compound **81**[9]. When assayed, this compound showed markedly greater luciferase agonistic activity than testosterone, thereby having potential as a new anti-inflammatory agent[9].

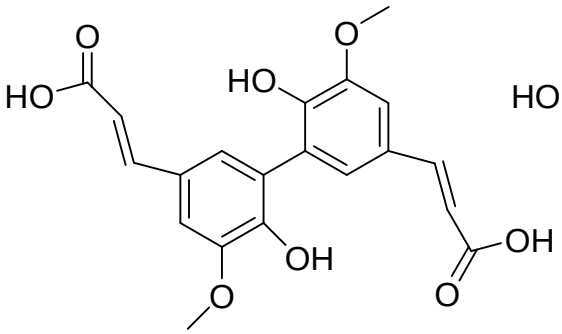

78

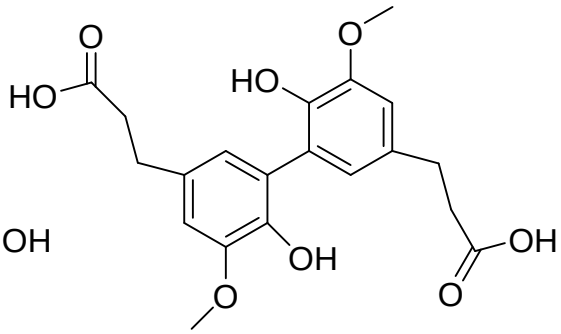

79

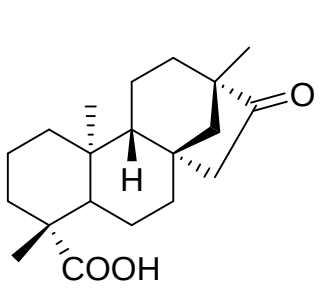

80

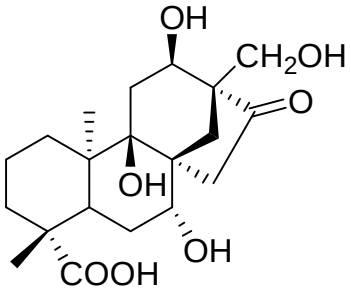

81

Although the use of microbial catalysis in synthetic organic chemistry does have many advantages, it also suffers from significant disadvantages: namely, low yields and the formation of side products[6]. Fortunately, there is much research underway to find ways to maximize the production of a compound of interest. Under the proper conditions, increases of 1000-fold in yield are possible[10].

In order to maximize the yield of a biotransformation, several steps may be taken. Screening for related higher-yielding species or strains, and developing greater-expressing mutants is an excellent way to increase yields. Additionally, optimization of growth conditions such as medium composition, temperature, pH, and aeration can have a significant effect on the yield. Adding limiting precursors that inhibit steps in biosynthesis after the desired metabolite is produced is another option. These steps can not only increase the yield of the desired metabolite, but also work to improve the process by eliminating side products.

3.1.1 The Role of Biotransformations in the Modeling of Drug Metabolism

Before a new pharmaceutical is approved for use for the treatment of a particular ailment, it undergoes extensive testing to ensure its safety and efficacy. Part of this testing process includes determining the metabolic fate of the compound. As discussed in

Chapter 1, when a foreign substance is ingested it is transformed (metabolized) by GST and other detoxification enzymes into something that is often more polar and more water soluble, thereby making it easier to excrete[11,12]. In addition, it is often the metabolized form of the drug that is the active constituent. For instance, metabolism of the cholesterol-lowering drug, Compactin (**82**) produces the active form of the drug, pravastatin (**83**)[12].

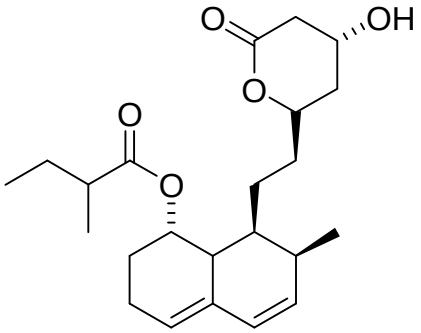

82

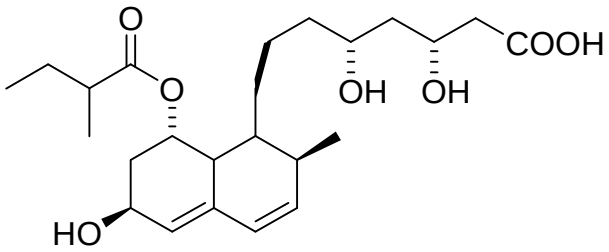

83

The reactions of greatest interest in drug metabolism include aromatic hydroxylations, N-dealkylations, O-dealkylations, N-oxidations, and S-oxidations [11,12]. The enzymes most often responsible for these reactions are the cytochrome P_{450} oxidases, which are found both in fungi and in mammals, predominantly in the liver but also in the kidneys, lungs, intestines, and other organs[11,12].

A general cytochrome P_{450} oxygenation mechanism is shown in Scheme 3.1. Briefly, the oxidized cytochrome P_{450} (Fe^{3+}) first complexes with a substrate, near the iron site of the heme protein[13]. This complex is rapidly reduced via cytochrome P_{450} reductase to produce the Fe^{2+} form[13]. Next, a molecular oxygen (O_2) / cytochrome / substrate complex is formed[13]. The iron atom is then oxidized back to its Fe^{3+} form by reducing the oxygen to an oxide[13]. Reduction by cytochrome P_{450} reductase reduces the P_{450} enzyme to its Fe^{2+} form again[13]. Finally, through a rearrangement the bond between

the molecular oxygen is cleaved, resulting in one oxygen being incorporated into the substrate while the other accepts two protons to become water, and cytochrome P_{450} is oxidized back to its Fe^{3+} form[13].

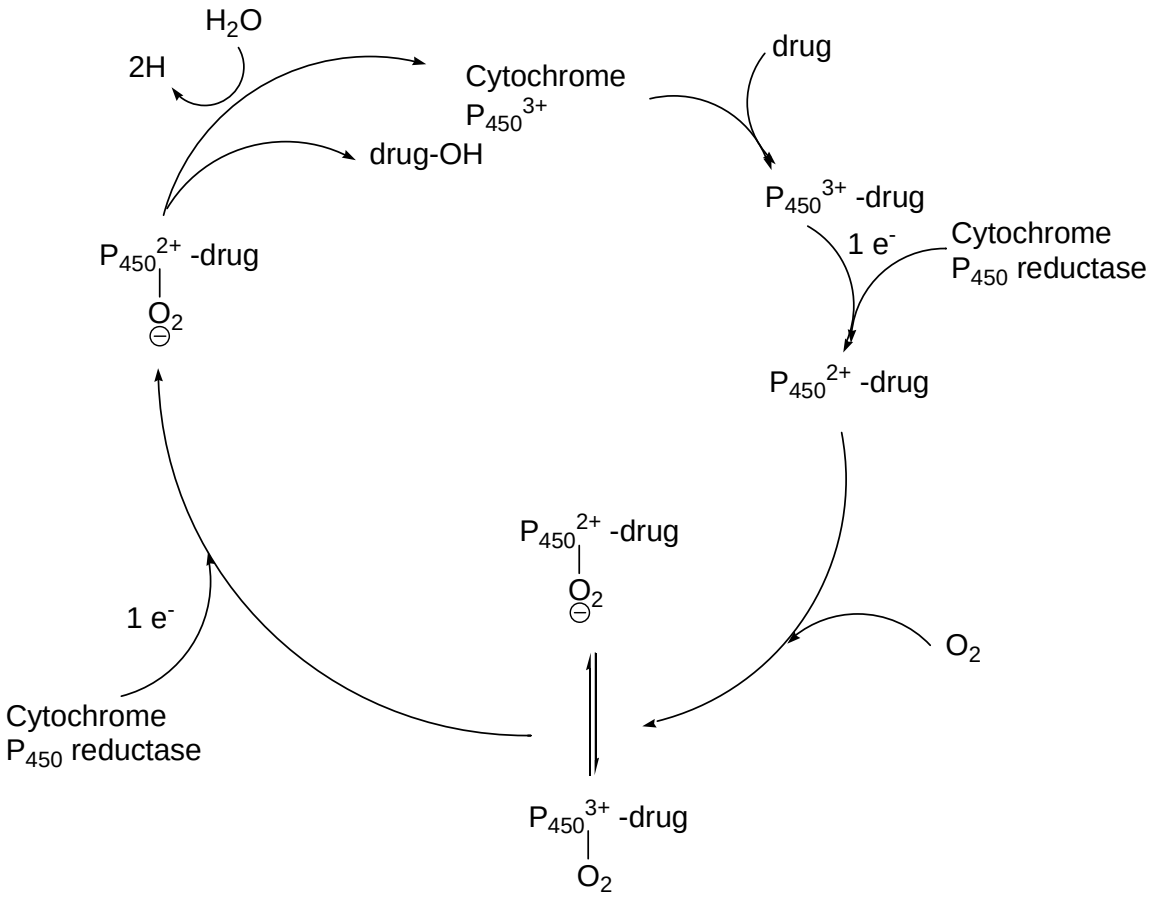

Scheme 3.1. General oxygenation mechanism of drugs by cytochrome P_{450}.

Upon transformation of the substance, the resulting metabolite may be either more or less toxic to the user, depending on the nature of the substance. It is therefore essential that the metabolic fates of the drug be known. Traditionally, such metabolic investigations involved the administration of the drug to a series of laboratory animals such as rats, dogs, rabbits, and guinea pigs, and collecting their body fluids and examining them for the presence and identification of metabolites[12]. These *in vivo*

studies, however, are plagued by several limitations such as the cost of animals, the ethical controversies about the use of animals in biomedical research, and the toxicity of drugs limiting the amount administered and therefore the quantities of metabolites isolated[12]. Even with the highly sensitive mass spectroscopic and NMR techniques available today the process is quite difficult.

This has lead to the use of microbial models in drug metabolism studies. As fungi are eukaryotes, they generally carry out many of the same enzymatic reactions as mammals and are therefore ideal for use in drug metabolism studies. In these studies, the drug of interest is incubated with the fungus and the resulting metabolites are isolated, identified, and assayed for toxicity. The use of fungi in drug metabolism studies has several advantages: being less expensive, having no ethical issues, and permitting the administration of compounds at a higher dose to permit the isolation of higher quantities of metabolites for toxicological study[12].

3.1.2 Matrine (84) and Oxymatrine (85)

Sophora flavescens is a small legumous plant found in China, Japan, and in some parts of Europe which is utilized extensively in ancient Chinese medicine[14]. Phytochemical studies have resulted in the isolation of a number of different compounds, including the two chief bioactive components, matrine (**84**) and oxymatrine (**85**)[15-17].

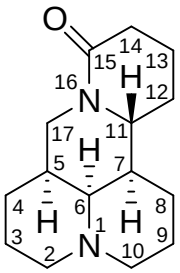

84

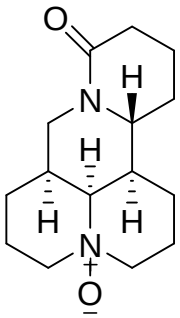

85

Recent biological studies on matrine (**84**) have demonstrated a wide variety of bioactivities, most notably anti-cancer activity. In one study, treatment of gastric carcinoma cells in vitro with matrine (**84**) resulted in the inhibition of cancer cell proliferation and induction of apoptosis[14]. In a related study, when matrine (**84**) was administered in conjunction with 5-fluorouracil, a synergistic effect in the suppression of gastric tumors was observed[18]. Moreover, it was also demonstrated that matrine (**84**) could induce apoptosis in cells deficient in p53, an important regulatory protein which is involved in controlling abnormal cell division and therefore preventing tumor formation[19].

In addition to having a direct effect on the growth of tumor cells, matrine (**84**) has also been shown to be effective in the treatment of cancer cachexia, a complex disorder which commonly occurs during the advanced stages of cancer and is characterized by progressive weight loss in association with anorexia, asthenia, anemia, and alterations in immune function[16]. It has been previously demonstrated that much of the pathology of cachexia results from the overproduction of the pro-inflammatory cytokines tumor necrosis factor α (TNF-α) and interleukin 6 (IL-6)[16]. When administered to mice, matrine (**84**) was able to attenuate the cachexia symptoms and decrease the serum levels of TNF-α and IL-6[16].

As well as possessing significant anti-cancer activities, matrine (**84**) has been shown to be useful in the treatment of other diseases and disorders, especially hepatic diseases. In several studies, the hepatoprotective effect of matrine (**84**) has been demonstrated. When one group of Chinese patients was given matrine (**84**), the incidences of liver cirrhosis and subsequent hepatocellular carcinoma were greatly reduced in comparison to a control group[20]. Furthermore, matrine (**84**) was found to reduce the rate of rejection in liver transplant patients, thereby increasing the survival rate[21]. When administered intramuscularly, matrine (**84**) was shown to be an effective treatment for viral chronic hepatitis B[22].

Lastly, along with the aforementioned bioactivities, matrine (**84**) has been shown to possess anti-inflammatory[23], anti-collagenase[24], and weak antifungal activities[25].

Oxymatrine (**85**) demonstrates many of the same bioactivities as matrine (**84**), such as anti-cancer activity; oxymatrine (**85**) has been shown to induce apoptosis[26,27] and inhibit cell proliferation[28] in a number of different cancer cell lines. Secondly, oxymatrine (**85**) has been utilized in the treatment of liver diseases including viral hepatitis B[29], and the reduction of hepatic fibrosis[30]. Moreover, oxymatrine (**85**) has also demonstrated other collagen regulatory activities, and has been utilized in the attenuation of pulmonary fibrosis[31]. Thirdly, oxymatrine (**85**) has also demonstrated weak antifungal activity[25].

Interestingly, part of the reason for oxymatrine (**85**) and matrine (**84**) possessing similar biological activities may be that under certain circumstances, oxymatrine (**85**) is actually a prodrug of matrine (**84**)[32-34]. When administered orally to mice, it was found that oxymatrine (**85**) was metabolized into matrine (**84**), and therefore, matrine (**84**) was the active molecule[32].

Even so, oxymatrine (**85**) does possess some of its own unique biological activities. First of all, oxymatrine (**85**) has been shown to possess weak MAOI inhibitory activities[35]. Secondly, oxymatrine (**85**) has shown significant potential in the treatment of gastrointestinal problems, specifically colitis and other gastrointestinal inflammatory disorders[36], as well as enteroviral infections[37]. In these studies, however, it is unknown whether matrine (**84**) or oxymatrine (**85**) was the active molecule responsible for the bioactivities. Lastly, oxymatrine (**85**) has been utilized in the treatment of contact dermatitis; the mode of action by which symptoms are relieved is believed to be the upregulation of the production of $CD4^+$ and $CD25^+$ T-cells[38].

3.1.3 Harmine (87) and Related *Harmala* Alkaloids

Peganum harmala is a small perennial which grows wild in the semi-arid regions of the Indo-Pakistan sub-continent, Iran, Africa, and in the Mediterranian Sea[39,40]. It has also been recently introduced and naturalized to Australia and the United States[39,40]. This plant has been used extensively in folk medicine to treat a number of ailments[39,40], but is better known, however, for the four major β-carboline alkaloids obtained from the seeds of the plant, harman (**86**), harmine (**87**), harmaline (**88**), and harmalol (**89**), which have often been used recreationally for their hallucinogenic effects[40,41].

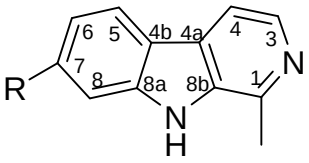

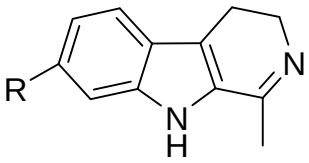

86: R = H
87: R = OMe

88: R = OMe
89: R = OH

Pharmacological study on these compounds, however, has revealed a number of interesting biological activities. Firstly, *harmala* alkaloids have demonstrated moderate to

good AChE inhibitory activities of less than 55 μM[42]. Furthermore, when administered to mouse brain mitochondria, both harmaline (**88**) and harmalol (**89**) exhibited a protective effect against dopamine-induced oxidative damage, exemplifying their anti-oxidant activities and their potential in the treatment of neurological disorders[43,44]. Additionally, these four alkaloids have been shown to be potent monoamine oxidase inhibitors, indicating their potential as antidepressants[40]. Secondly, these compounds have displayed weak to moderate antibacterial activities against a number of common Gram positive and Gram negative pathogens[39]. Thirdly, compounds **86**-**89** have shown to be useful in the treatment of cardiovascular problems including hypertension and arrhythmia[45]. The benefit of these compounds in the treatment of these cardiac disorders may be related to their ability to inhibit the activity of calcium channels[46]. Lastly, when administered to rabbit jejunum, these compounds caused a relaxation of spontaneous contractions within the muscle, thus demonstrating their spasmolytic activity[47].

Currently, there have been relatively few reports of microbial transformations of the four aforementioned compounds. Incubation of harmaline (**88**) and harmalol (**89**) with *Rhodotorula rubra* gave 2-acetyl-3-(2-acetamidoethyl)-7-methoxyindole (**90**) and 2-acetyl-3-(2-acetamidoethyl)-7-hydroxyindole (**91**), respectively[48]. Fermentation of harman (**86**) with *Cunninghamella echinulata*, resulted in the isolation of harman-6-hydroxide (**92**) and harman-N-oxide (**93**)[48].

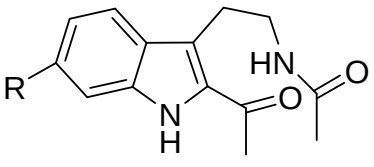

90: R = OCH_3
91: R = OH

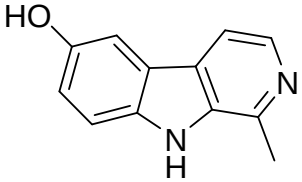

92

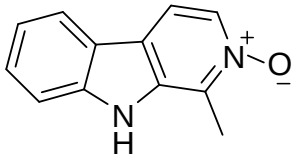

93

Given the medicinal potential of both the *Sophora* and *harmala* alkaloids, attempts were made to prepare new derivatives of some of these compounds by microbial transformation. These efforts will be described in the remainder of this chapter.

3.2 RESULTS AND DISCUSSION

3.2.1 Biotransformation of Matrine (84) and Oxymatrine (85)

In the screening experiment, matrine (**84**) and oxymatrine (**85**) were incubated in the liquid cultures of *Penicillum chrysogeneum* (ATCC 9480), *Cunninghamella blakesleena* (ATCC 9245 and 8688A), *Cunninghamella bainieri* (ATCC 9244), *Curvularia lunata* (ATCC 12017), and *Fusarium sp*. Only the biotransformation of oxymatrine was observed in the fermentation flasks of *P. chrysogeneum C. bainieri, C. lunata, Fusarium sp.,* and both strains of *C. blakesleena.* Analytical TLC of the microbial reaction mixtures indicated that **85** was metabolized into the same product in all fermentation experiments. The R_f values of the biotransformation product was similar to that of matrine (**84**). Based on the identical results it was decided to perform a scale-up experiment using *P. chrysogeneum* to permit characterization of the biotransformation product.

The crude product was first isolated by preparative TLC and then further purified by high performance liquid chromatography (HPLC) (see experimental). The retention time of the biotransformed product (~19 min; Figure A-31) was similar to that of matrine (**84**) (~19 min; Figure A-30) and that helped to characterize the biotransformed product as matrine (**84**).

For confirmation of the identity of the transformed product, ^{1}H- and ^{13}C-NMR spectra of this product were acquired. These spectral data were identical to those of matrine (**84**) [49]. Complete ^{1}H- and ^{13}C-NMR spectral data of **84** and **85** are given in Table 3.1.

The ^{1}H-NMR spectrum ($CDCl_3$, 400 MHz) of matrine (**84**) differed from oxymatrine (**85**) at several positions, most notably H_2-2, H-6, H_2-10, H-11, and H_2-17. In the ^{1}H-NMR spectrum of matrine (**84**), the C-2 and C-10 methylene protons resonated as mutiplets at δ 1.95 and 1.43, and at δ 2.82 and 1.97, respectively. In the ^{1}H-NMR spectrum of oxymatrine (**85**), these protons resonated at δ 3.15 and 3.09, and at δ 3.12 and 3.07, respectively. The C-17 methylene protons appeared as a triplet and double doublet at δ 3.02 (J = 12.8 Hz) and 4.36 (J = 4.5, 12.8 Hz), respectively, for matrine (**84**); while in oxymatrine (**85**) they appeared at δ 4.20 (J = 12.8 Hz) and 4.38 (J = 4.5, 12.8 Hz). In matrine, H-6 and H-11 resonated as multiplets at δ 2.09 and 3.79, respectively. In oxymatrine (**85**), these signals appeared at δ 3.06 and 5.11, respectively. The differences observed in these chemical shifts can be attributed to the presence of the *N*-oxide in oxymatrine (**85**). This oxyanion causes N-1 to be positively charged, thereby deshielding these protons through the electron-withdrawing effect of the positive charge. As a result, the resonances for these protons are all shifted downfield in oxymatrine (**85**), relative to matrine (**84**).

The differences between the ^{13}C-NMR spectra ($CDCl_3$, 100 MHz) of matrine (**84**) and oxymatrine (**85**) are even more diagnostic as the resonances corresponding to the carbons bonded to N-1 significantly differ between compounds **84** and **85**. In matrine (**84**), these carbons resonated at δ 57.3 (C-2), 63.7 (C-6), and 57.2 (C-10). In oxymatrine (**85**), these carbons resonated at δ 69.2 (C-2), 67.1 (C-6), and 69.5 (C-10). As in the proton spectrum, the downfield shift of these carbons in the ^{13}C-NMR spectrum of oxymatrine (**85**) can be attributed to the deshielding electron-withdrawing effect of the *N*-oxide.

Table 3.1. ^{1}H (400 MHz) and ^{13}C (100 MHz) NMR data for **84** and **85** ($CDCl_3$).

	84		**85**	
Position	δH (J in Hz)	δC (multiplicity)	δH (J in Hz)	δC (multiplicity)
1	-	-	-	-
2	α 2.79, m β 1.95, m	57.3 ($-CH_2-$)	α 3.15, m β 3.09, m	69.2 ($-CH_2-$)
3	α 1.43, m β 1.73, m	21.1 ($-CH_2-$)	α 2.75, m β 1.56, m	17.1 ($-CH_2-$)
4	α 1.68, m β 1.52, m	27.7 ($-CH_2-$)	α 1.79, m β 1.68, m	26.1 ($-CH_2-$)
5	1.71, m	35.3 (-CH-)	1.85, m	34.5 (-CH-)
6	2.09, m	63.7 (-CH-)	3.06,m	67.1 (-CH-)
7	1.45, m	43.2 (-CH-)	1.57, m	42.7 (-CH-)
8	α 1.90, m β 1.40, m	26.4 ($-CH_2-$)	α 2.04, m β 1.55, m	24.7 ($-CH_2-$)
9	α 1.64, m β 1.43, m	20.7 ($-CH_2-$)	α 2.67, m β 1.53, m	17.2 ($-CH_2-$)
10	α 2.82, m β 1.97, m	57.2 ($-CH_2-$)	α 3.12, m β 3.07, m	69.5 ($-CH_2-$)
11	3.79, m	53.2 (-CH-)	5.11, m	52.9 (-CH-)
12	α 2.09, m β 1.41, m	27.1 ($-CH_2-$)	α 2.19, m β 1.26, m	28.5 ($-CH_2-$)
13	α 1.60, m β 1.81, m	18.9 ($-CH_2-$)	α 1.66, m β 1.79, m	18.6 ($-CH_2-$)
14	α 2.41, m β 2.22, m	32.8 ($-CH_2-$)	α 2.24, m β 2.44, m	32.9 ($-CH_2-$)
15	-	169.4 (-C-)	-	170.1 (-C-)
16	-	-	-	-
17	α 3.02, t, (12.8) β 4.36, dd, (4.5, 12.8)	41.4 ($-CH_2-$)	α 4.20, t, (12.8) β 4.38, dd, (5.3, 12.8)	41.7 ($-CH_2-$)

3.2.1.1 Time Based Analysis of the Biotransformation of Oxymatrine (**85**).

Analytical TLC of the biotransformation of oxymatrine (**85**) indicated that oxymatrine (**85**) started to be metabolized into matrine (**84**) by *P. chrysogeneum* after 48 hours.

3.2.1.2 Importance of findings

The results presented above provide a new useful method for the production of matrine (**84**), a less bioavailable compound (0.02-0.09%), by biologically transforming oxymatrine (**85**), a more bioavailable compound (0.7-3.2%)[50]. Although the total synthesis of matrine (**84**) has been reported[51], and given that oxymatrine (**85**) will spontaneously convert into matrine (**84**) at temperatures greater than 206 °C[52], matrine (**84**) could also be produced industrially by heating oxymatrine (**85**), both alternatives are considerably more detrimental to the environment. The former utilizes large amounts of toxic reagents and the latter would require the input of large amounts of energy to permit heating to the high temperature required at an industrial scale. In contrast, for reasons described in the introduction, the biotransformation procedure is more environmentally favorable. Furthermore, from a regulatory standpoint, compounds produced by means of biofermentation are more accepted, generally undergoing less scrutiny by government agencies as those produced by other means.

3.2.2 Biotransformation of Harmine (87)

In a similar manner to the biotransformation of oxymatrine (**85**), harmine (**87**) was incubated in separate flasks on an analytical scale with the fungi mentioned in section 3.2.1 as well as *Mucor plumbeus* (ATCC 4740) and *Penicillum crustosum* (ATCC 90174) to screen for potential biotransformations. Analytical TLC of these fermentation mixtures showed that *M. plumbeus* may be capable of bioconverting harmine via the presence of a spot which had an R_f that was approximately 0.05 units higher. HPLC analysis of the crude extract provided further evidence of a possible transformation,

showing a small shoulder peak extending from the peak identified as harmine (~18-20 min; Figure A-38). To permit the characterization of the product, the transformation was carried out on a preparative scale and the product was isolated using a combination of prep. TLC and HPLC (see experimental). The product was then characterized using a combination of 1D- and 2D-NMR experiments, as well as ultraviolet spectroscopy and mass spectrometry.

The ^{1}H-NMR spectrum (DMSO-d_6, 400 MHz) of the product was similar to that of harmine (**87**) but showed downfield shifts of H-3 and H-4 compared to harmine (**87**). In harmine (**87**), H-3 and H-4 resonated at δ 7.79 and 8.15, respectively. In the biotransformation product, H-3 and H-4 resonated at δ 8.39 and 8.35, respectively. This could only be possible if N-2 was carrying a positive charge. As there were no additional proton resonances present in the ^{1}H-NMR spectrum of the product, this suggested that N-2 was bonded to an electronegative heteroatom.

The ^{13}C-NMR spectrum (DMSO-d_6, 100 MHz) of the product displayed resonances for all thirteen carbons as in the ^{13}C-NMR spectrum (DMSO-d_6, 100 MHz) of harmine (**87**). As in the proton spectrum, many of the carbon resonances were shifted somewhat downfield. Again, given the absence of any additional carbons and the shift in the carbon resonances, the presence of an oxygen atom bonded to N-2 was further supported.

In the chemical ionization mass spectrum, peaks at *m/z* 211 and 212 were observed. It has been reported in the literature[53] that these peaks are characteristic of harmine-*N*-oxide (**94**), corresponding to [M-17] and [M-16], respectively. The molecular ion peak was not observed in this instance but this is common in N-oxides[53]. Further

evidence for the structure of the product being **94** came from the UV spectrum, which showed maxima at 210, 246, and 324 nm. These values were also consistent with an *N*-oxide[53].

Chemical shift assignments, which are shown in Table 3.2 were made by comparison to the literature[53] as well as extensive use of the HMBC and HSQC spectra. Key HMBC correlations are shown in Figure 3.1. Notable HMBC correlations include the methyl protons (δ 2.98) coupling with C-1 (δ 137.5) and C-8b (δ 133.8); H-4 (δ 8.46) coupling with C-4a (δ 131.9), C-4b (δ 113.8), and C-8b; H-5 (δ 8.35) coupling with C-7 (δ 162.6) and C-8a (δ 145.2); H-8 (δ 7.14) coupling with C-8a and C-7; and the methoxy protons (δ 3.95) coupling with C-7.

From the above NMR, UV, and mass spectroscopic data the harmine biotransformation product was identified as harmine-*N*-oxide (**94**). This compound has been previously isolated from *Banisteropsis caapi*[53] and a similar biotransformation has previously been performed by Ibrahim[54], who reported the *N*-oxidation of harmine (**87**) by *Cunninghamella elegans.*

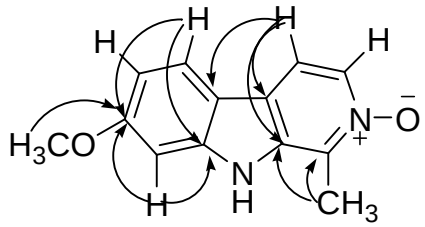

Figure 3.1. Important HMBC interactions in **94**.

Table 3.2. ^{1}H (400 MHz) and ^{13}C (100 MHz) NMR data for **94** and $^{1}H/^{13}C$ one-bond shift correlations as determined by HSQC (DMSO-d_6).

Position	δH (J in Hz)	δC
1[b]	-	137.5
3[c]	8.39, d, (6.3)	113.9
4[c]	8.46, d, (6.3)	129.3
4a[d]	-	131.9
4b[d]	-	113.8
5	8.35, d, (8.9)	124.5
6	7.06, dd, (2.3, 8.9)	112.3
7	-	162.6
8	7.14, d, (2.2)	94.4
8a	-	145.2
8b[b]	-	133.8
Me	2.98, s	16.1
OMe	3.95, s	55.7

[a]Multiplicity was determined with the help of the HSQC spectrum.
[b]The chemical shift assignments for these positions may be interchangeable
[c]The chemical shift assignments for these positions may be interchangeable
[d]The chemical shift assignments for these positions may be interchangeable

3.2.2.1 Acetylcholinesterase Inhibitory Assay

As mentioned in section 3.1.3, *harmala* alkaloids have shown good AChE inhibitory activity[42]. In an effort to study the structure-activity relationship, compounds **87** and **94** were evaluated for AChE inhibitory activity. While both compounds displayed good activity, compound **94**, with an IC_{50} value of 40.3 µM, was unfortunately less active than harmine (**87**; IC_{50} = 34.6 µM). This may perhaps indicate N-2 is an important pharmacophore which contributes to the AChE inhibitory activity of the *harmala* alkaloids. Further study is required to verify this hypothesis and identify other pharmacophores within the *harmala* alkaloids.

3.3 EXPERIMENTAL

3.3.1 General

The general experimental procedures of chromatography and spectroscopy utilized in this experimental work were the same as discussed in Chapter 2.

3.3.2 Microorganisms

Mucor plumbeus (ATCC 4740), *Cunninghamella bainieri* (ATCC 9244), *Cunninghamella blakesleena* (ATCC 9245 and 8688A), *Curvularia lunata* (ATCC 12017), *Penicillum chrysogeneum* (ATCC 9480), and *Penicillum crustosum* (ATCC 90174) were purchased from ATCC. *Fusarium sp.* was provided by the Department of Biology, the University of Winnipeg. All organisms were maintained on Potato Dextrose Agar and stored in a refrigerator at 4°C.

3.3.3 Preparation of Media

The soy broth medium was prepared by mixing dextrose (20 g), yeast extract (5 g), sodium chloride (5 g), potassium hydrogen phosphate (5 g), and soy flour (5 g) in 1 L of double distilled water. The pH was adjusted to 7.0 prior to autoclaving.

3.3.4 General Incubation Experiment

Six fungi, *Cunninhamella bainieri* (ATCC 9244), *Cunninghamella blakesleena* (ATCC 9245 and 8688A), *Curvularia lunata* (12017), *Penicillum chrysogeneum* (ATCC 9480), and *Fusarium sp*. were screened for their capability to metabolize matrine (**84**; Indofine Chemical Co., Hillsborough, NJ) and oxymatrine (**85**; Indofine Chemical Co.,

Hillsborough, NJ) at an analytical scale. In addition to these fungi, *Mucor plumbeus* (ATCC 4740) and *Penicillum crustosum* (ATCC 90174) were screened for their capability to metabolize harmine (**87**; Indofine Chemical Co., Hillsborough, NJ) at an analytical scale. During these analytical experiments it was discovered that the biotransformation of oxymatrine (**85**) into matrine (**84**) could be accomplished using *C. bainieri* (ATCC 9244), *C. blakesleena* (ATCC 9245 and 8688A), *C. lunata* (ATCC 12017), *P. chrysogeneum* (ATCC 9480), and *Fusarium sp*. as a biocatalyst. It was also discovered that the biotransformation of harmine (**87**) into harmine-N-oxide (**94**) could be accomplished using *M. plumbeus* as a biocatalyst. To permit further study, preparative scale biotransformation experiments were carried out. Both analytical and preparative fermentation experiments were conducted using standard two-stage fermentation experiments. For the preparation of the stage I liquid culture, thirteen 250 mL flasks (each containing 100 mL of liquid culture media) were inoculated with microorganisms to be screened and incubated at 30 °C on a shaker rotating at 150 RPM for 48 hours. Stage II cultures were prepared by adding either oxymatrine (**85**; 65 mg), matrine (**84**; 65 mg), or harmine (**87**; 65 mg) to the flasks containing the different micoorganisms as a solution in methanol (compounds **84** and **85**)/dimethylformamide (compound **87**) to effect a final substrate concentration of 0.05 mg/mL. These fermentation experiments were also monitored by including two controls, a “culture control” and a “substrate control” to eliminate the possibility that the culture media has affected any chemical transformations on the substrates. The culture control contained only fermentation blanks in which the microorganisms were grown under identical conditions but without substrates, while the substrate control consisted of substrate in sterile liquid media. All of

these flasks were returned to the shaker and incubated for an additional 14 days. After this time, these culture media were extracted with chloroform/ethyl acetate and the crude extracts were concentrated under reduced pressure. The products of these microbial reactions were isolated and analyzed as described below.

3.3.5 Isolation and Analysis of the Biotransformation Products

*3.3.5.1 Matrine (**84**)*

The crude extracts of the oxymatrine biotransformation reactions were analyzed by TLC using ethyl acetate:methanol:diethylamine (40:60:0.05). Dragendorf's spray reagent was utilized in this analysis to aid in the visualization of the starting materials and any biotransformed products.

The crude chloroform extract obtained from the liquid culture of *P. chrysogeneum* (771 mg) was subjected to prep. TLC using ethyl acetate-methanol-diethylamine (90.5:4.8:4.8) to isolate the impure product (13 mg). Compound **84** (5 mg) was obtained by injecting the crude product dissolved in methanol onto an Agillent 4 µm Zorbax C_{18} HPLC column (4.6 x 250 mm) and eluting isocratically with methanol:water:diethylamine (45:55:0.07) at a flow rate of 0.8 mL/min. The peak which eluted at approximately 19 minutes (Figure A-31) was collected. This HPLC purification was carried out on a Waters HPLC system equipped with a binary pump (Waters 1525) and a photodiode array (PDA) detector (Waters 2996). The effluent was monitored at 220 nm and the wavelength of maximum absorption.

Matrine (**84**); white amorphous solid, 5 mg; UV (MeOH): λ_{max} 205 nm; IR (CCl_4): ν_{max} 2933, 1619 cm^{-1}; ^{1}H-NMR ($CDCl_3$, 400 MHz) = see Table 3.1; ^{13}C-NMR ($CDCl_3$, 100 MHz) = see Table 3.1

*3.3.5.2 Harmine-N-oxide (**94**)*

The crude extracts from the Harmine biotransformation procedure were analyzed by TLC using chloroform:acetone:diethylamine (5:4:1). The starting material and product band were visualized on the TLC plate under UV light (254 nm) and with the aid of Dragendorf's spray reagent. The subsequent HPLC analysis was performed (with the same column and instrument as before) using a mixture of acetonitrile (eluent A) and 0.01 M phosphate buffer, pH 6.5 (eluent B) at a constant flow rate of 1 mL/min. After column equilibration with a mixture of 10% A (v/v) and 90% B (v/v), a linear gradient was programmed to 75% A (v/v) over 23.5 min and maintained for an additional 9 minutes. The effluent was monitored at 254 nm, 304 nm, and the wavelength of maximum absorption.

The crude ethyl acetate extract obtained from the liquid culture of *M. Plumbeus* (400 mg) was subjected to prep. TLC using ethyl acetate:acetone:diethylamine (5:4:1) to isolate the impure product (43 mg). Part of this (4 mg) was dissolved in approximately 5 mL of ethanol and injected over multiple runs onto the HPLC, eluting with a gradient mixture of acetonitrile (eluent A) and 0.1% trifluoroacetic acid (v/v) (eluent B) at a flow rate of 1 mL/min. After equilibrating the column with eluent A, a linear gradient was programmed to 70% A over 15 min. The peak which eluted at approximately 5.5 to 7.5

minutes (see Figure A-39) was collected in two portions, separated by the boundary of the shoulder peak, to obtain compound **94** (3 mg).

Harmine-N-oxide (**94**) pale yellow amorphous solid, 3 mg; UV λ_{max} (MeOH) = 210, 246, and 324 nm; PCI-MS = *m/z* 212, 211, 197, 170, 169; ^{1}H- NMR (DMSO-d_6, 400 MHz) = see Table 3.2; ^{13}C-NMR (DMSO-d_6, 100 MHz) = see Table 3.2.

3.3.6 Time-Based Measurement of the Bioconversion of Oxymatrine (85)

Using a similar two-stage protocol as to that given in 3.3.4, 10 mg of oxymatrine (**85**) was incubated in a 500 mL flask containing 200 mL of liquid culture medium inoculated with a 48 h culture of *P. chrysogeneum.* At 24 h intervals 3 mL samples were removed from the flask and extracted with chloroform. The crude extracts were concentrated under a stream of nitrogen and analyzed by TLC as described in section 3.3.5.1.

3.3.7 Acetylcholinesterase Inhibitory Assay

3.3.7.1 Reagents

Electric eel acetylcholinesterase and the other reagents used in the acetylcholinesterase inhibitory assay, except the 5-5'-dithiobis(2-nitrobenzoic acid) (DTNB), were purchased from Sigma-Aldrich. The DTNB was purchased from EMD.

3.3.7.2 Bioassay Procedure

The acetylcholinesterase inhibitory activity was measured by following Ellman's methodology[55] with slight modifications. In order to evaluate the inhibitory activity of compounds **87** and **94**, the assay was carried out at room temperature in 0.1 M, pH 8 sodium phosphate buffer. In a typical assay, 176 µL buffer, 2 µL enzyme (with an initial effective assay activity of 0.25 U/mL), and 2 µL of the test compound solution (prepared in ethanol) were mixed and incubated for 30 minutes. The reaction was then initiated by the addition of 10 µL of 0.01 M DTNB (prepared in 0.1 M pH 7 sodium phosphate buffer) and 10 µL of 0.075 M acetylthiocholine iodide. Hydrolysis of acetylthiocholine was monitored by the formation of the yellow 5-thio-2-nitrobenzoate anion as a result of the reaction of DTNB with thiocholine, released by the enzymatic hydrolysis of acetylthiocholine, at a wavelength of 406 nm. The assay was carried out in triplicate in a 96-well microplate reader (KC-4 Biokinetic reader, Bio-TEK instrumentation, USA). The percentage of inhibition was calculated using the formula:

$[(E-S)/E] \times 100$

where E is the activity of the enzyme without test compound and S is the activity of the enzyme with test compound. The IC_{50} values were calculated by plotting a concentration response curve.

3.4 REFERENCES

1. Loughlin, W. A. *Bioresour. Technol.* **2000**, *74*, 49-62.

2. Borges, K. B.; Borges, W. de S.; Duran-Patron, R.; Pupo, M. T.; Bonato, P. S.; Collado, I. G. *Tetrahedoron Asymmetry* **2009**, *20*, 385-397.

3. Grogan, G. *Annu. Rep. Prog. Chem., Sect. B* **2009,** *10*5, 206-231.

4. Holland, H. L. *Curr. Opin. Chem. Bio.* **1998**, *2*, 77-84.

5. Simeo, Y.; Sinisterra, J. V. *Mini Rev. Org. Chem.* **2009**, *6*,128-134.

6. Grogan, G. *Practical Biotransformations: A Beginner's Guide*; Wiley: Chichester, United Kingdom, 2009.

7. Venisetty, R. K.; Ciddi, V. *Curr. Pharm. Biotechnol.* **2003**, *4*, 153-167.

8. Russell, W. R.; Scobbie, L.; Chesson, A.; Richardson, A. J.; Stewart, C. S.; Drew, J. E.; Duthie, G. G. *Nutr. Cancer* **2008**, *60*, 636-642.

9. Chang, S.; Yang, L.; Lo, C.; Liaw, J.; Wang, L.; Lin, S *J. Nat. Prod.* **2008**, *71*, 87-92.

10. Demain, A. L. *J. Ind. Microbiol. Biotechnol.* **2006**, *33*, 486-495.

11. Asha, S.; Vidyavathi, M. *Biotechnol Adv.* **2009**, *27*, 16-29.

12. Azerad, R. *Adv. Biochem. Eng. Biotechnol*. **1999**, *63*, 169-218.

13. Frey, P. A.; Hegman, A. D. *Enzymatic Reaction Mechanisms*; Oxford University Press: New York, 2007.

14. Dai, Z.J.; Gao, J.; Ji, Z.Z.; Wang, X.J.; Ren, H.T.; Liu, X.X.; Wu, W.Y.; Kang, H.F.; Guan, H.T. *J. Ethnopharmacol.* **2009**, *123*, 91–96.

15. Shirataki, Y.; Motohashi, N. *Top. Heterocycl. Chem.* **2009**, *16*, 41-91.

16. Zhang, Y.; Wang, S.; Li, Y.; Xiao, Z.; Hu, Z.; Zhang, J. *Int. Immunoharmacol.* **2008**, *8*, 1767-1722.

17. Bohlmann, F.; Rahtz, D.; Arndt, C. *Chemische Berichte* **1958**, *9*1, 2189-93.

18. Hu, M. J.; Wu, Y. L.; Zhang, Y. P.; Zhang, S.; Qiao, M. M.; Fu, H. *Chinese. J. Dig. Dis.* **2005**, *6*, 68-71.

19. Jiang, H.; Hou, C.H.; Zhang, S.B.; Xie, H.Y.; Zhou, W.Y.; Jin, Q.H.; Cheng, X.D.; Qian, R.L.; Zhang, X.J. *Eur. J. Pharmacol.* **2007**, *559*, 98-108.

20. Xu-ying, W.; Ming, L.; Xiao-dong, L.; Ping, H. *Chem. Bio. Interact.* **2009**, *18*1, 15-19.

21. Xu, X.; Ling, Q.; Gao, F.; He, Z.L.; Xie, H.Y.; Zheng S.S. *Am. J. Chin. Med.*. **2009**, *37*, 27-34.

22. Long, Y.; Lin, X.T.; Zeng, K.L.; Zhang, L. *Hepatobilliary Pancreatic Dis. Int*. **2004**, *3*, 69-72.

23. Suo, Z.; Liu, Y.; Ferreri, M.; Zhang, T.; Liu, Z.; Mu, X.; Han, B. *J. Ethnopharmacol.* **2009,** *125*, 404–409.

24. Jung, E.; Lee, J.; Huh, S.; Lee, J.; Hwang, H.; Kim, Y.; Kim, Y.W.; Byun, S.Y.; Park,*D. BioFactors.* **2008**, *33*, 121–128.

25. Yang, X.; Zhao, B. *J. Forest. Res.* **2006**, *17*, 323-325.

26. Jin, Y.; Hu, J.; Wang, Q.; Li, Z. Chen, Y. *J. Huazhong Univ. Sci. Technol.[Med. Sci.]* **2008**, *28*, 314-316.

27. Ho, J. W.; Hon, P. L. N.; Chim, W. O. *Anti Cancer Agent. Med Chem.* **2009**, *9*, 823-826.

28. Song, G.; Luo, Q.; Qin, J.; Wang, L.; Shi. Y.; Sun, C. *Colloids Surf. B* **2006**, *48*, 1-5.

29. Lin, M.; Yang, L.; Peng, Y. P.; Zheng, J. K. *J. Int. Med. Res.* **2009**, *37*, 1411-1419.

30. Shi, G.; Li, Q. *World J. Gastroenterol.* **2005**, *1*1, 268-271.

31. Chen, X.; Sun, R.; Hu, J.; Mo, Z. Yang, Z.; Liao, D.; Zhong, N. *Basic Clin. Pharmacol. Toxicol.* **2008**, *103*, 278-286.

32. Xie, M.; Zhou, W.; Zhang, Y. *Chin. Med. J.* **1983**, *96*, 145-150.

33. Wang, S.; Wang, G.; Li, X.; Sun, J.; Ma, R.; Sheng, L. *J. Chomatogr. B* **2005**, *817*, 319-325.

34. Wu, X.L.; Hang, T.J.; Shen, J.P.; Zhang, Y.D. *J. Pharm. Biomed. Ana.* **2006**, *4*, 918-924.

35. Hwang, J.S.; Lee, S.A.; Hong, S.S.; Lee, K.S.; Lee, M.K.; Hwang, B.Y.; Ro, J.S. *Arch Pharm Res.* **2005**, *28*,190-194.

36. Fan, H.; Chen, R.; Shen, L.; Lv, J.; Xiong, P.; Shou, Z. Zhuang, X. *J. Huazhong Univ. Sci. Technol.[Med. Sci.]* **2008**, *28*, 415-420.

37. Chia; John, K. S. US patent 20100022575, 2010.

38. Li, J.; Wu, B.; Xie, H.; Zhang, J.; Yi, M.; Li, J. *Xiandai Yixue Zazhi* **2008**, *18*, 993-999.

39. Ahmad, A.; Khan, K. A.; Sultana, S. Siddiqui, B. S.; Begum, S.; Faizi, S.; Siddiqui, S. *J. Ethnopharmacol.* **1992**, *35*, 289-294.

40. Herraiz, T.; Gonzalez, D.; Ancin-Azpilicueta, C.; Aan, V. J.; Guillen, H. *Food. Chem. Toxicol.* **2010**, *48*, 839-845.

41. McKenna, D. J.; Towers, G. H. N. *Phytochemistry* **1981**, *20*, 1001-1004.

42. Agbaji, A. S.; Gerassimidis, K.; Hider, R. C. *Comp. Biochem. Physiol.* **1984**, *78C*, 211-216.

43. Lee, C. S.; Han, E. S.; Jang, Y. Y.; Han, J. H.; Ha, H. W.; Kim, D. E. *J. Neurochem.* **2000**, *75*, 521-531.

44. Moura, D. J.; Richter, M. F.; Boeira, J. M.; Henriques, J. A. P.; Saffi, J. *Mutagenesis* **2007**, *22*, 293-302.

45. Aarons, D. H.; Rossi, V.; Orzechowski, R. F. *J. Pharm. Sci.* **1977**, *66*, 1244-1248.

46. Karaki, H.; Kishimoto, T.; Ozaki, H.; Sakata, K.; Umeno, H.; Urakawa, N. *Br. J. Pharmac.* **1986**, *89*, 367-375.

47. Begum, S.; Hassan, S. I.; Siddiqui, B. S.; Ifzal, R.; Perwaiz, S.; Kiran, T.; Shaheen, F.; Ghayur, M. N.; Gilani, A. H. *Nat. Prod. Res.* **2006**, *20*, 213-227.

48. Herath, W.; Mikell, J. R.; Ferreira, D.; Kahn, I. A. *Chem. Pharm. Bul.* **2003**, *51*, 646-648.

49. Bai, G.Y.; Wang, D.Q.; Yei, C.H.; Liu, M.L. *Appl. Mag. Reson.* **2002**, *23*, 113-121.

50. Chen, X.; Yi, C.; Yang, X.; Wang, X. *J. Chromatogr. B* **2004**, *812*, 149-163.

51. Mandell, L.; Singh, K. P., Gresham, J. T.; Freeman, W. J. *J. Am. Chem. Soc*. **1965**, *87*, 5234-5236.

52. Chen, N.; Han, Z.; Luan, L. Wu, Y. *Chromatographia* **2009**, *70*, 299-303.

53. Hashimoto, Y.; Kawanshi, K. *Phytochemistry* **1975**, *14*, 1633-1635.

54. Ibrahim, A. S. *Bull. Fac. Pharm (Cairo Univ.)* **2006**, *44*, 355-359.

55. Ellman, G. L.; Courtney, K. D.; Andres, V. Jr.; Featherstone, R. M. *Biochem. Pharmacol.* **1961**, *7*, 88-95.

CONCLUSIONS

In summary, phytochemical studies on the crude methanolic extract of *M. chamomilla* resulted in the isolation of matriisobenzofuran (**72**), apigenin (**73**), apigenin-7-*O*-β-glucopyranoside (**74**), scopoletin (**75**), and fraxidin (**76**). The structures of these compounds were determined using spectroscopic methods. Matriisobenzofuran (**72**) was identified as a new natural product. Compounds **72-76** showed different levels of anti-GST properties. Compound **72** was found to be the most potent compared to the rest of the isolates. The bioactivity data of **72** indicated that the IC_{50} value of this compound was close to ethacrynic acid (**48**), a standard GST inhibitor. A careful examination of structures **72-76** revealed that all of these compounds contained an α, β-unsaturated carbonyl functionality in their structures. The GST inhibitory activities of these compounds might have resulted from this common functional group as it would allow these compounds to readily form adducts with glutathione via Michael reactions. Further structure-activity relationship studies on these compounds are warranted in order to confirm this hypothesis and to determine the active pharmacophore required for GST inhibition. These compounds were also evaluated for antioxidant activity and displayed moderate to good free radical scavenging activity. Additionally, compounds **72-76** were screened for anti-leishmanial activity. Compounds **75** and **76** were significantly active in this assay while the remaining compounds were weakly active. Further, compounds **72-76** were not found to be active in the antibacterial and antifungal assays.

In the biotransformation experiments it was identified that the fungi, *Penicillum chrysogeneum* (ATCC 9480), *Cunninghamella bainieri* (ATCC 9244), *Cunninghamella blakesleena* (ATCC 9245 and 8688A), *Curvularia lunata* (ATCC 12017), and

Fusarium sp. were capable of converting oxymatrine (**85**) to matrine (**84**). Additionally, these studies aided in identifying the fungus, *Mucor plumbeus* (ATCC 4740), as being capable of transforming harmine (**87**) into harmine-*N*-oxide (**94**).

A**PPENDIX: SPECTRAL AND CHROMATOGRAPHIC DATA**

Figure A-1. ^{1}H-NMR spectrum of matriisobenzofuran (**72**) in $CDCl_3$.

Figure A-2. ^{13}C-NMR spectrum of matriisobenzofuran (**72**) in $CDCl_3$.

Figure A-3. DEPT spectrum of matriisobenzofuran (**72**) in $CDCl_3$.

Figure A-4. COSY spectrum of matriisobenzofuran (**72**) in $CDCl_3$.

Figure A-5. HSQC spectrum of matriisobenzofuran (**72**) in $CDCl_3$.

Figure A-6. HMBC spectrum of matriisobenzofuran (**72**) in $CDCl_3$.

Figure A-7. ^{1}H-NMR spectrum of apigenin (**73**) in acetone-d_6.

Figure A-8. ^{13}C-NMR spectrum of apigenin (**73**) in acetone-d_6.

Figure A-9. COSY spectrum of apigenin (**73**) in acetone-d_6.

Figure A-10. HSQC spectrum of apigenin (**73**) in acetone-d_6.

Figure A-11. HMBC spectrum of apigenin (**73**) in acetone-d_6.

Figure A-12. ^{1}H-NMR spectrum of apigenin-7-*O*-β-glucopyranoside (**74**) in DMSO-d_6

Figure A-13. ^{13}C-NMR spectrum of apigenin-7-*O*-β-glucopyranoside (**74**) in DMSO-d_6.

Figure A-14. DEPT spectrum of apigenin-7-*O*-β-glucopyranoside (**74**) in DMSO-d_6.

Figure A-15. COSY spectrum of apigenin-7-*O*-β-glucopyranoside (**74**) in DMSO-d_6

Figure A-16. HSQC spectrum of apigenin-7-*O*-β-glucopyranoside (**74**) in DMSO-d_6

Figure A-17. HMBC spectrum of apigenin-7-*O*-β-glucopyranoside (**74**) in DMSO-d_6.

Figure A-18. ROESY spectrum of apigenin-7-*O*-β-glucopyranoside (**74**) in DMSO-d_6.

Figure A-19. ^{1}H-NMR spectrum of scopoletin (**75**) in $CDCl_3$.

Figure A-20. ^{13}C-NMR spectrum of scopoletin (**75**) in $CDCl_3$.

Figure A-21. COSY spectrum of scopoletin (**75**) in $CDCl_3$.

Figure A-22. HSQC spectrum of scopoletin (**75**) in $CDCl_3$.

Figure A-23. HMBC spectrum of scopoletin (**75**) in $CDCl_3$.

Figure A-24. ROESY spectrum of scopoletin (**75**) in $CDCl_3$.

Figure A-25. ^{1}H-NMR spectrum of fraxidin (**76**) in $CDCl_3$.

Figure A-26. ^{13}C-NMR spectrum of fraxidin (**76**) in $CDCl_3$.

Figure A-27. HSQC spectrum of fraxidin (**76**) in $CDCl_3$.

Figure A-28. HMBC spectrum of fraxidin (**76**) in $CDCl_3$.

Figure A-29. NOESY spectrum of fraxidin (**76**) in $CDCl_3$.

Figure A-30: HPLC chromatogram of matrine (**84**) (~19 min) and oxymatrine (**85**) (~3.5 min) standards.

Figure A-31: HPLC chromatogram of the semi-pure oxymatrine biotransformation product after prep TLC.

Figure A-32. ^{1}H-NMR spectrum of matrine (**84**) in $CDCl_3$.

Figure A-33. ^{13}C-NMR spectrum of matrine (**84**) in $CDCl_3$.

Figure A-34. ^{1}H-NMR spectrum of oxymatrine (**85**) in $CDCl_3$.

Figure A-35. ^{13}C-NMR spectrum of oxymatrine (**85**) in $CDCl_3$.

Figure A-36. ^{1}H-NMR spectrum of the oxymatrine biotransformation product in $CDCl_3$.

Figure A-37. ^{13}C-NMR spectrum of the oxymatrine biotransformation product in $CDCl_3$.

Figure A-38. HPLC chromatogram of the harmine (**87**) biotransformation crude ethyl acetate extract.

Figure A-39. Sample HPLC chromatogram from the isolation of **94**.

Figure A-40. ^{1}H-NMR spectrum of harmine (**87**) in DMSO-d_6.

Figure A-41. Expanded ^{1}H-NMR spectrum of harmine (**87**) in DMSO-d_6 showing the aromatic region.

Figure A-42. ^{13}C-NMR spectrum of harmine (**87**) in DMSO-d_6.

Figure A-43. ^{1}H-NMR spectrum of harmine-N-oxide (**94**) in DMSO-d_6.

Figure A-44. Expanded ^{1}H-NMR spectrum of harmine-*N*-oxide (**94**) in DMSO-d_6 showing the aromatic region.

Figure A-45. ^{13}C-NMR spectrum of harmine-N-oxide (**94**) in DMSO-d_6.

Figure A-46. HSQC spectrum of harmine-N-oxide (**94**) in DMSO-d_6.

Figure A-47. HMBC spectrum of harmine-N-oxide (**94**) in DMSO-d_6.

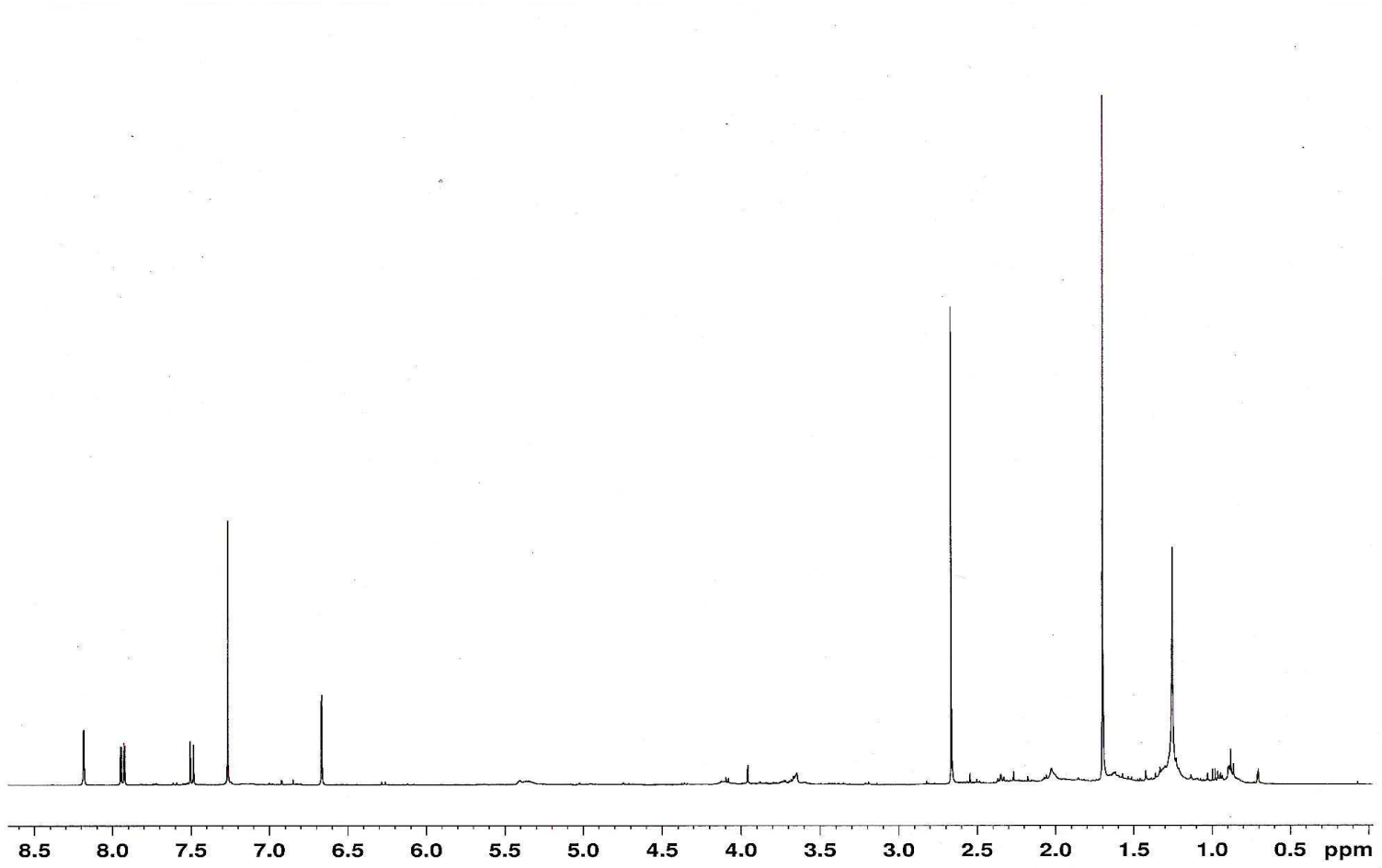

Figure A-1. ^{1}H-NMR spectrum of matriisobenzofuran (**72**) in $CDCl_3$.

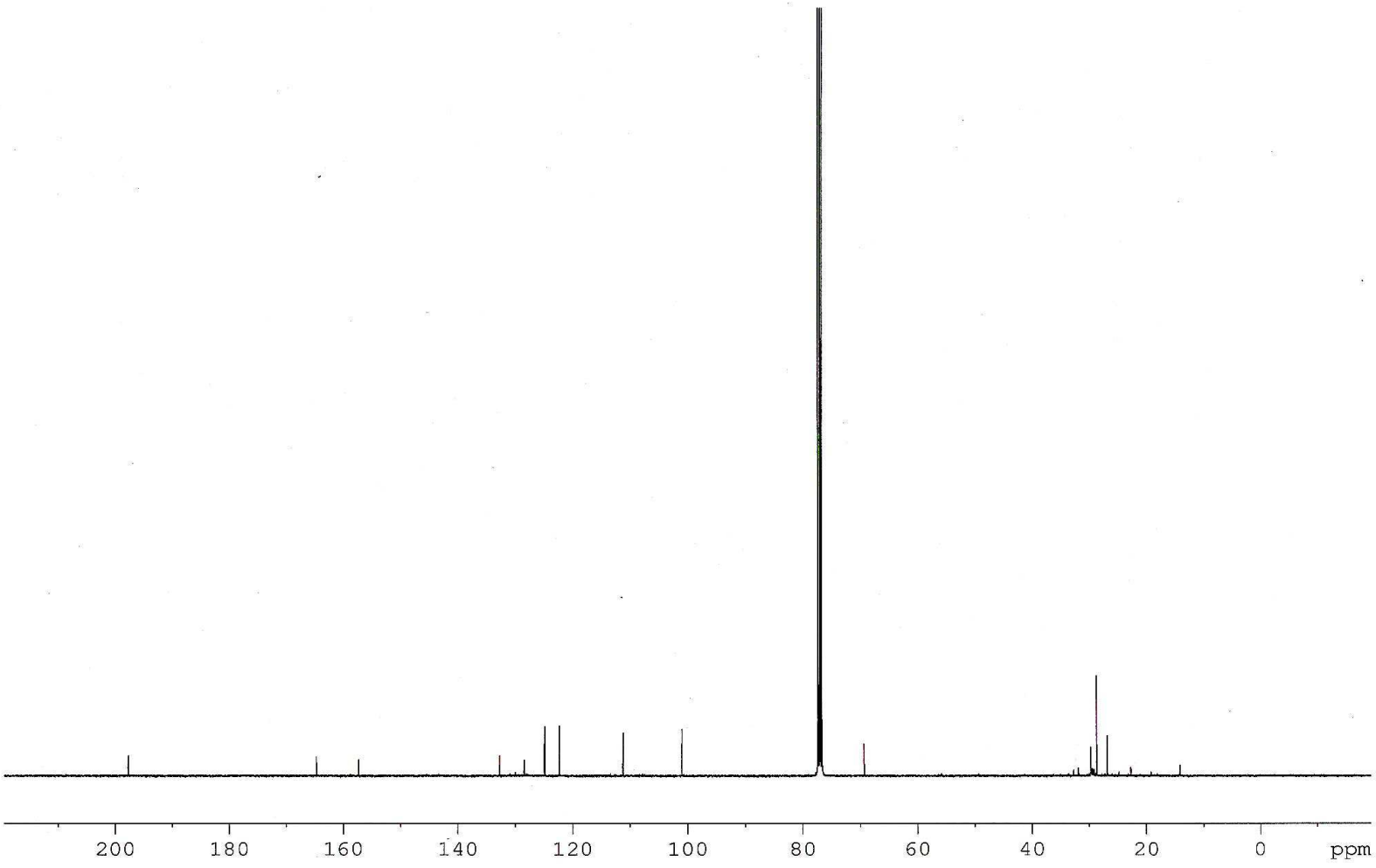

Figure A-2. ^{13}C-NMR spectrum of matriisobenzofuran (**72**) in $CDCl_3$.

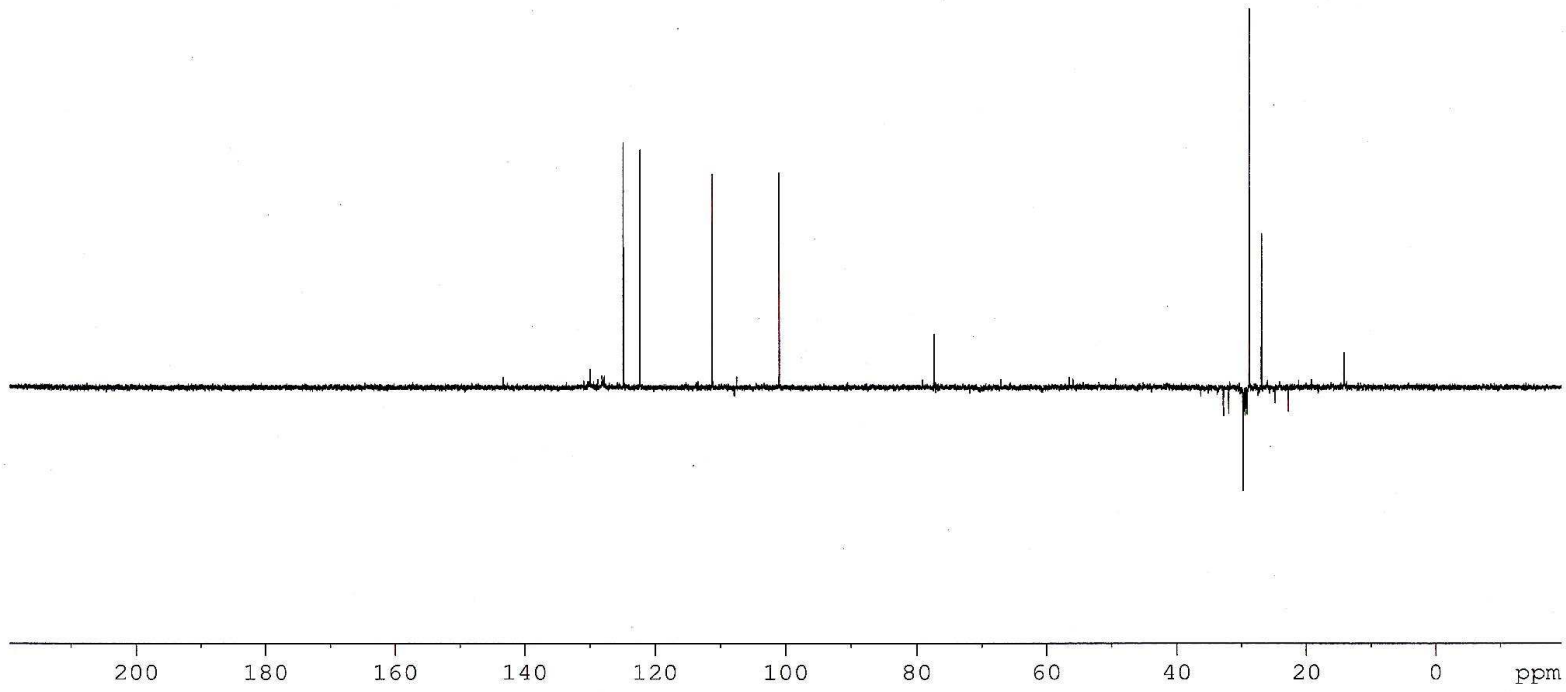

Figure A-3. DEPT spectrum of matriisobenzofuran (**72**) in $CDCl_3$.

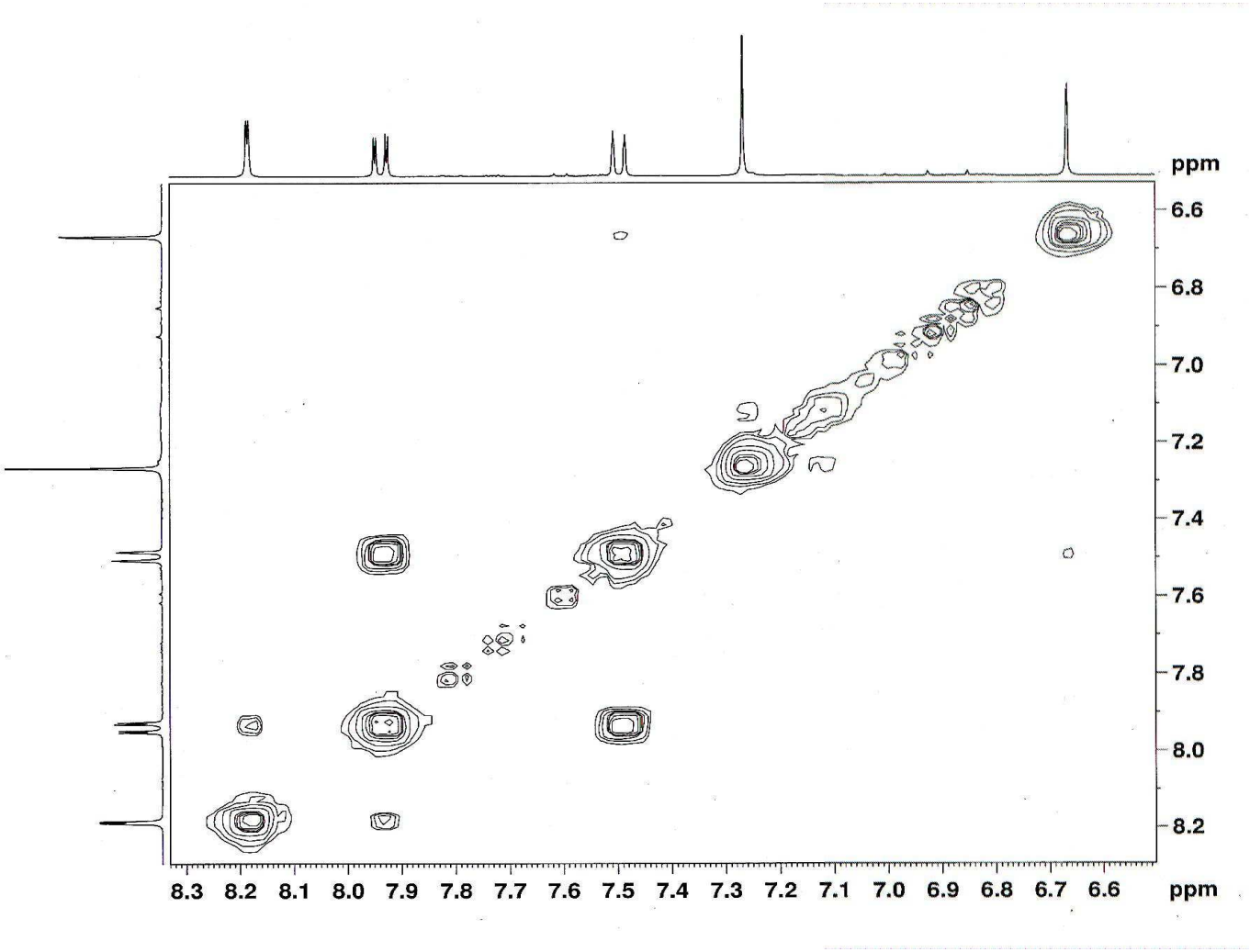

Figure A-4. COSY spectrum of matriisobenzofuran (**72**) in $CDCl_3$.

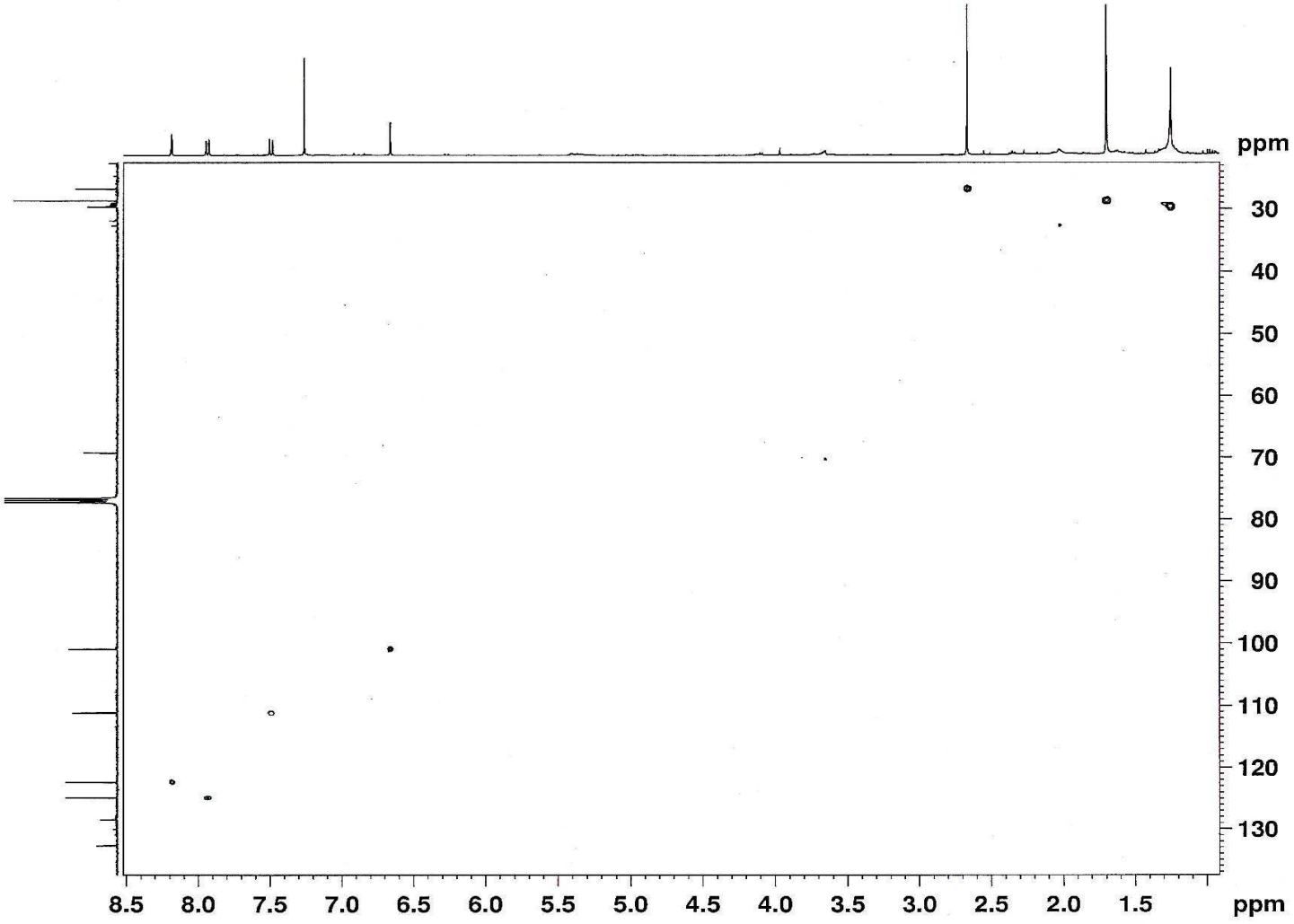

Figure A-5. HSQC spectrum of matriisobenzofuran (**72**) in $CDCl_3$.

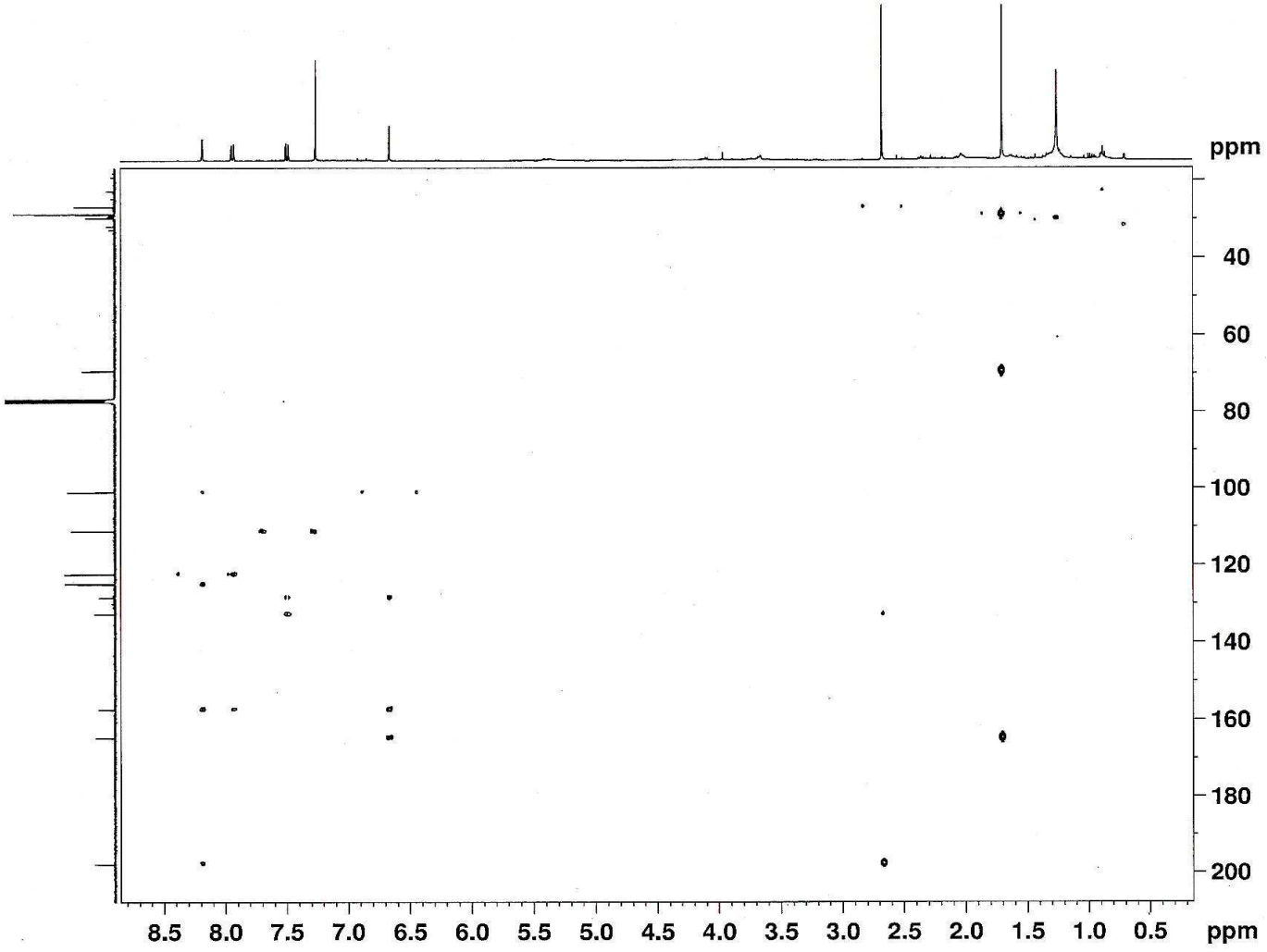

Figure A-6. HMBC spectrum of matriisobenzofuran (**72**) in $CDCl_3$.

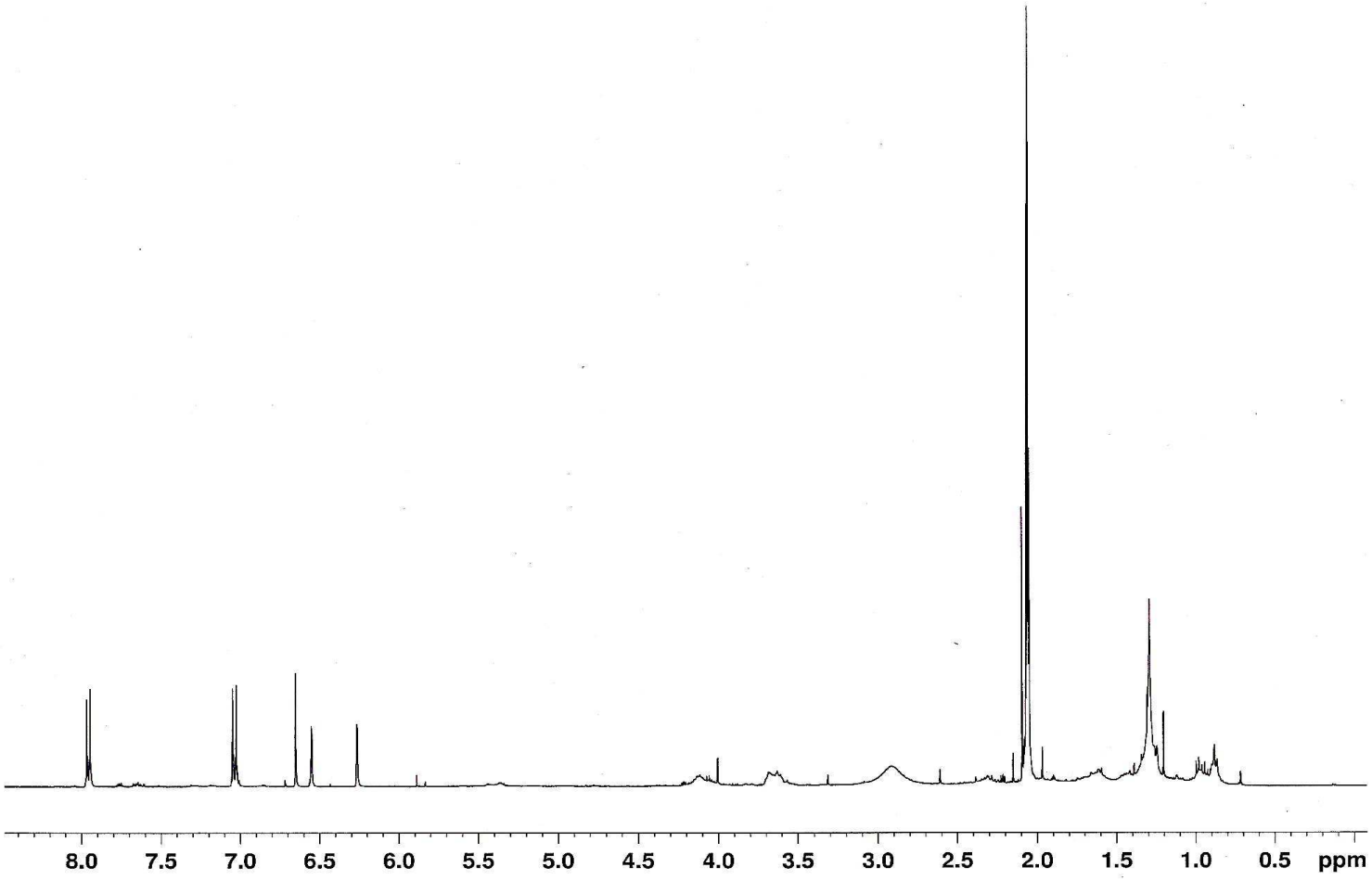

Figure A-7. ^{1}H-NMR spectrum of apigenin (**73**) in acetone-d_6.

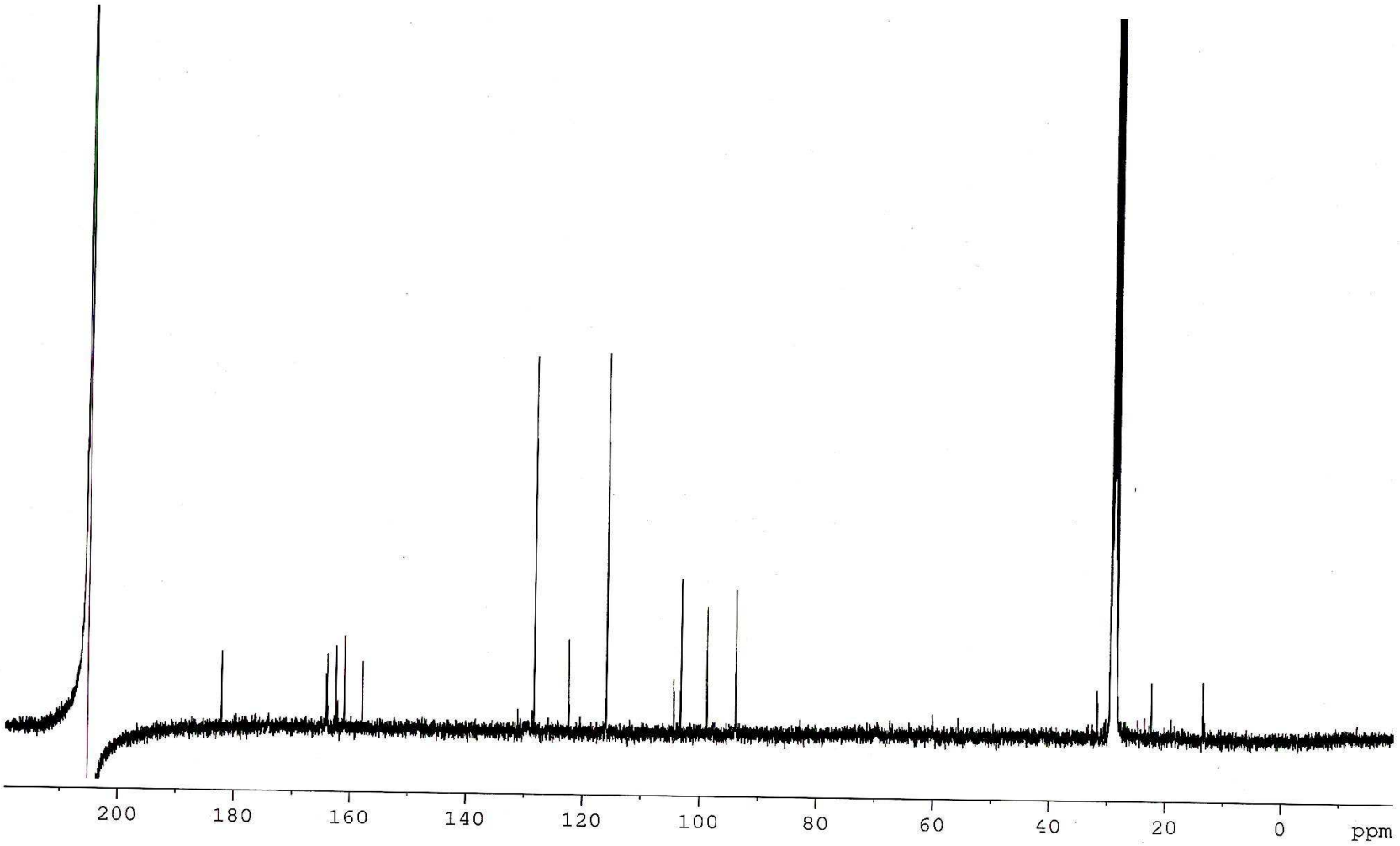

Figure A-8. ^{13}C-NMR spectrum of apigenin (**73**) in acetone-d_6.

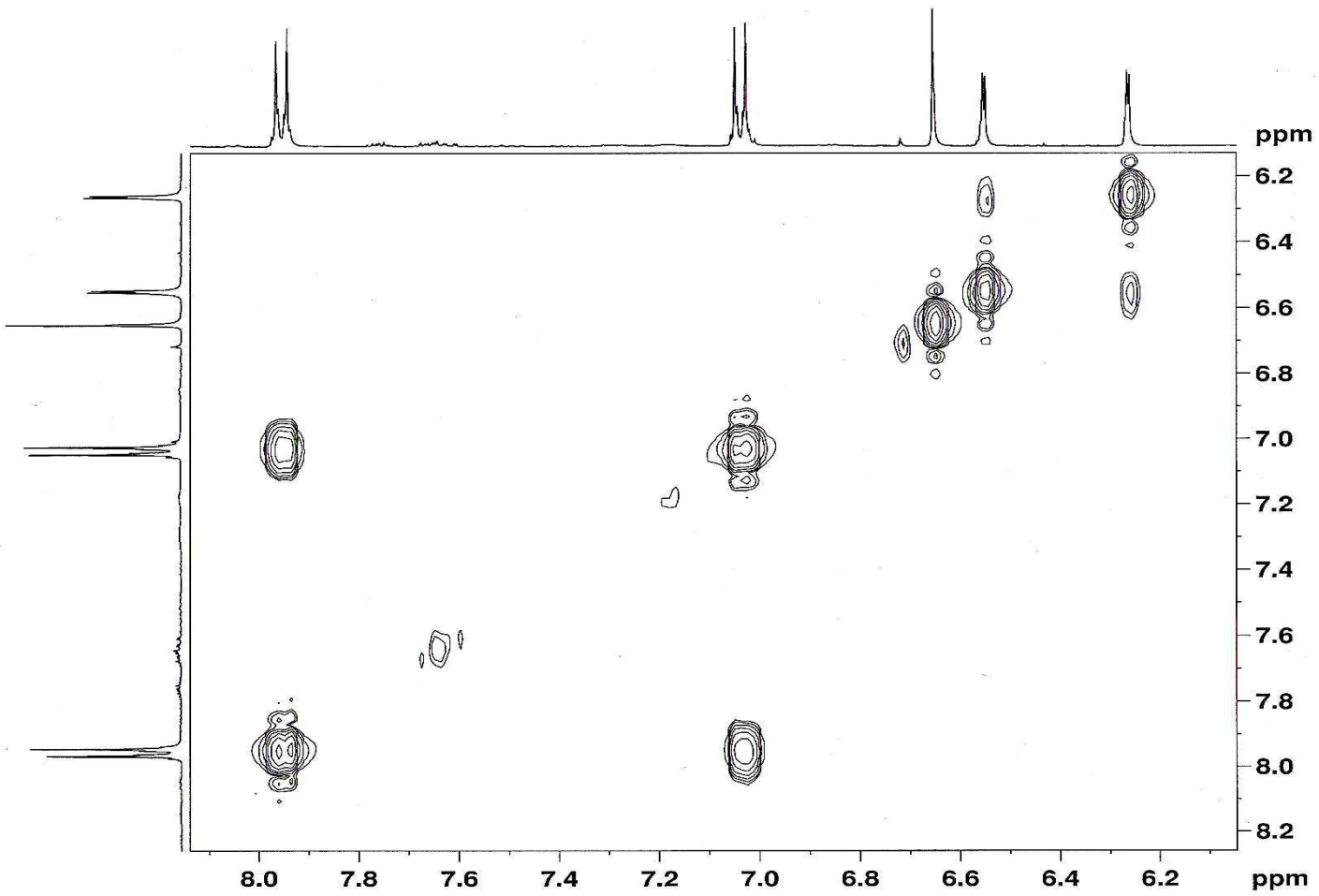

Figure A-9. COSY spectrum of apigenin (**73**) in acetone-d_6.

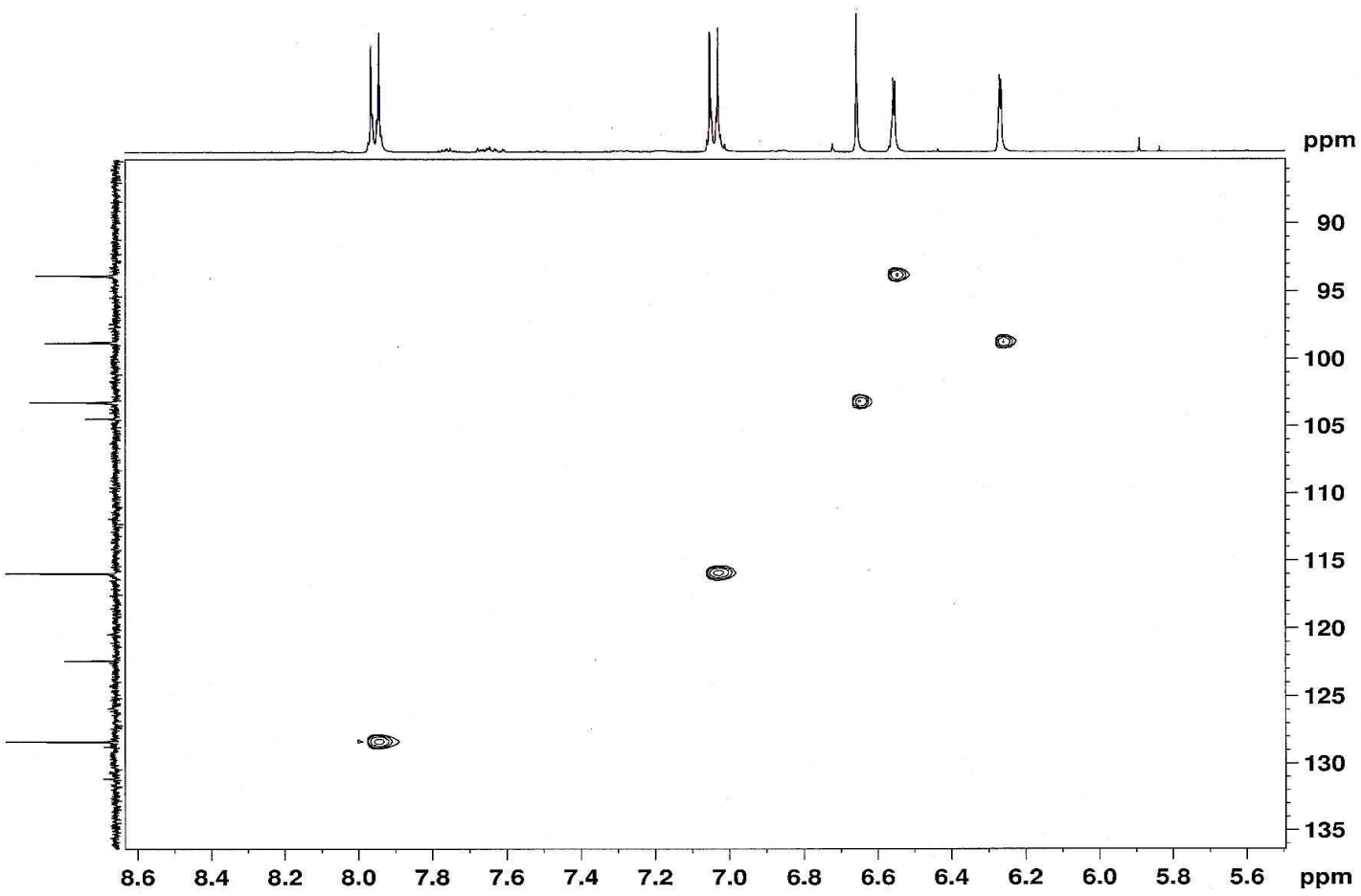

Figure A-10. HSQC spectrum of apigenin (**73**) in acetone-d_6.

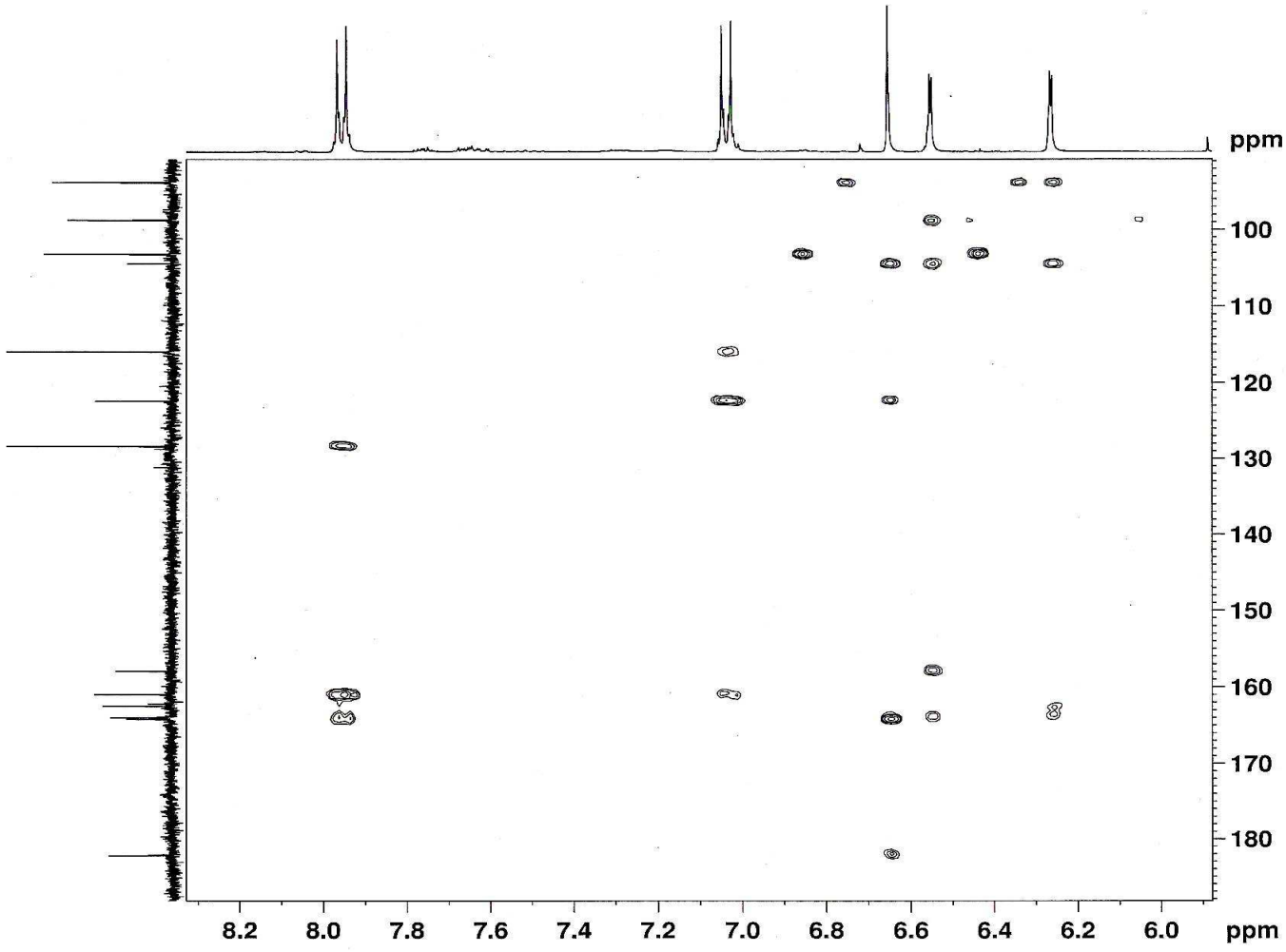

Figure A-11. HMBC spectrum of apigenin (**73**) in acetone-d_6.

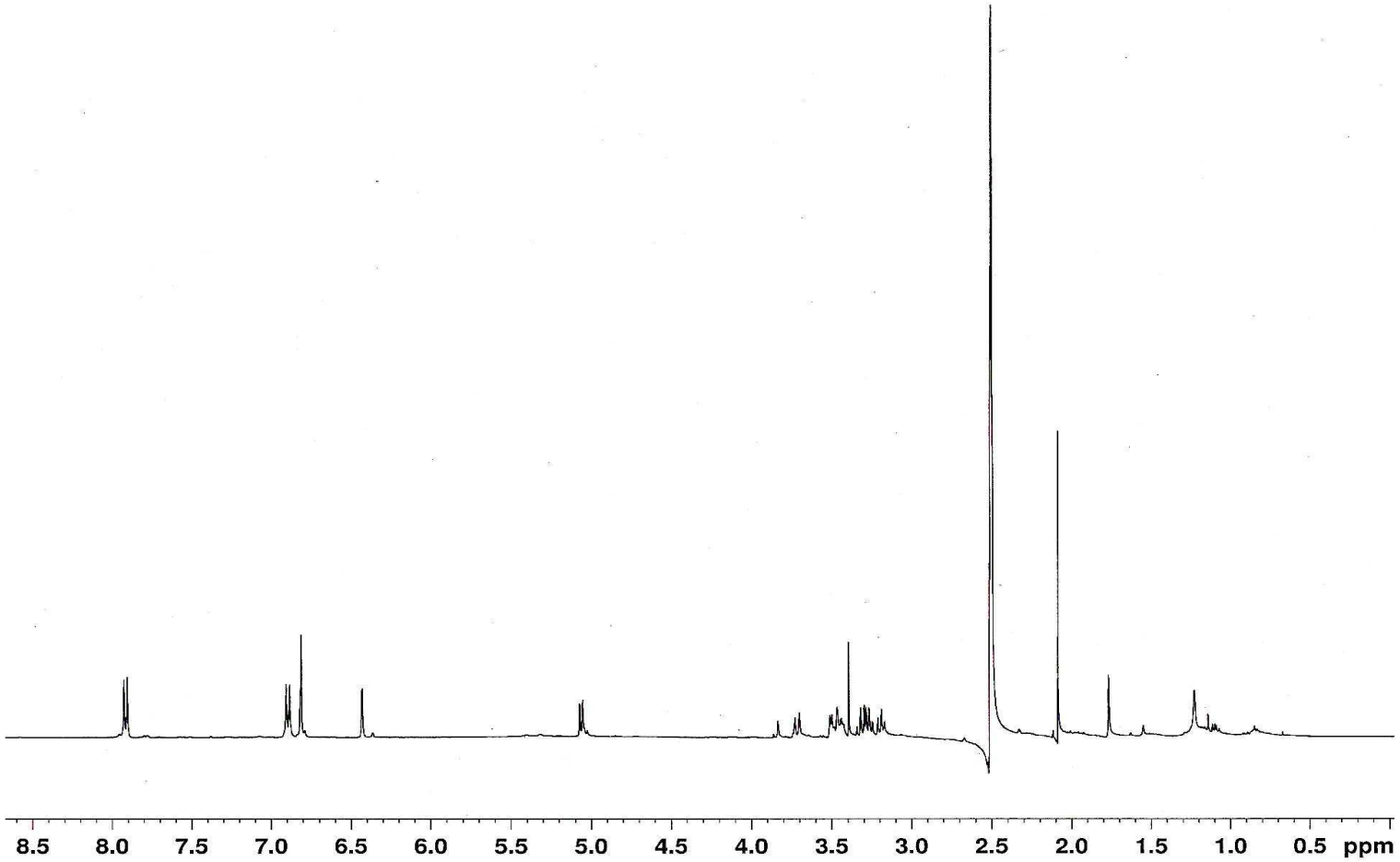

Figure A-12. ^{1}H-NMR spectrum of apigenin-7-*O*-β-glucopyranoside (**74**) in DMSO-d_6.

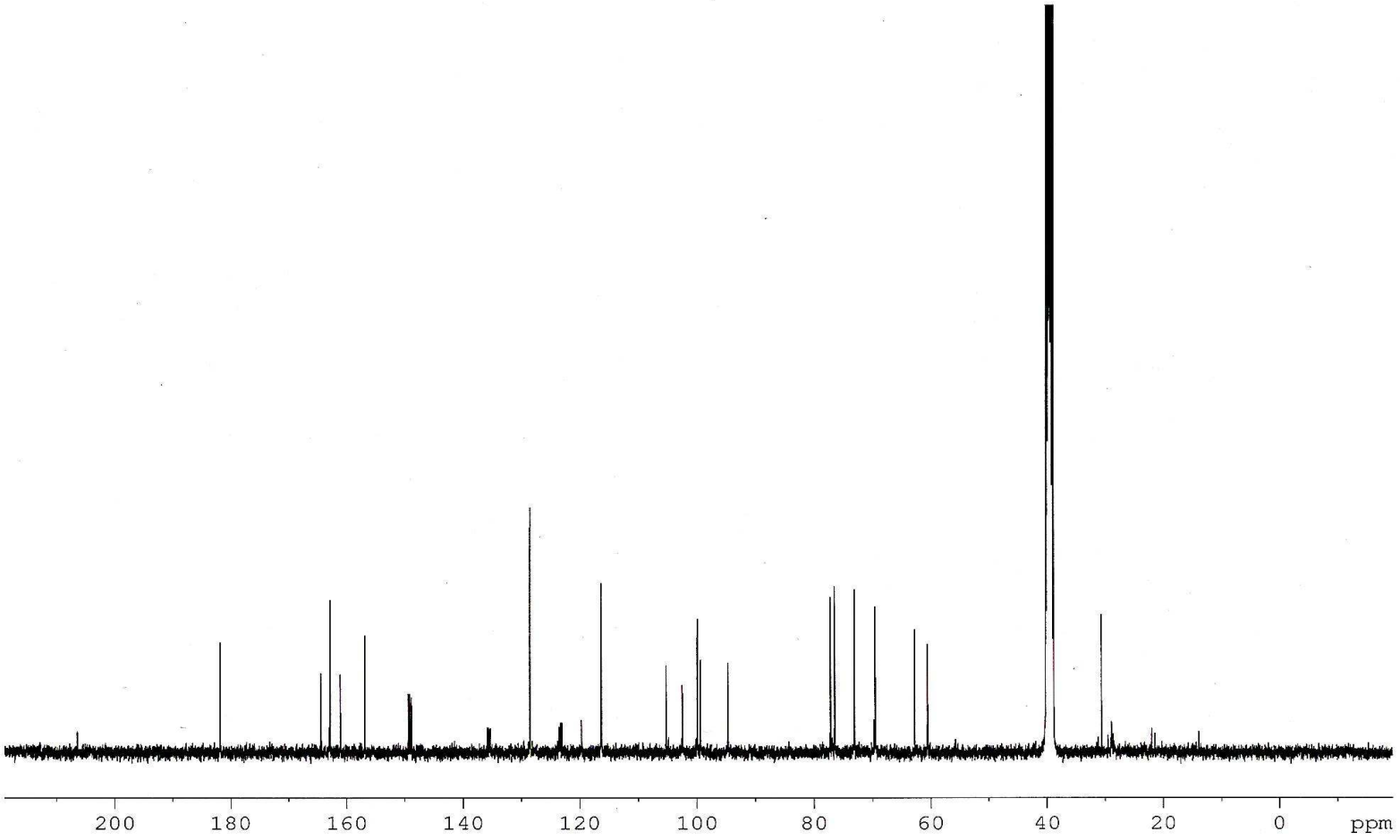

Figure A-13. ^{13}C-NMR spectrum of apigenin-7-*O*-β-glucopyranoside (**74**) in DMSO-d_6.

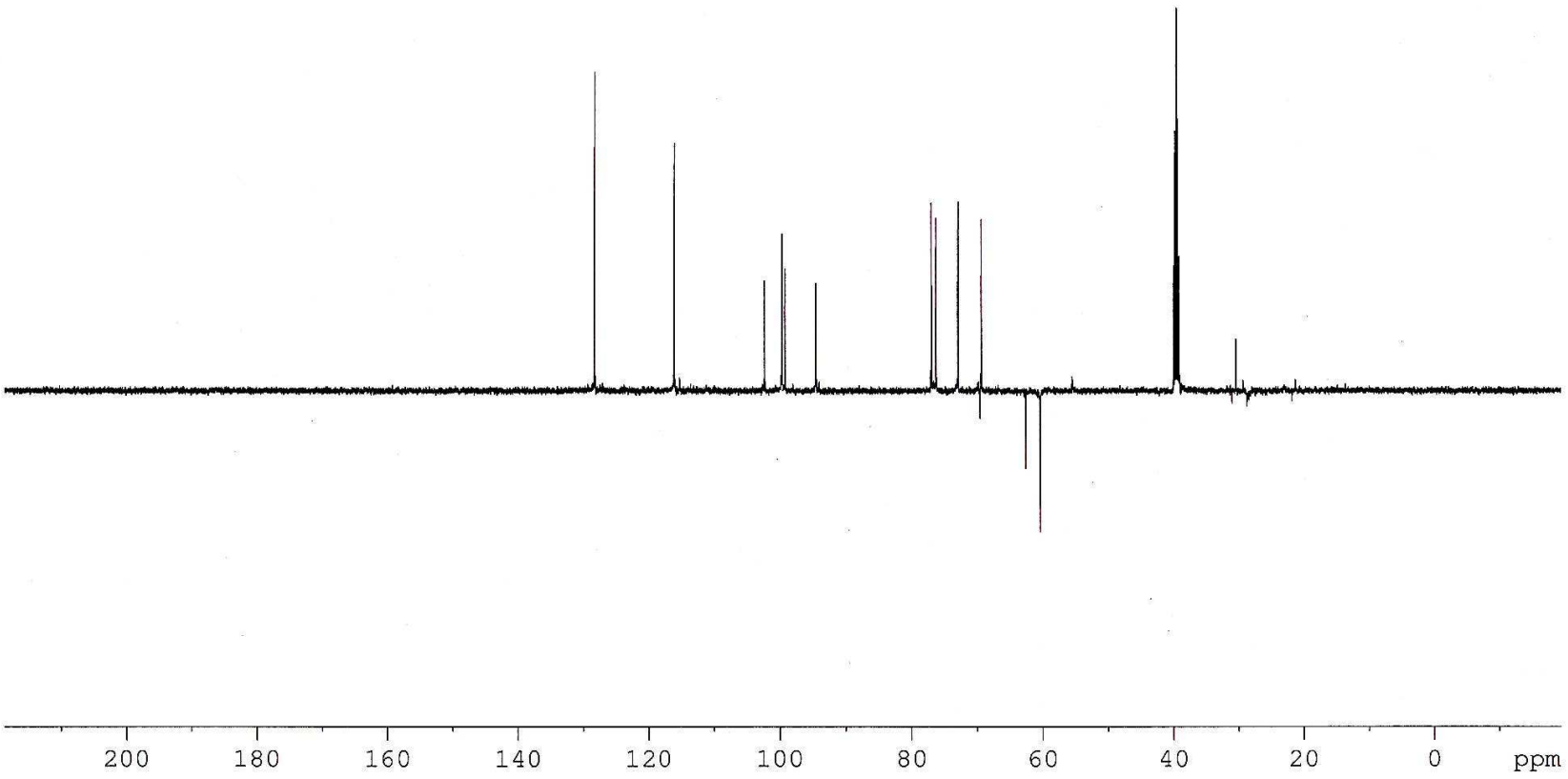

Figure A-14. DEPT spectrum of apigenin-7-*O*-β-glucopyranoside (**74**) in DMSO-d_6.

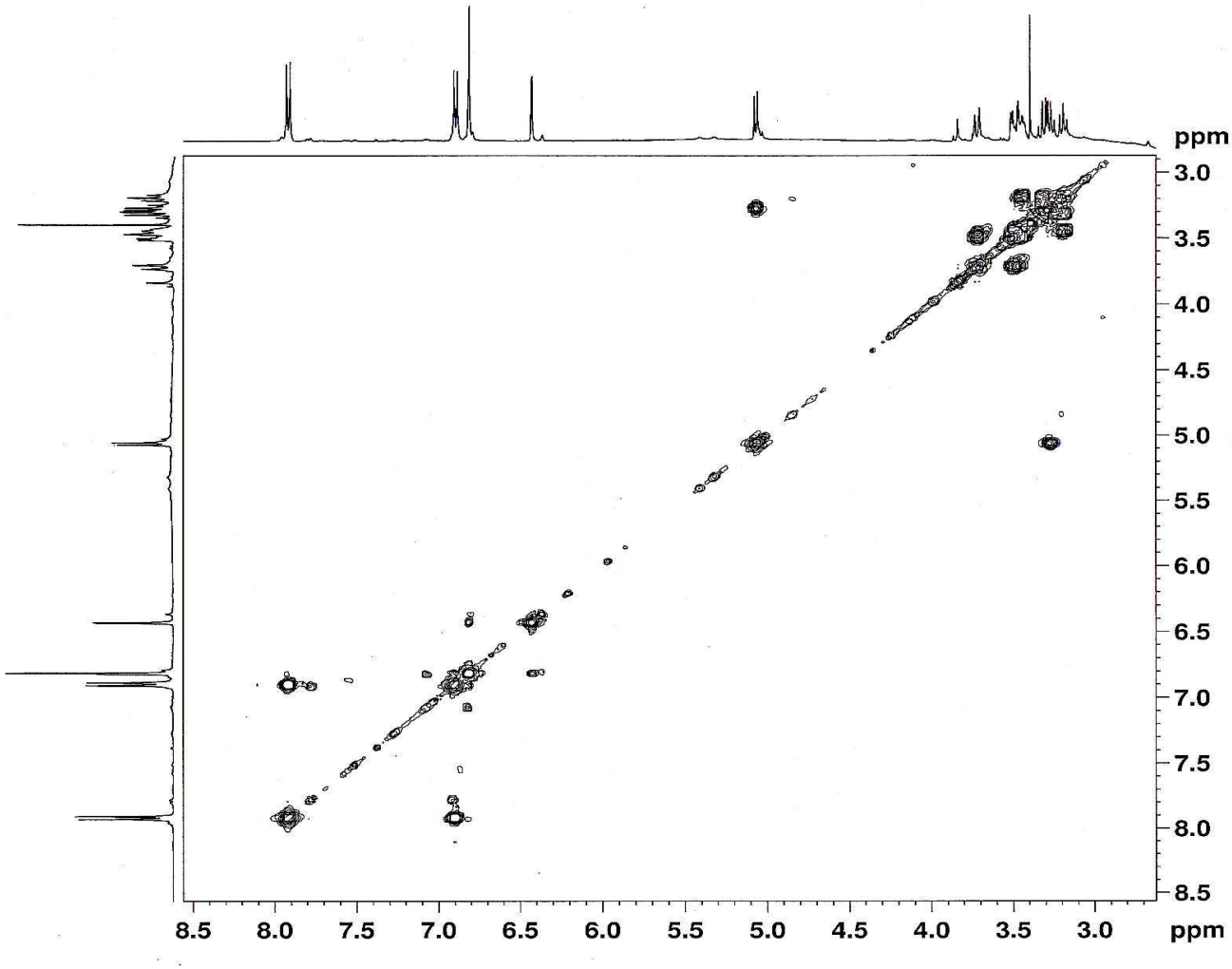

Figure A-15. COSY spectrum of apigenin-7-*O*-β-glucopyranoside (**74**) in DMSO-d_6.

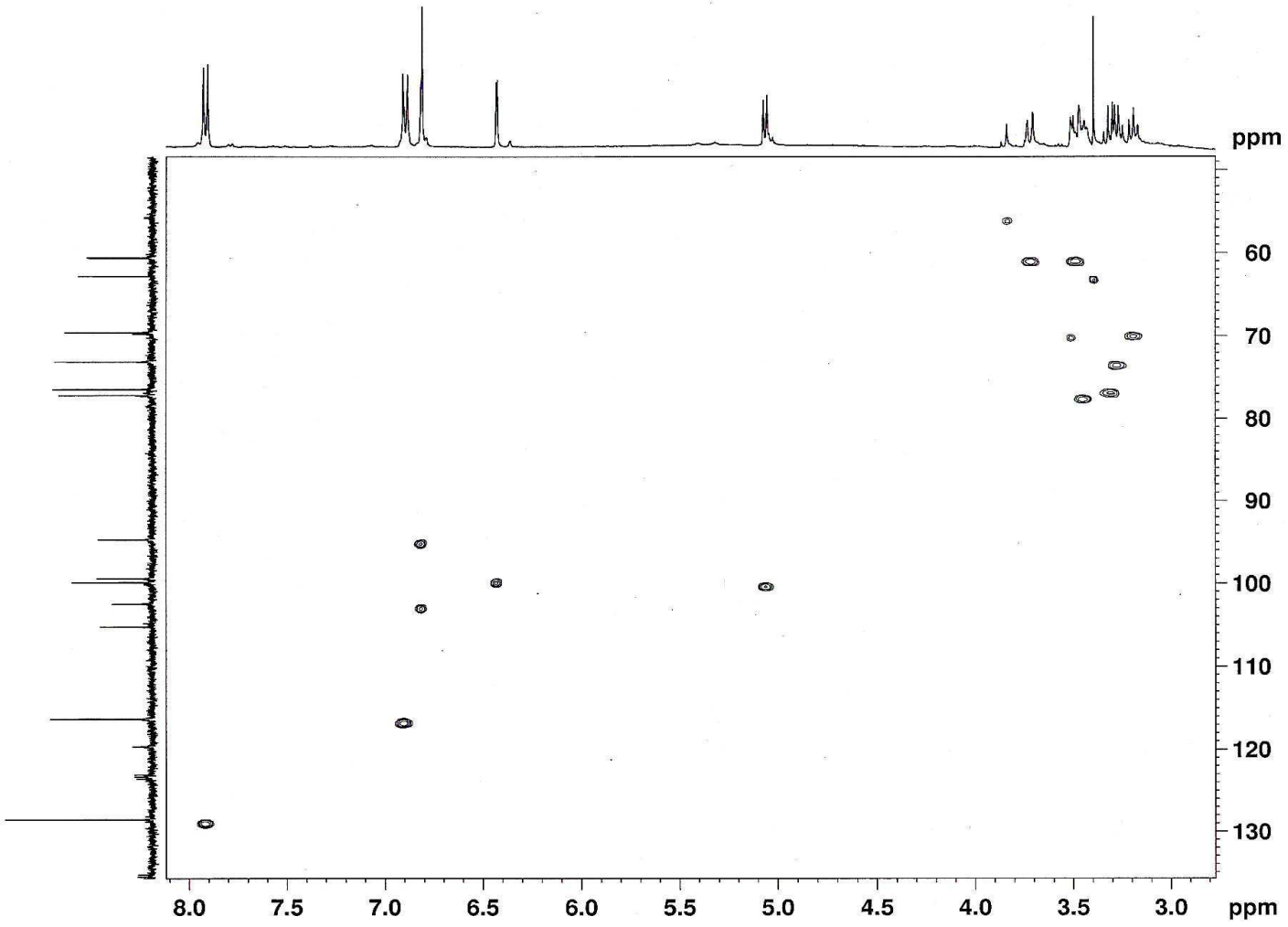

Figure A-16. HSQC spectrum of apigenin-7-*O*-β-glucopyranoside (**74**) in DMSO-d_6.

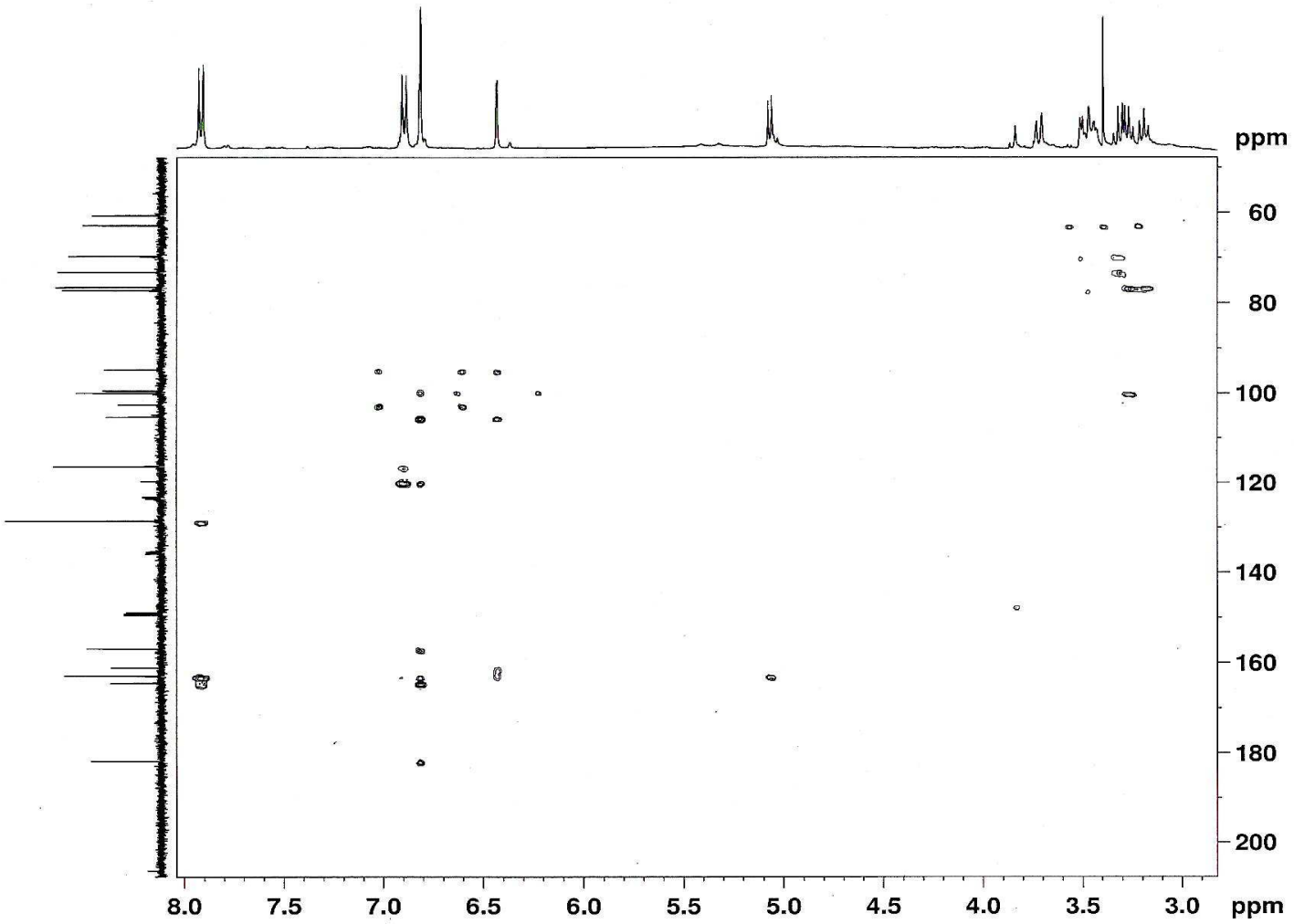

Figure A-17. HMBC spectrum of apigenin-7-*O*-β-glucopyranoside (**74**) in DMSO-d_6.

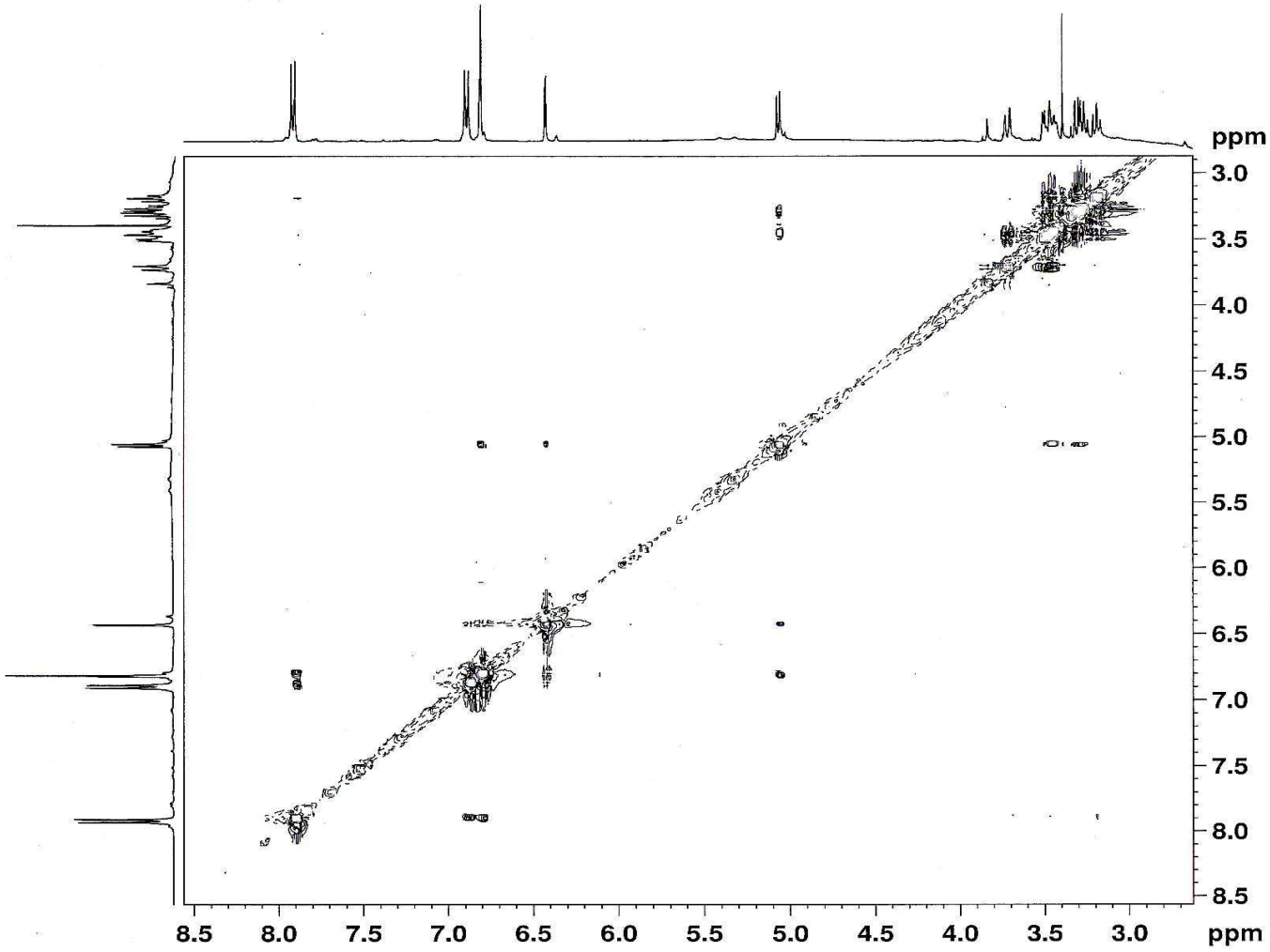

Figure A-18. ROESY spectrum of apigenin-7-*O*-β-glucopyranoside (**74**) in DMSO-d_6.

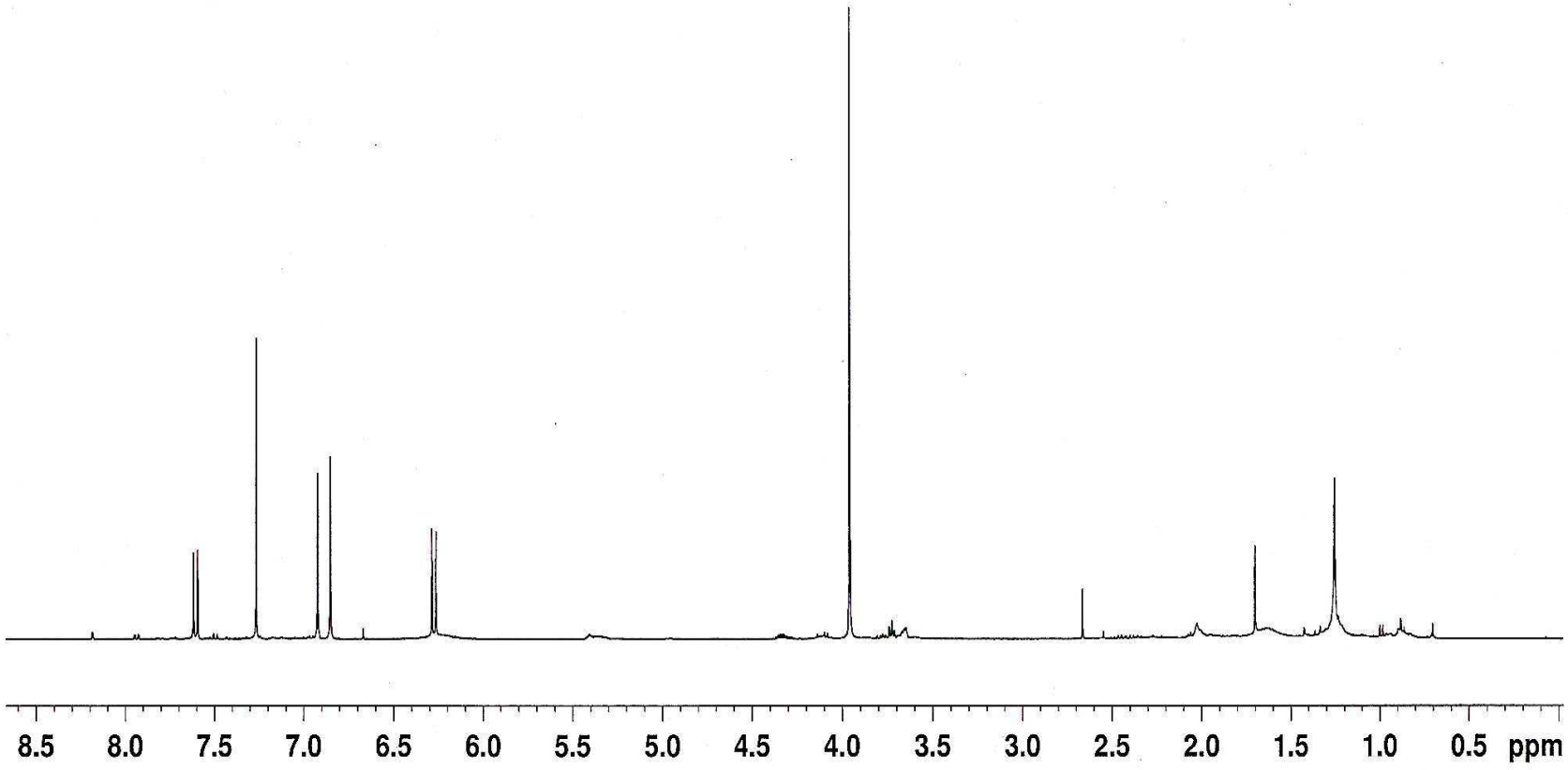

Figure A-19. ^{1}H-NMR spectrum of scopoletin (**75**) in $CDCl_3$.

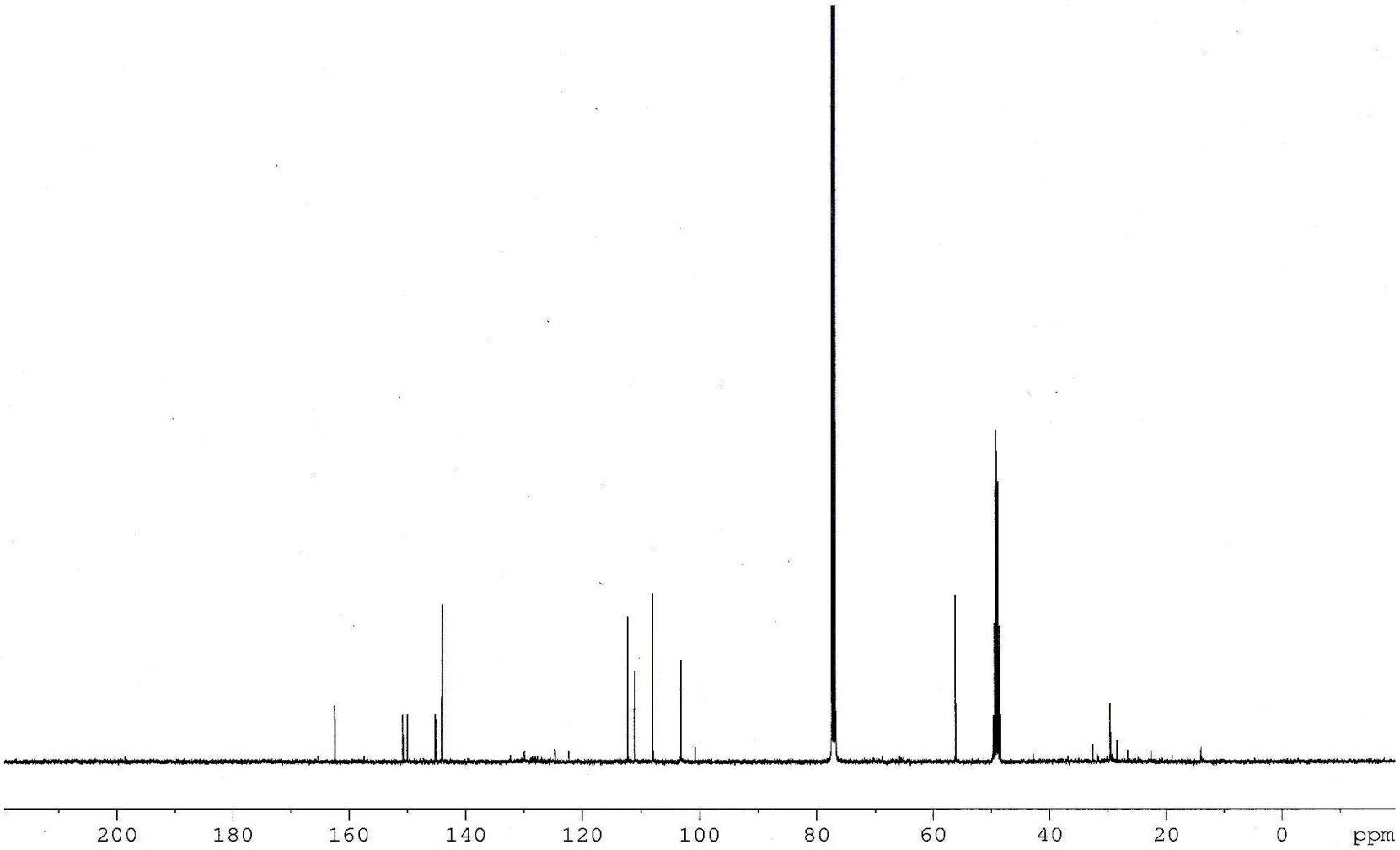

Figure A-20. ^{13}C-NMR spectrum of scopoletin (**75**) in $CDCl_3$.

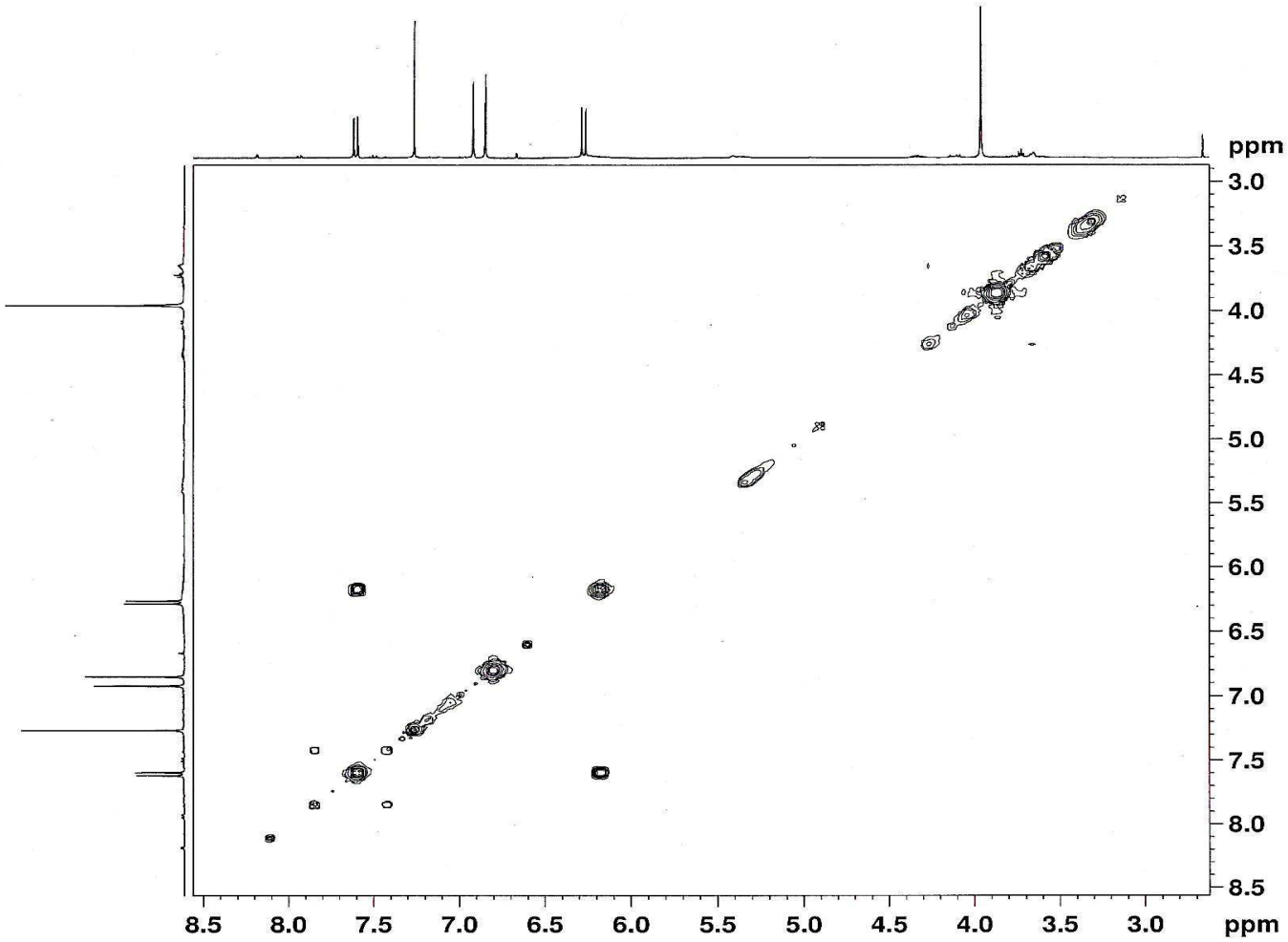

Figure A-21. COSY spectrum of scopoletin (**75**) in $CDCl_3$.

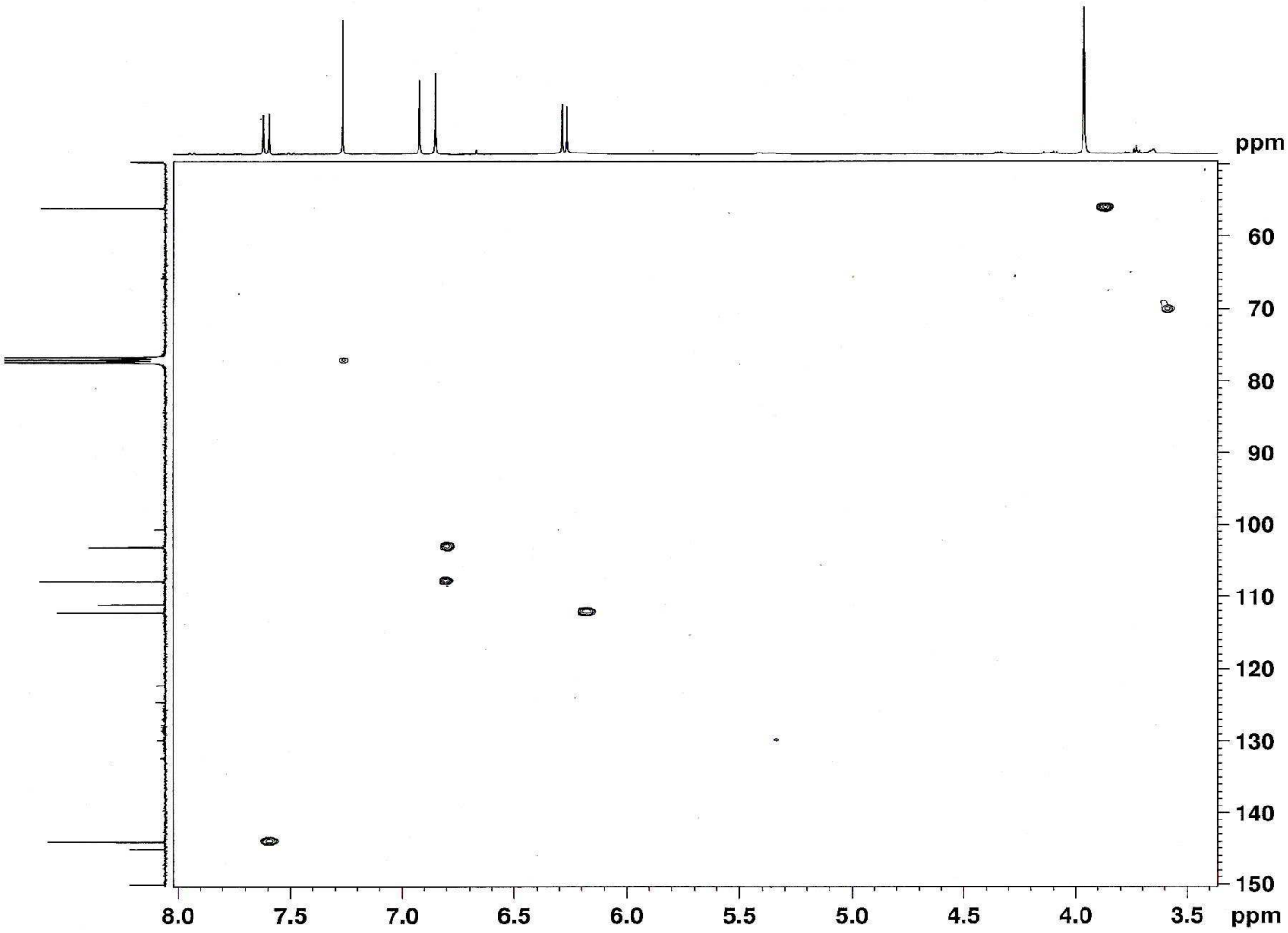

Figure A-22. HSQC spectrum of scopoletin (**75**) in $CDCl_3$.

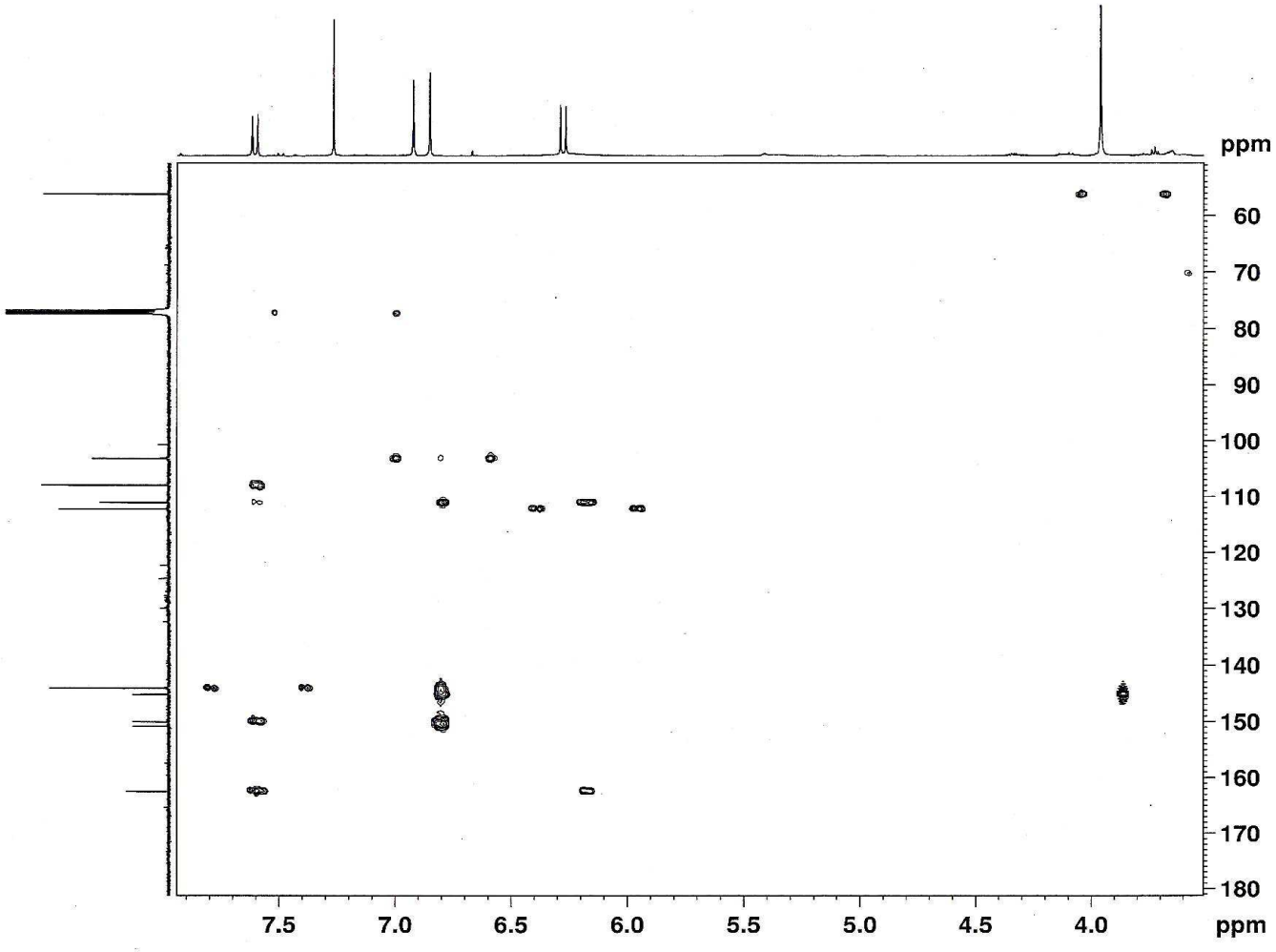

Figure A-23. HMBC spectrum of scopoletin (**75**) in $CDCl_3$.

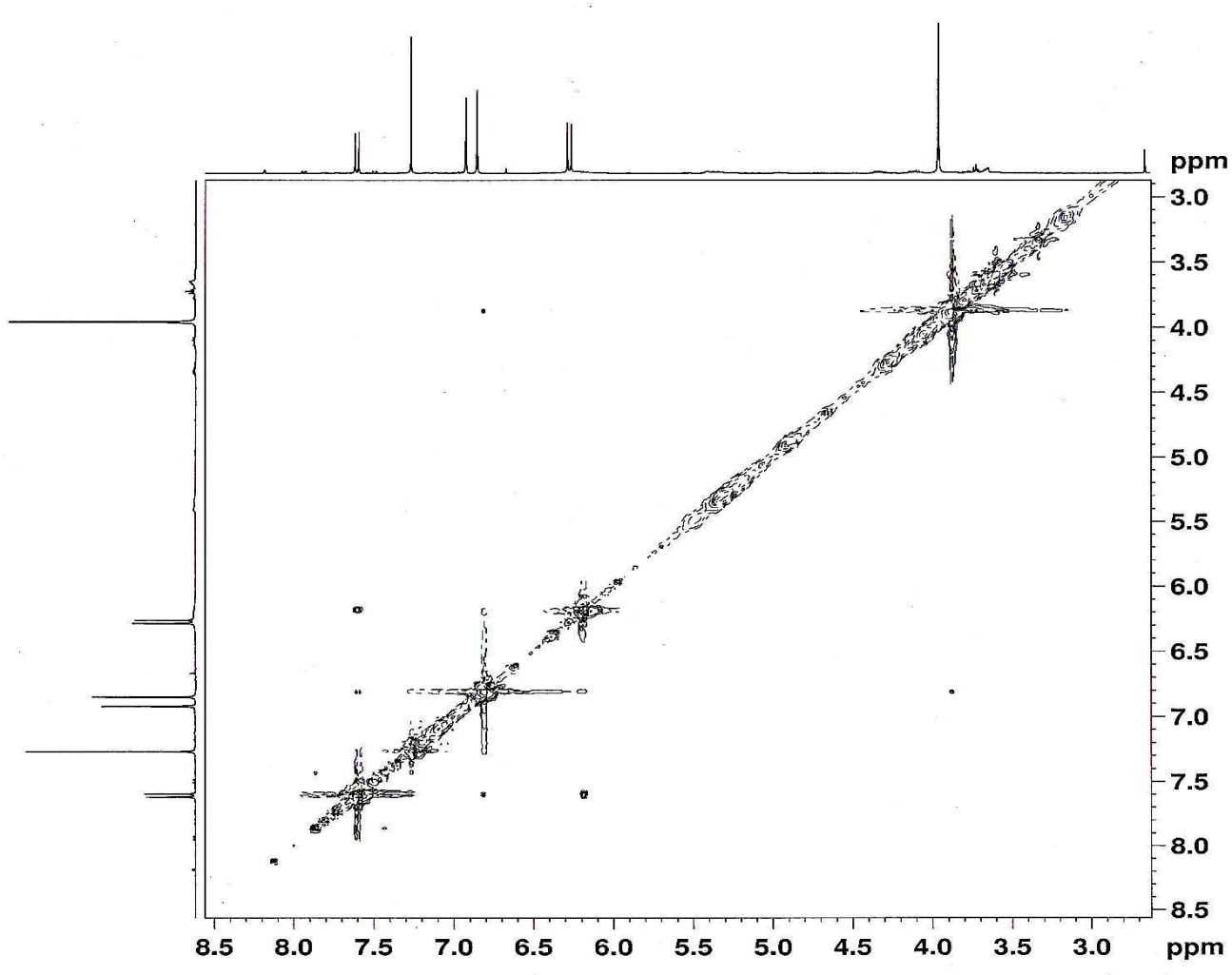

Figure A-24. ROESY spectrum of scopoletin (**75**) in $CDCl_3$.

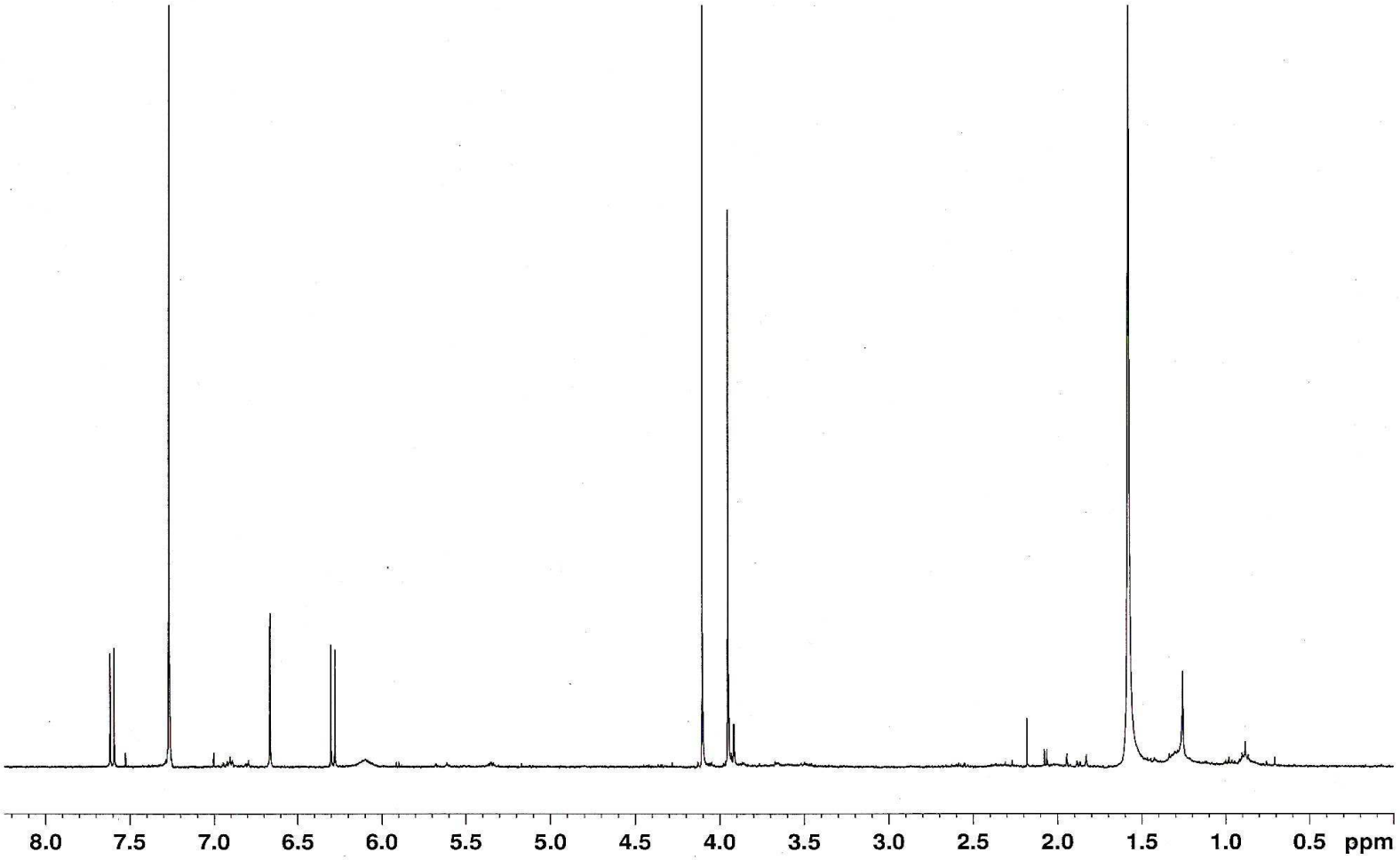

Figure A-25. ^{1}H-NMR spectrum of fraxidin (**76**) in $CDCl_3$.

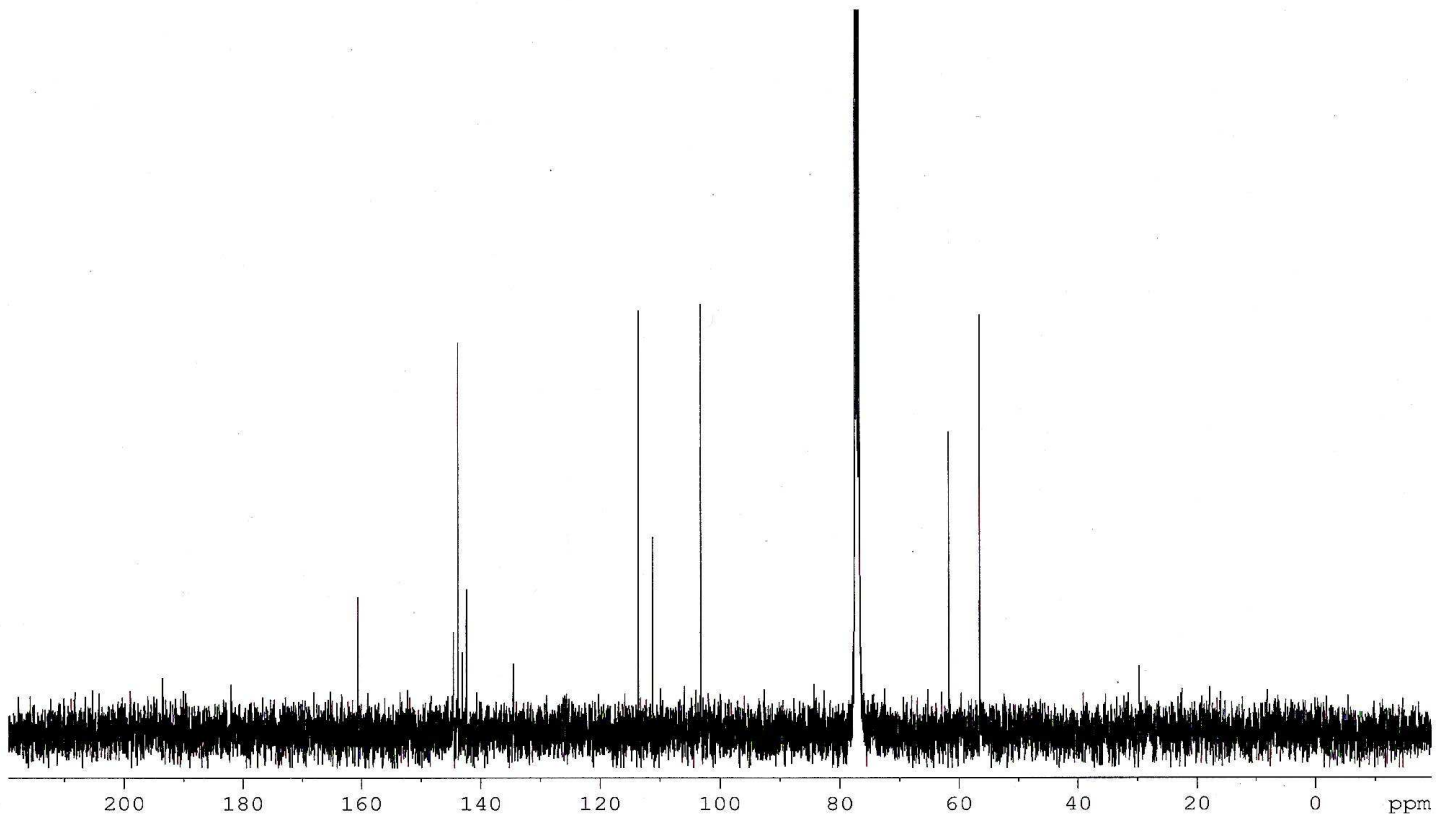

Figure A-26. ^{13}C-NMR spectrum of fraxidin (**76**) in $CDCl_3$.

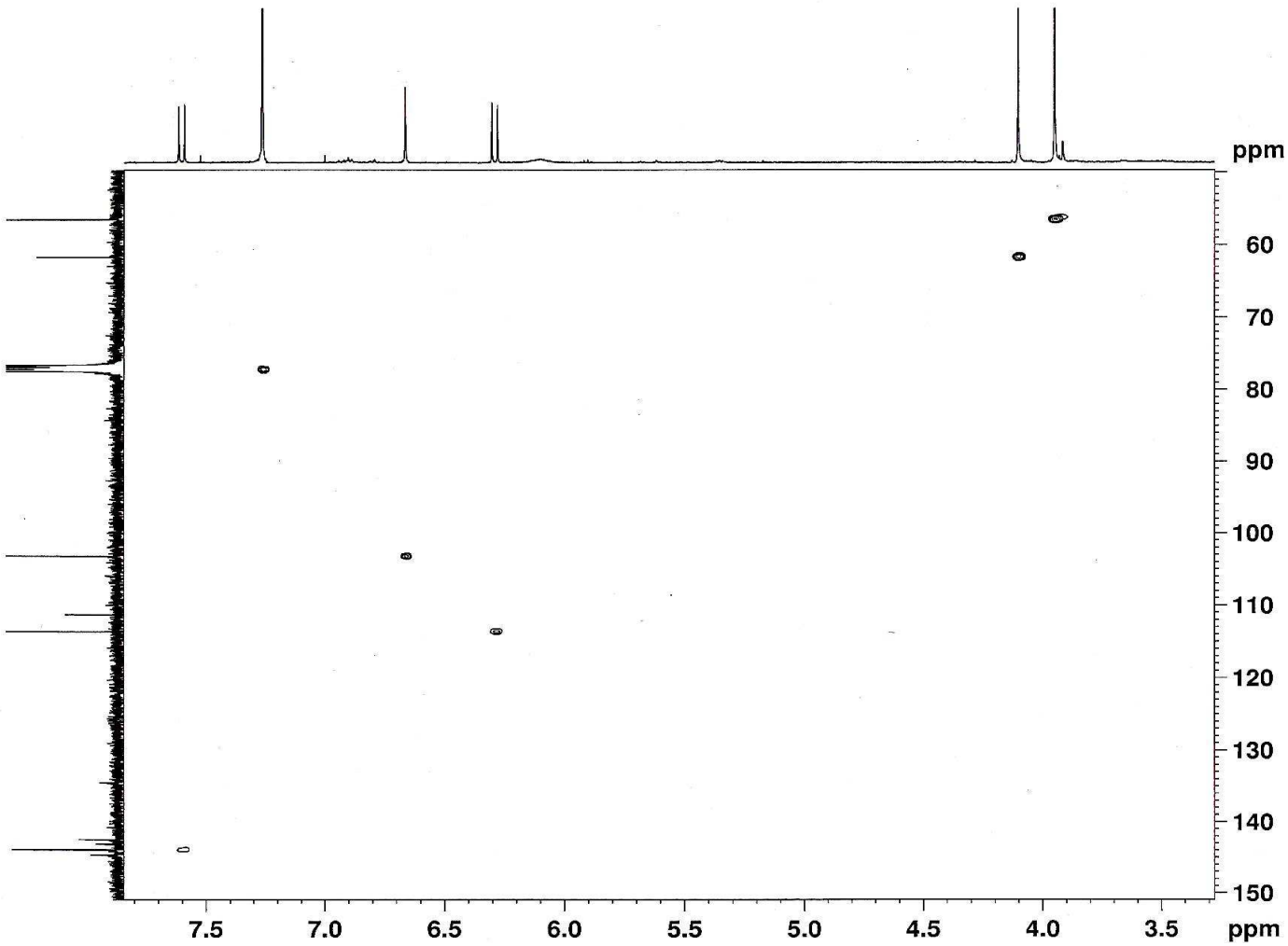

Figure A-27. HSQC spectrum of fraxidin (**76**) in $CDCl_3$.

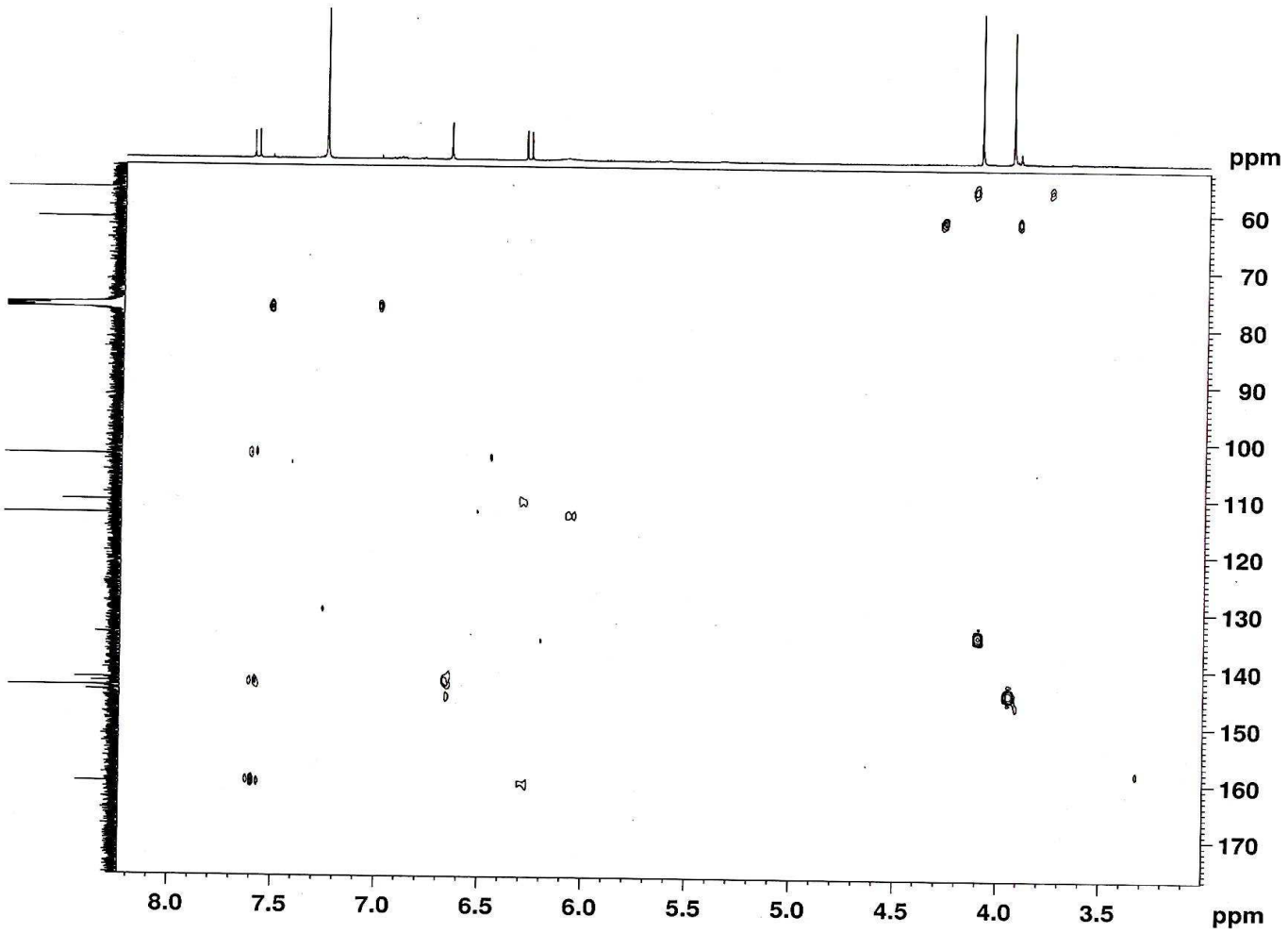

Figure A-28. HMBC spectrum of fraxidin (**76**) in $CDCl_3$.

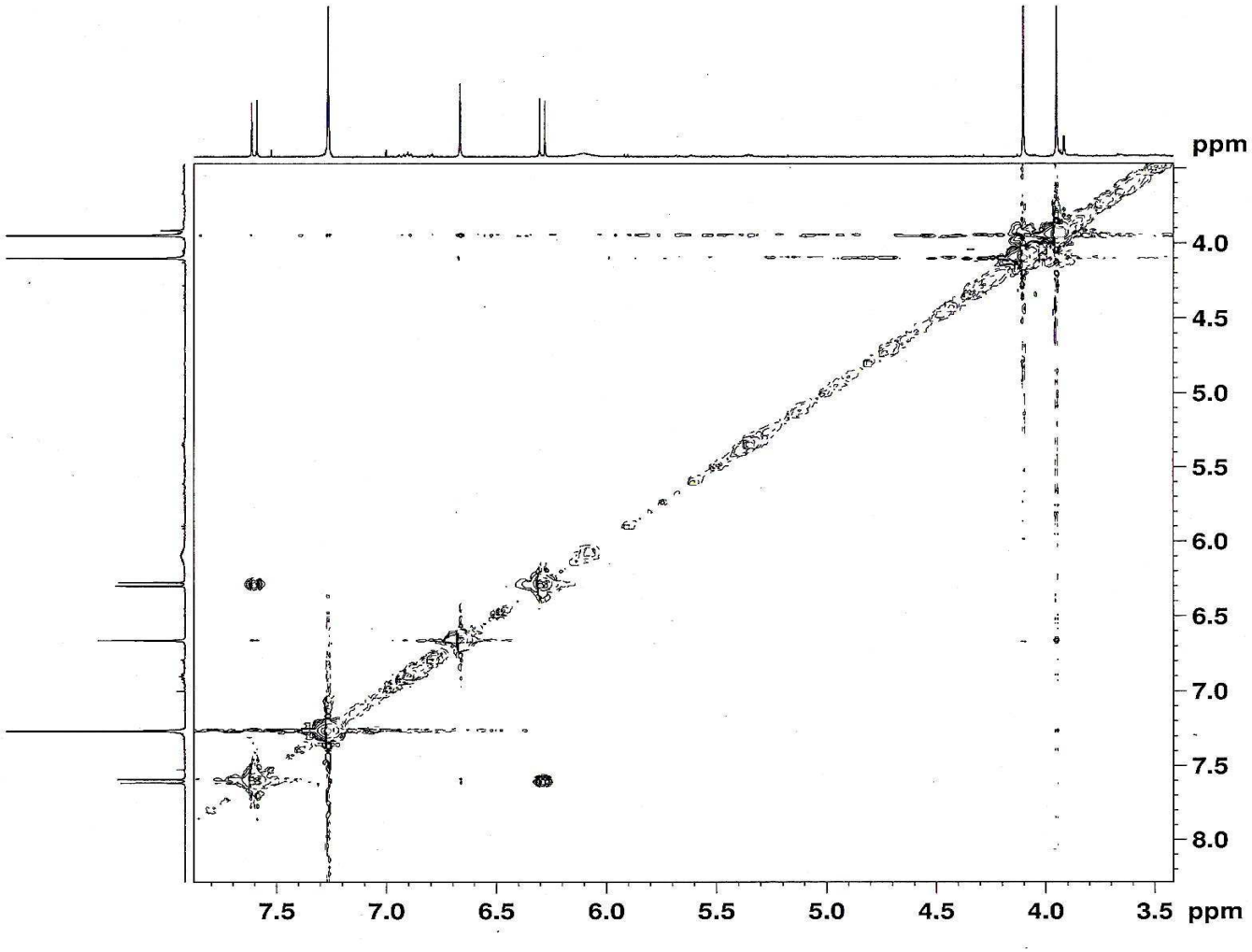

Figure A-29. NOESY spectrum of fraxidin (**76**) in $CDCl_3$.

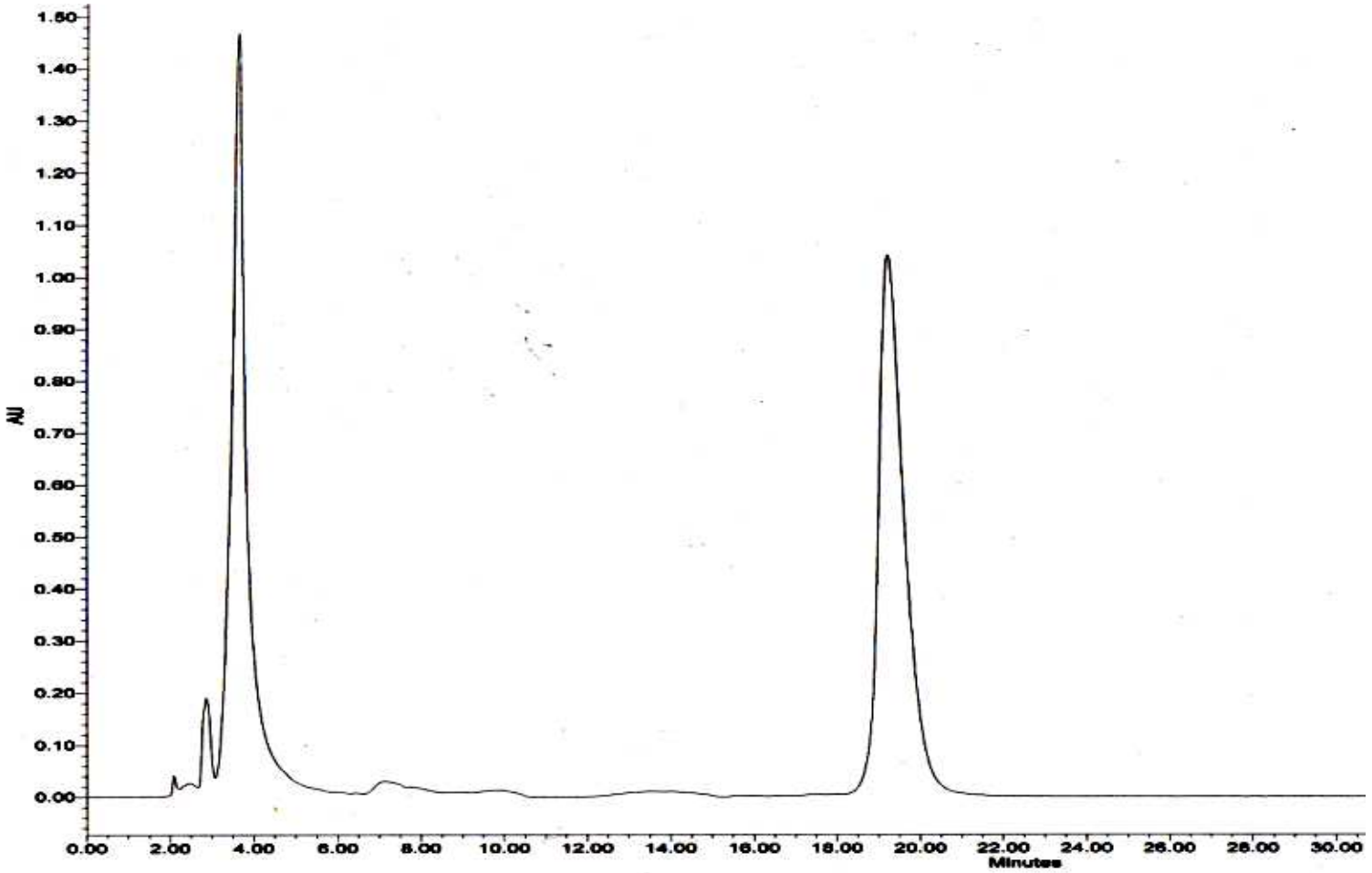

Figure A-30: HPLC chromatogram of matrine (**84**) (~19 min) and oxymatrine (**85**) (~3.5 min) standards.

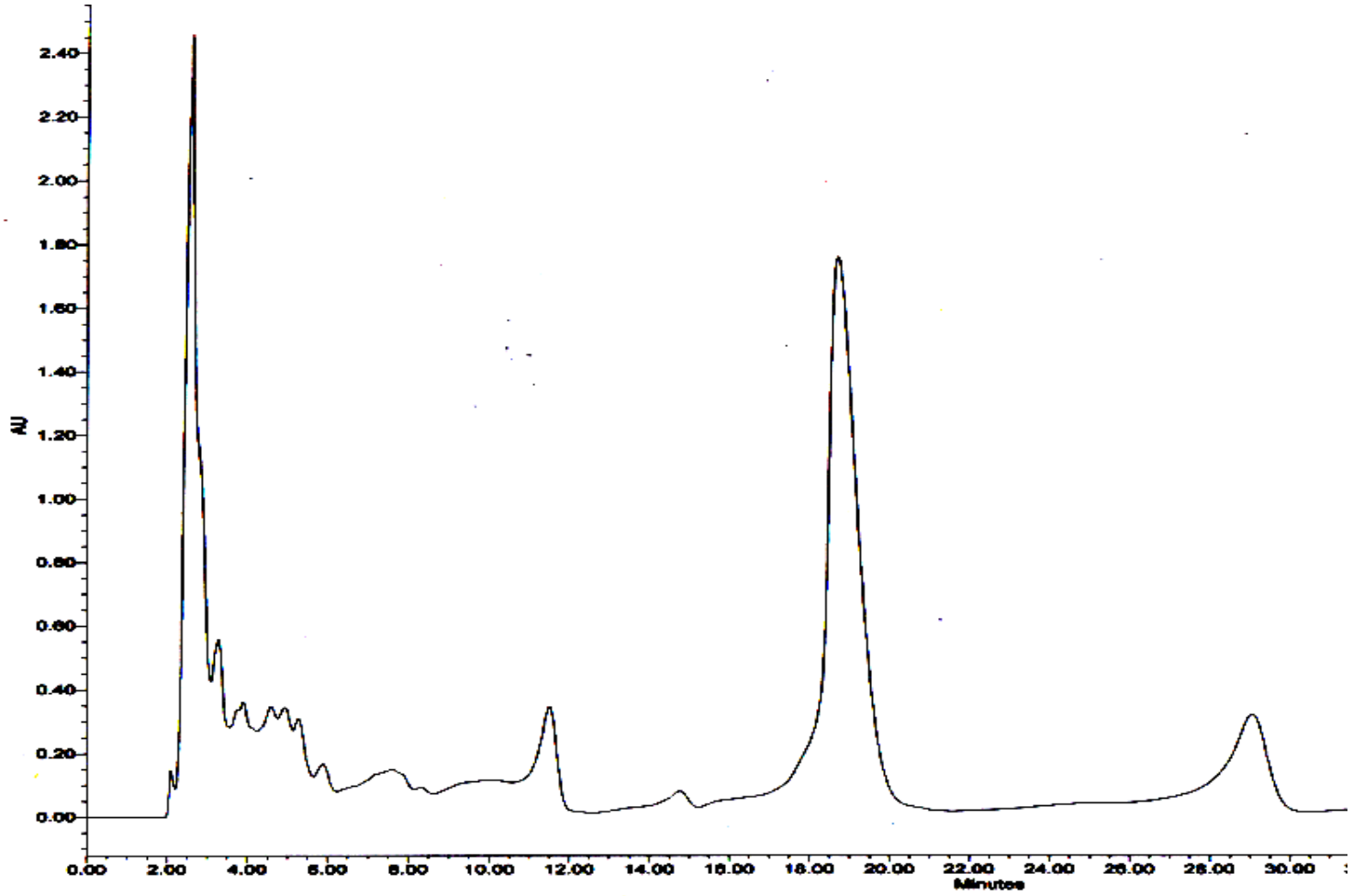

Figure A-31: HPLC chromatogram of the semi-pure oxymatrine biotransformation product after prep TLC.

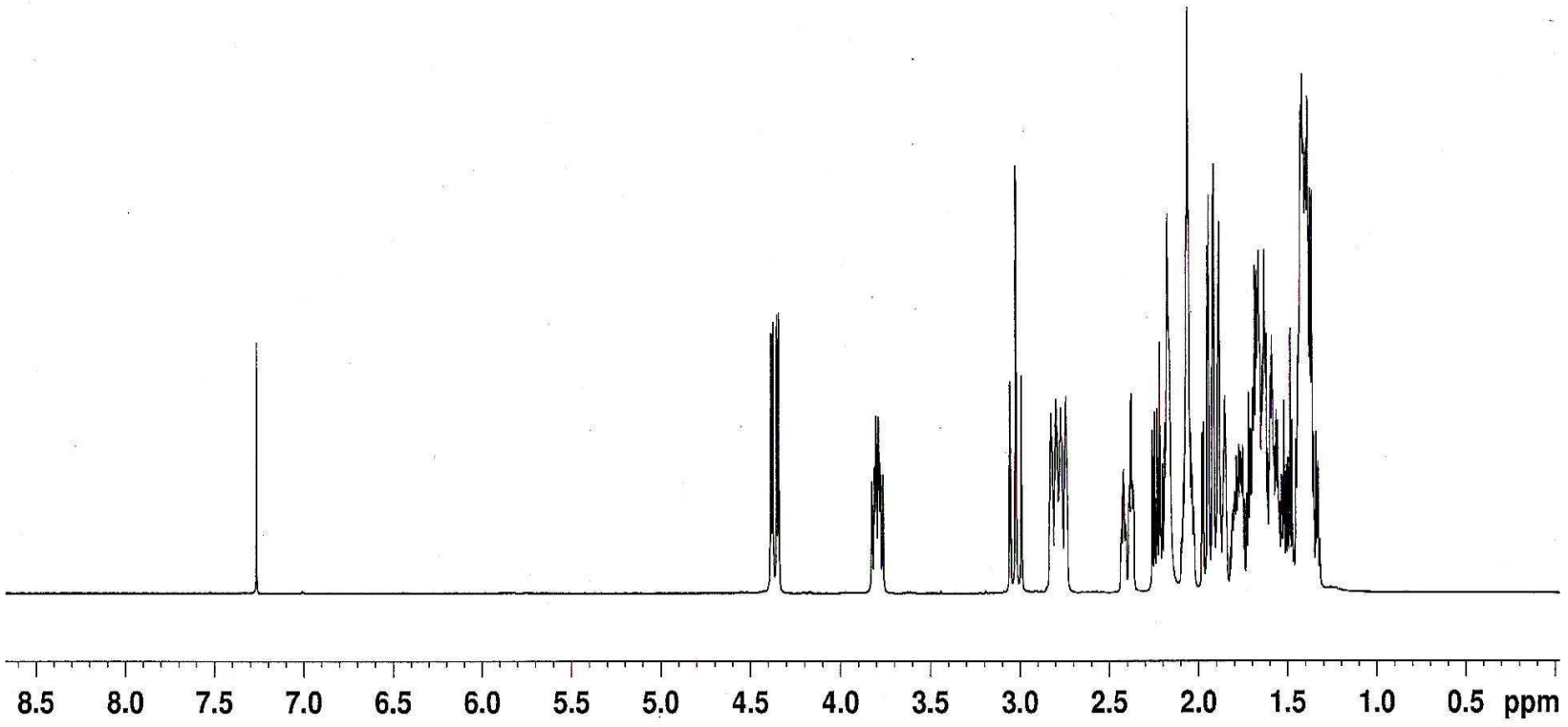

Figure A-32. ^{1}H-NMR spectrum of matrine (**84**) in $CDCl_3$.

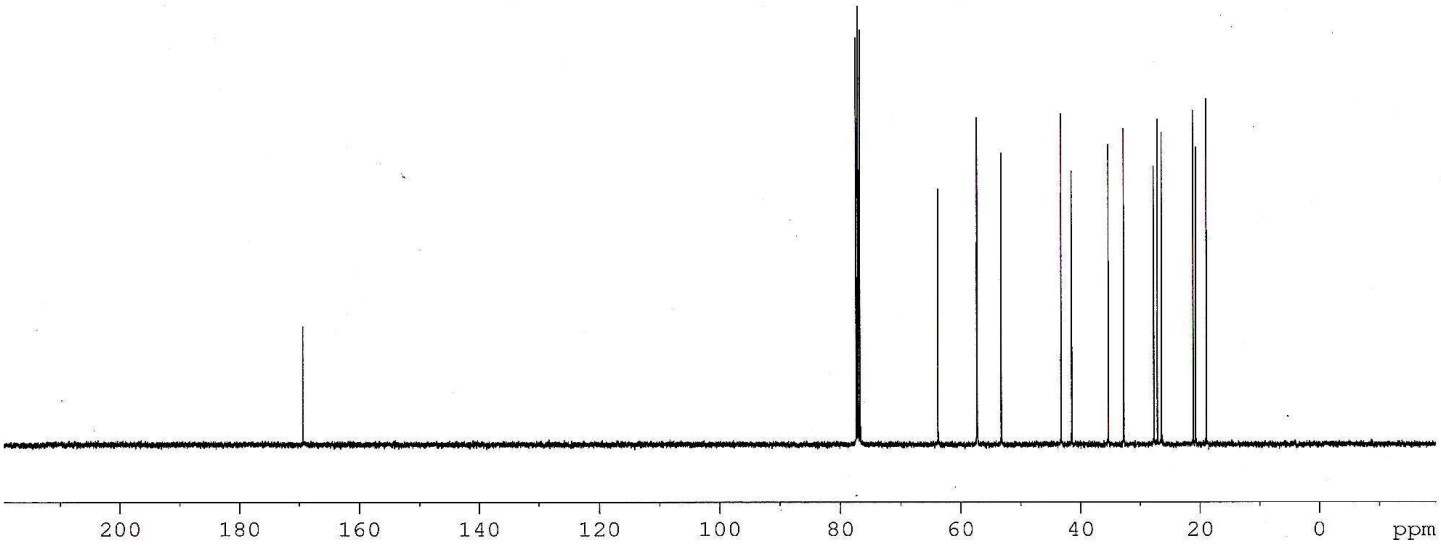

Figure A-33. ^{13}C-NMR spectrum of matrine (**84**) in $CDCl_3$.

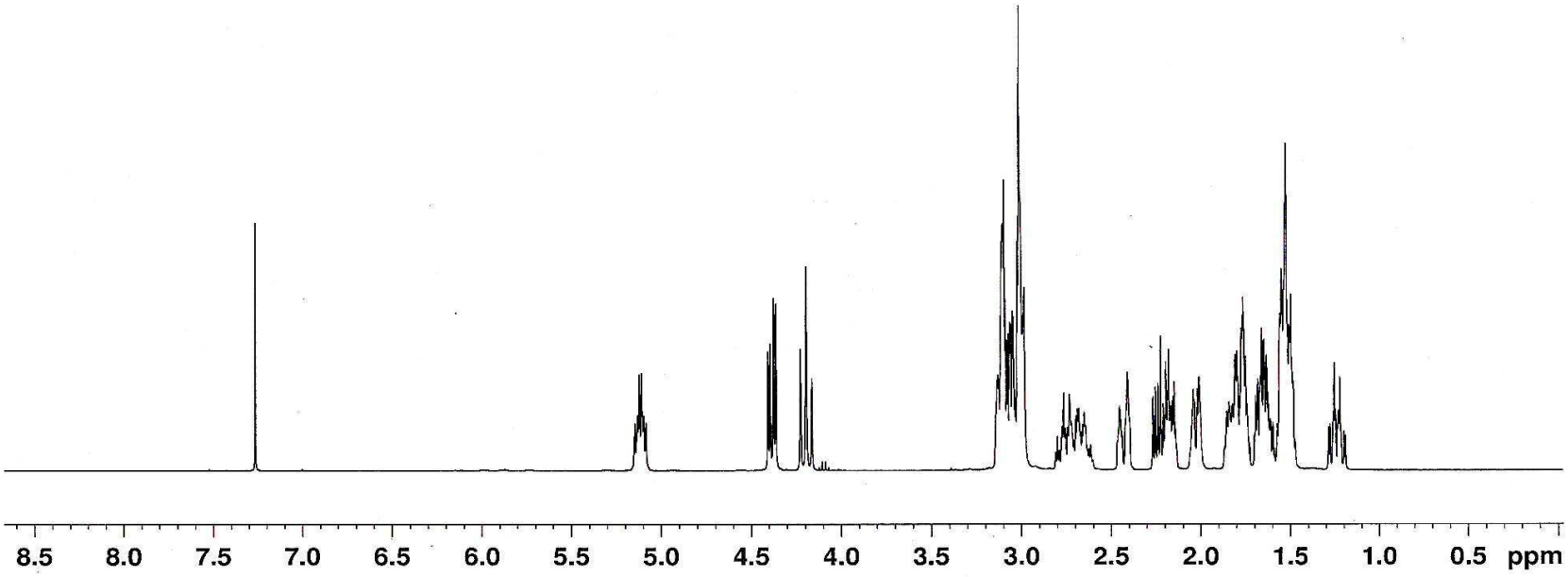

Figure A-34. ^{1}H-NMR spectrum of oxymatrine (**85**) in $CDCl_3$.

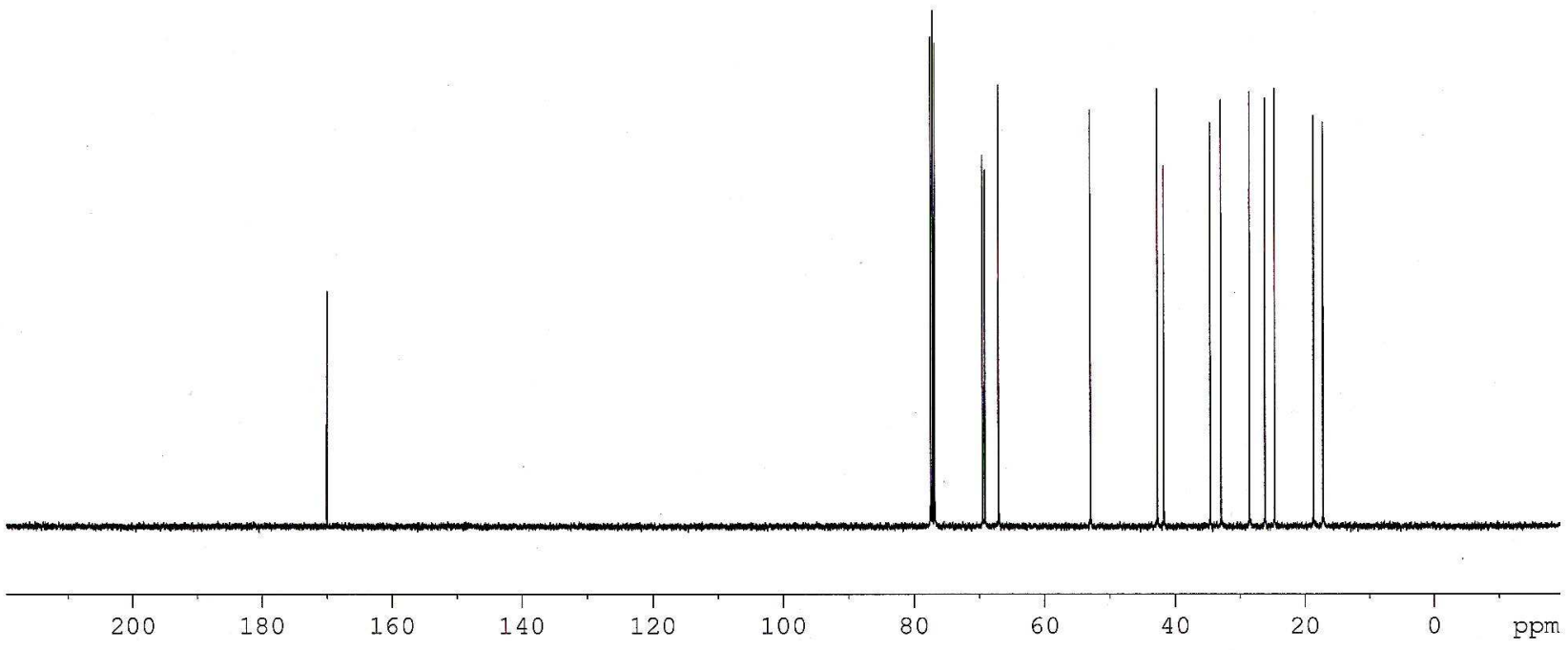

Figure A-35. ^{13}C-NMR spectrum of oxymatrine (**85**) in $CDCl_3$.

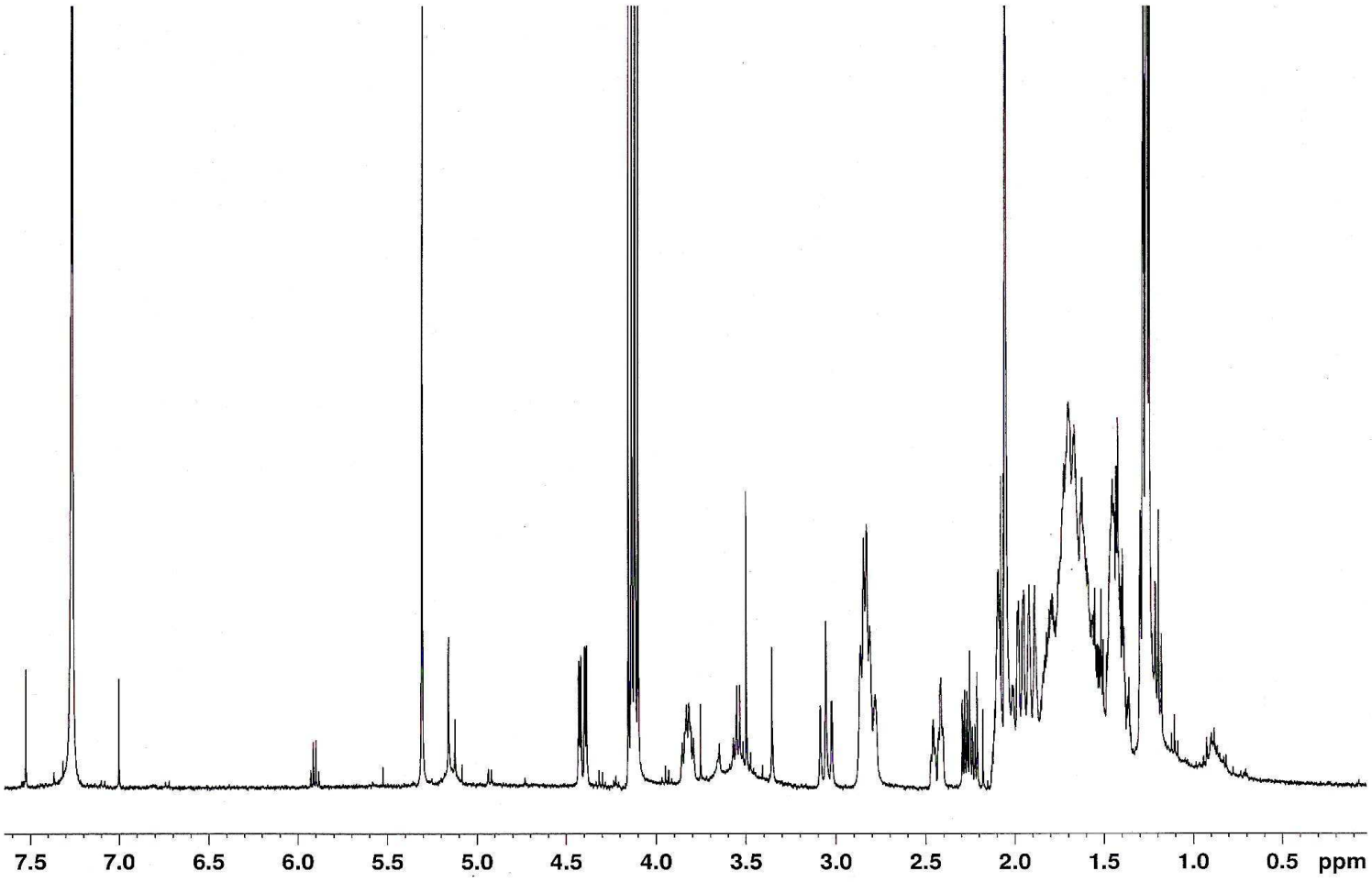

Figure A-36. ^{1}H-NMR spectrum of the oxymatrine biotransformation product in $CDCl_3$.

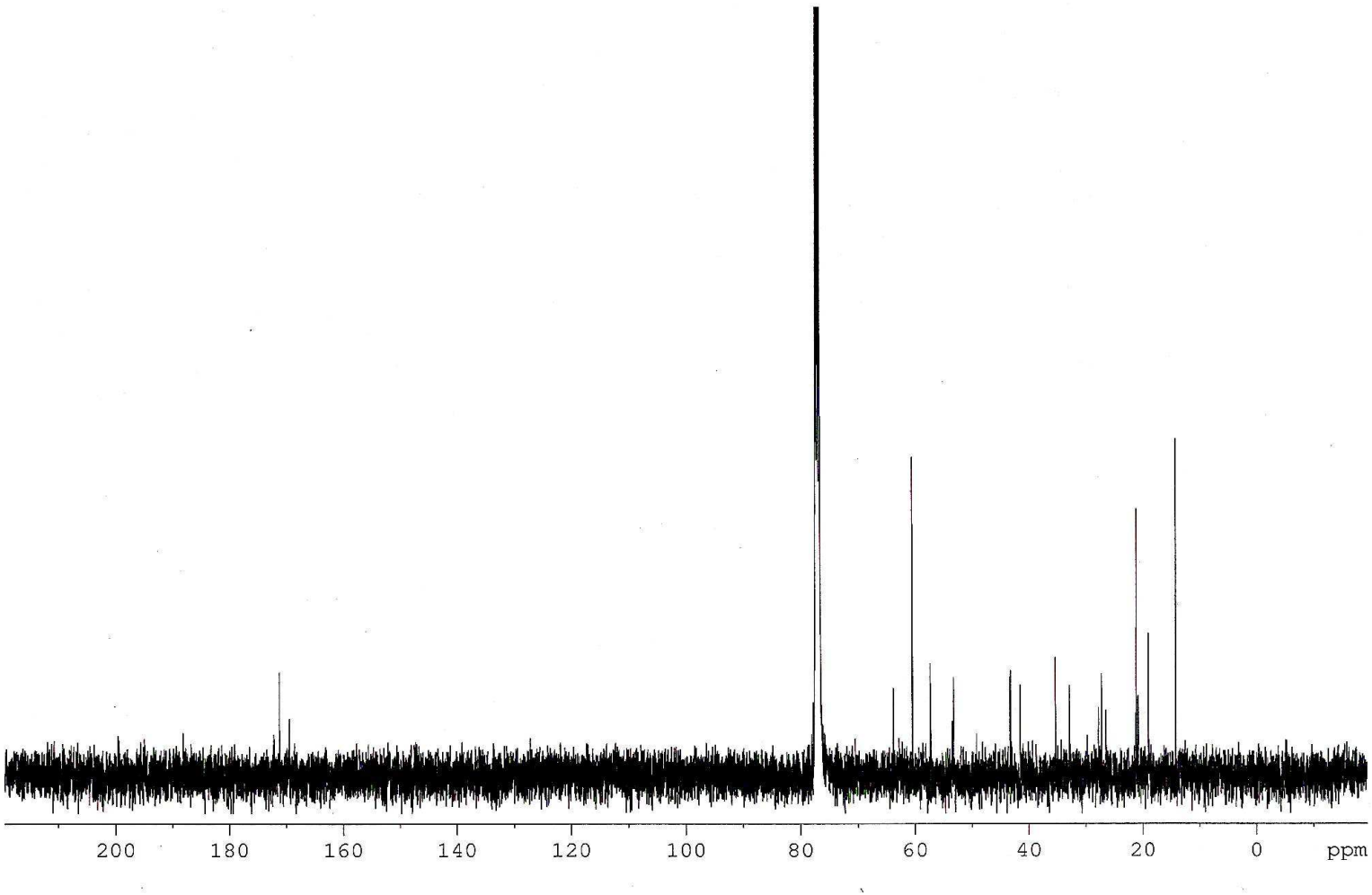

Figure A-37. ^{13}C-NMR spectrum of the oxymatrine biotransformation product in $CDCl_3$.

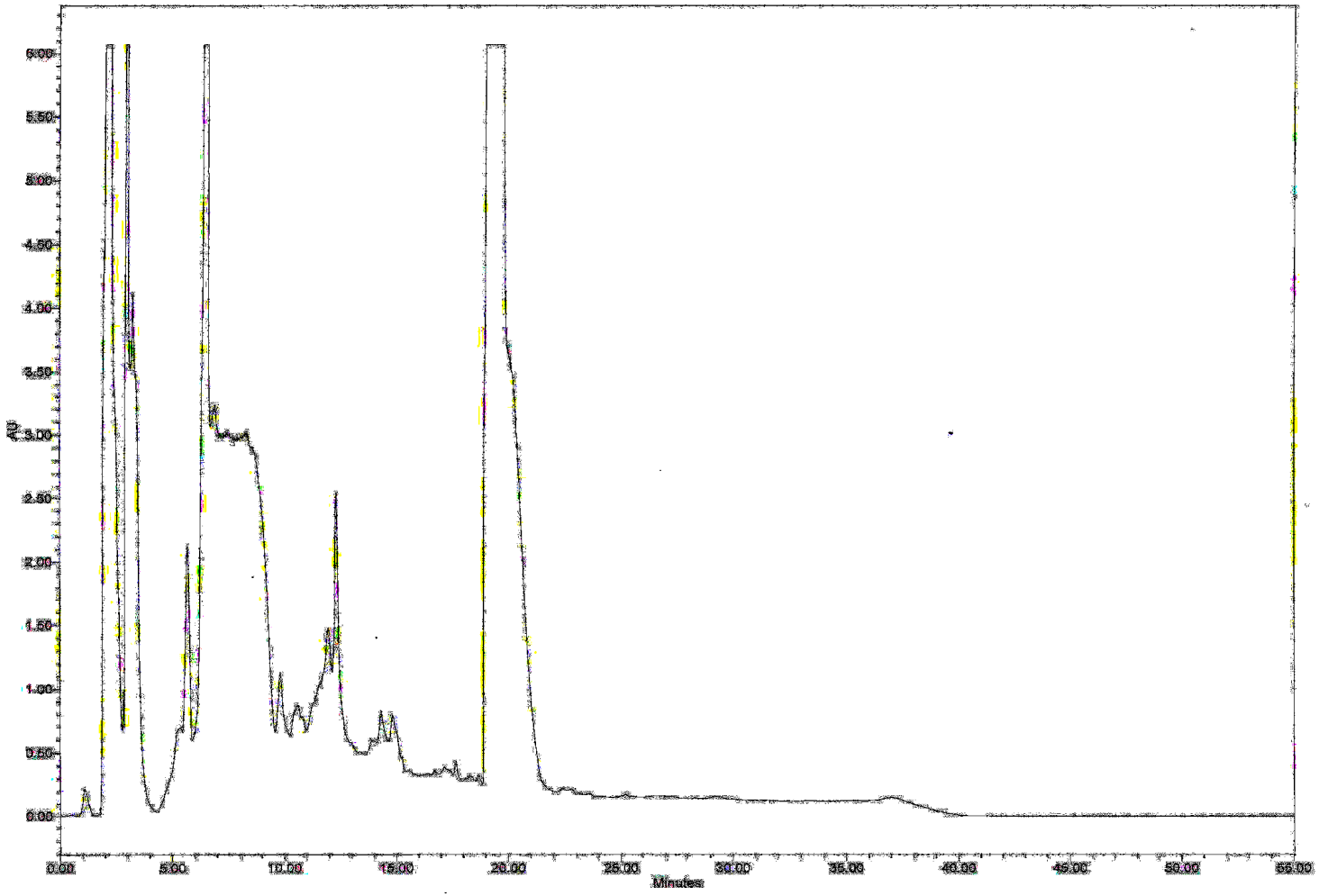

Figure A-38. HPLC chromatogram of the harmine (**87**) biotransformation crude ethyl acetate extract.

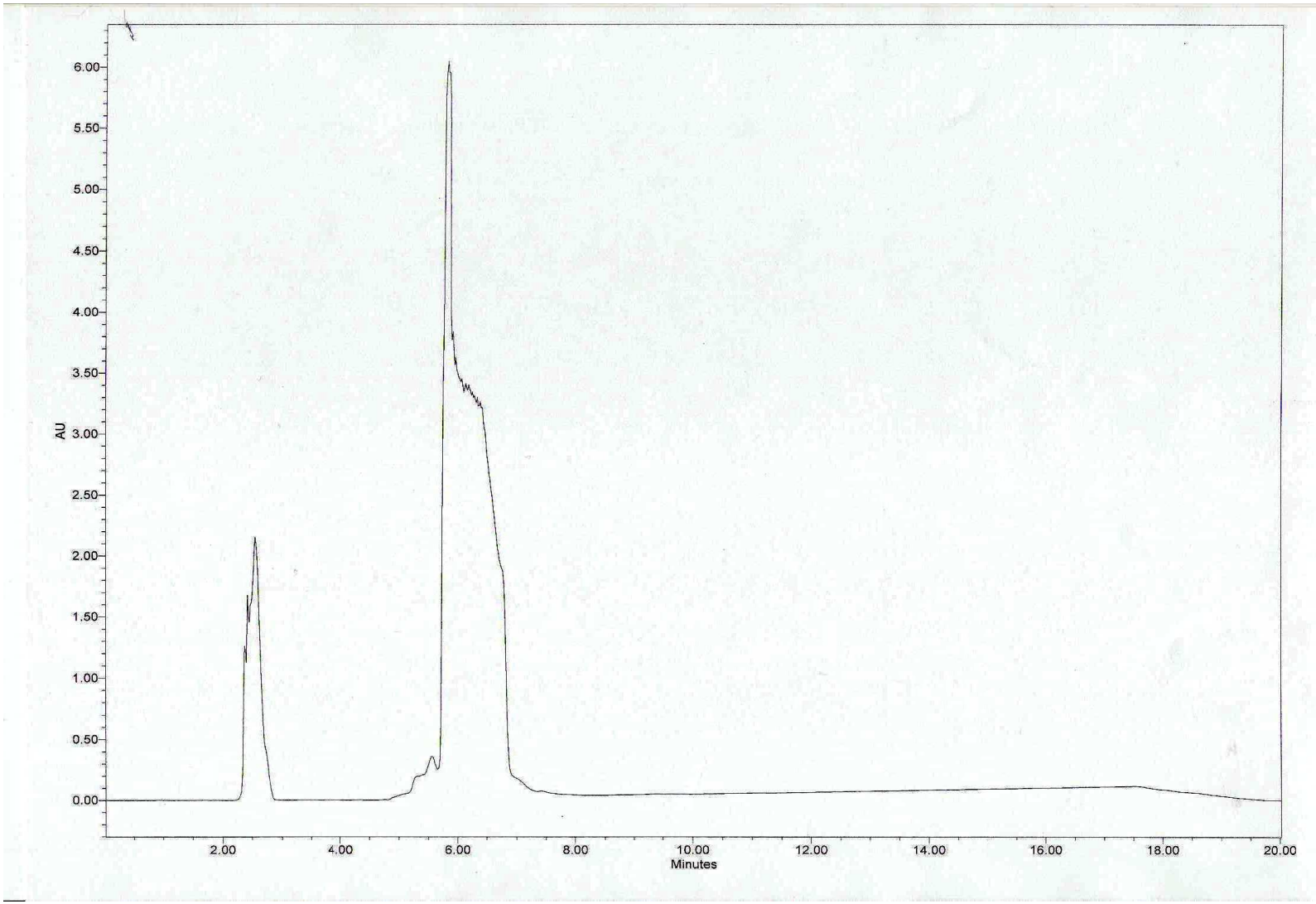

Figure A-39. Sample HPLC chromatogram from the isolation of **94**.

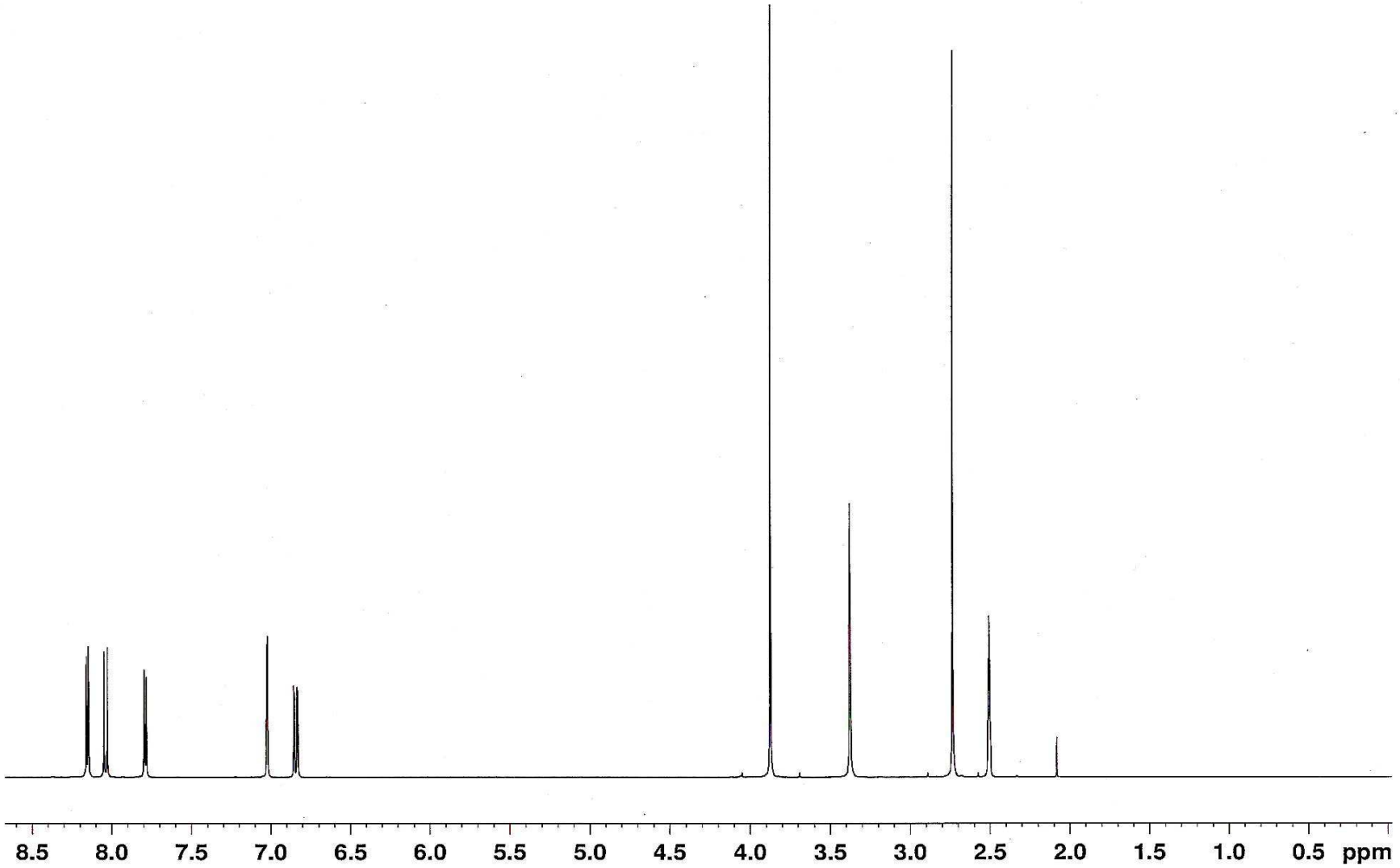

Figure A-40. ^{1}H-NMR spectrum of harmine (**87**) in DMSO-d_6.

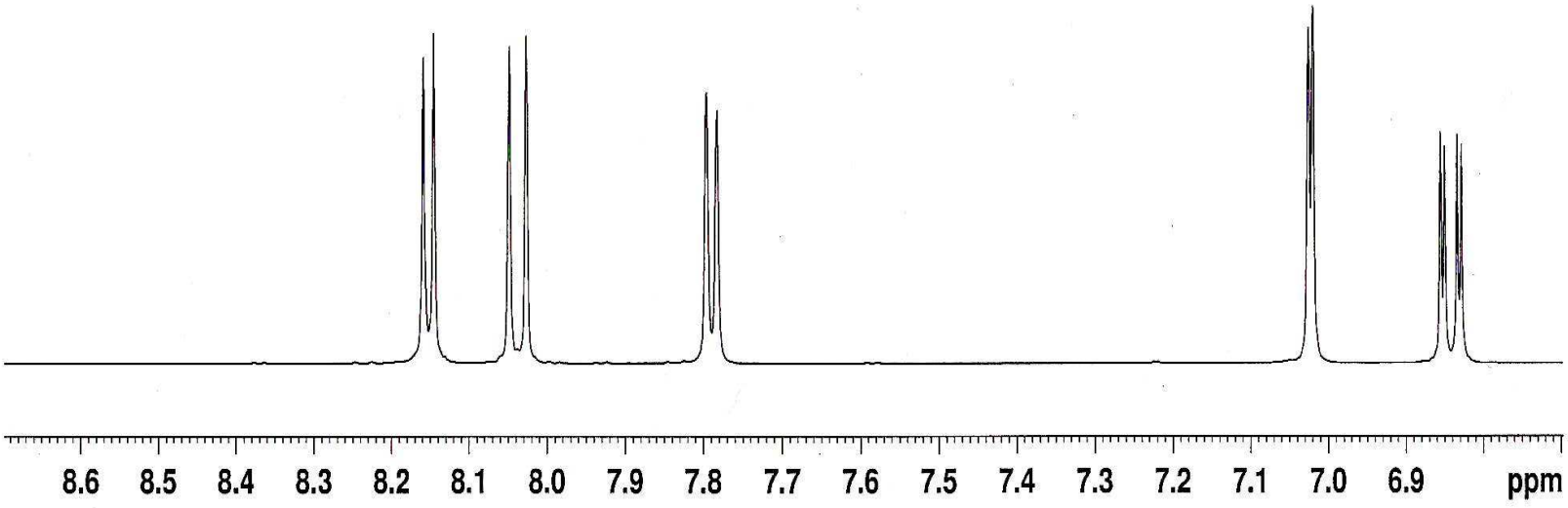

Figure A-41. Expanded ^{1}H-NMR spectrum of harmine (**87**) in DMSO-d_6 showing the aromatic region.

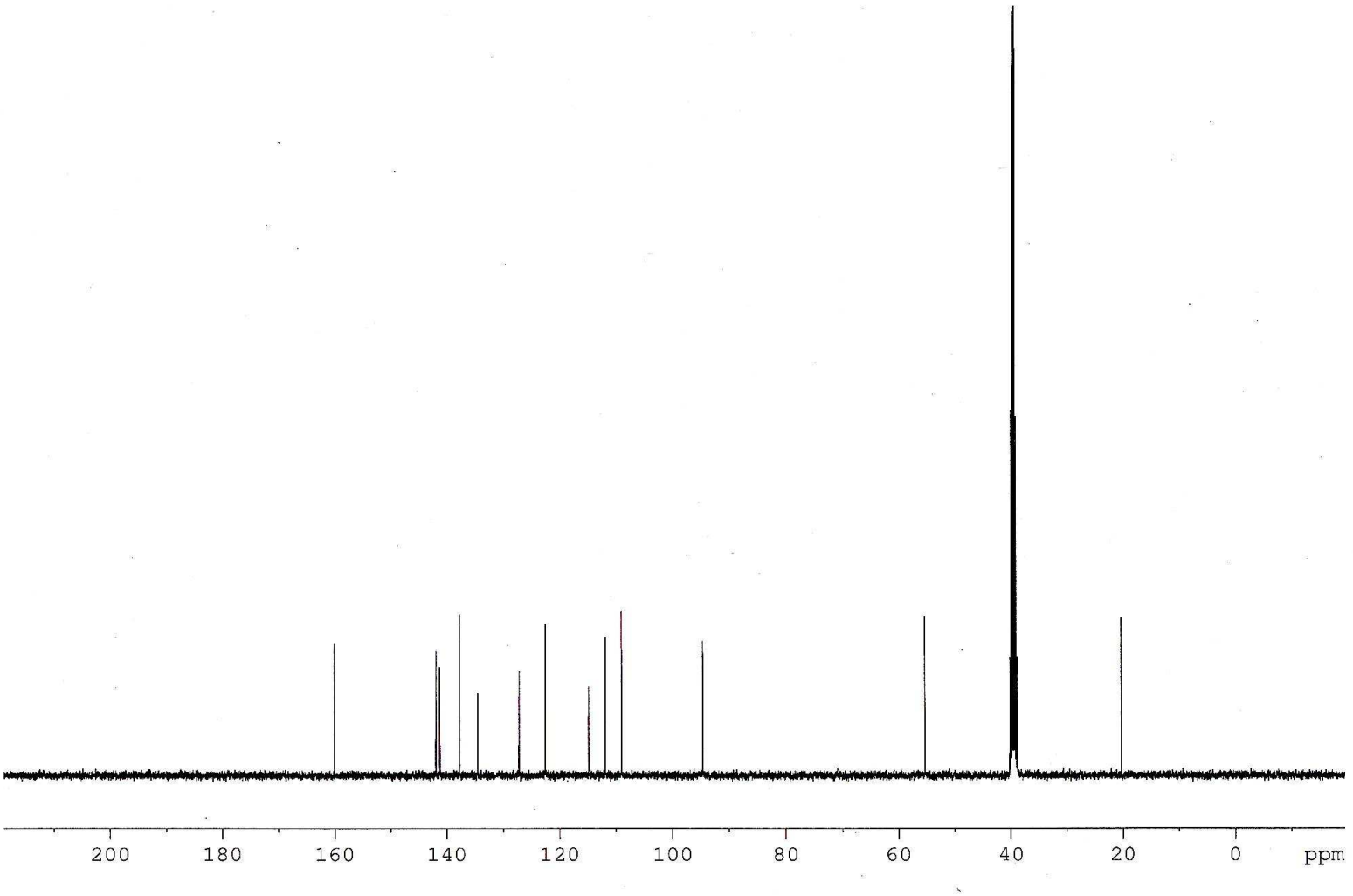

Figure A-42. ^{13}C-NMR spectrum of harmine (**87**) in DMSO-d_6.

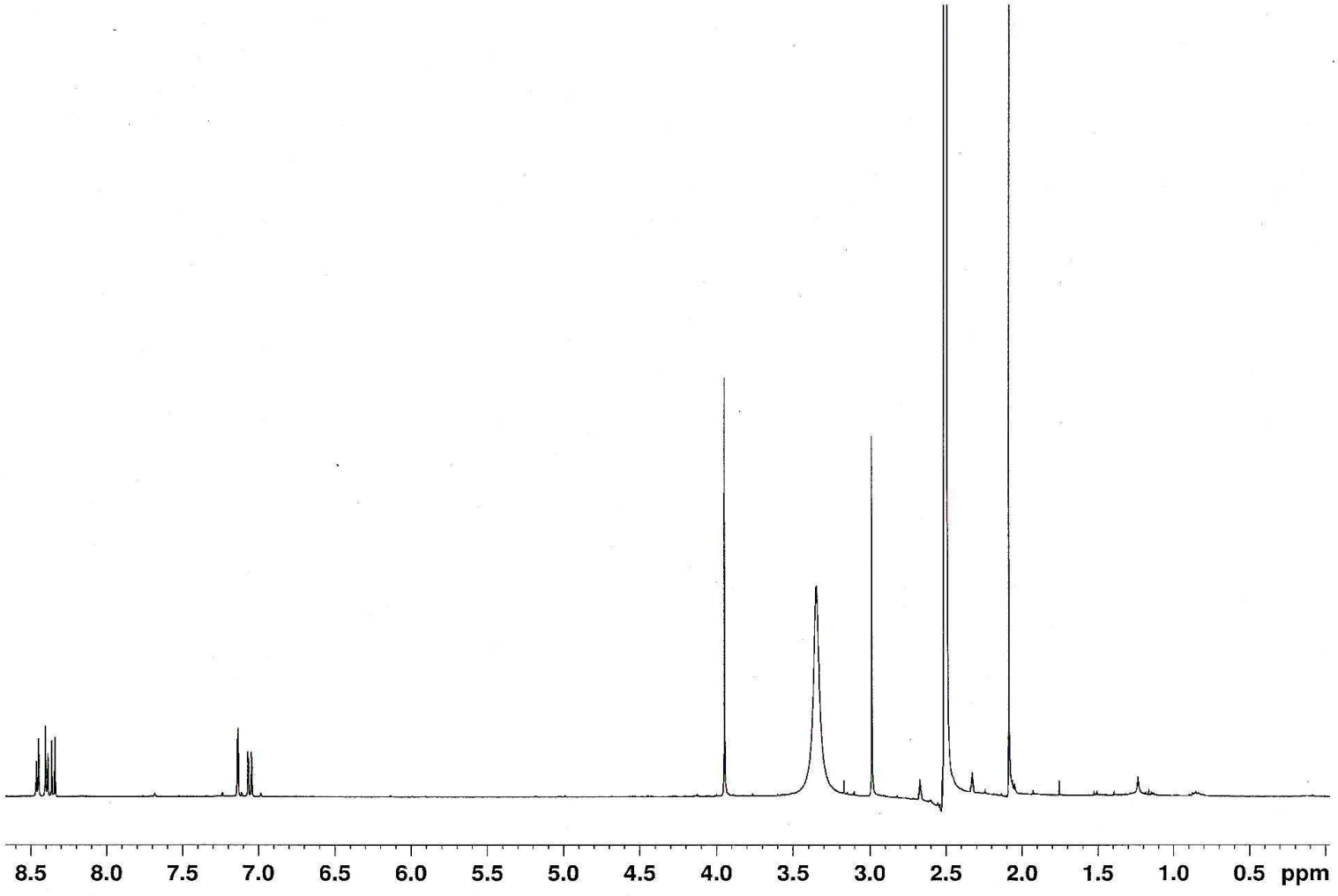

Figure A-43. ^{1}H-NMR spectrum of harmine-*N*-oxide (**94**) in DMSO-d_6.

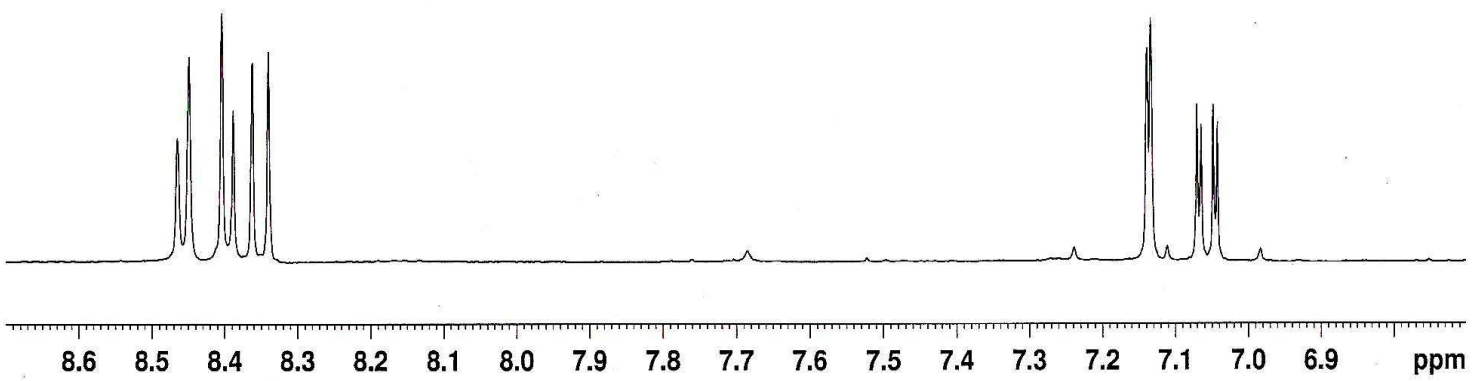

Figure A-44. Expanded ^{1}H-NMR spectrum of harmine-*N*-oxide (**94**) in DMSO-d_6 showing the aromatic region.

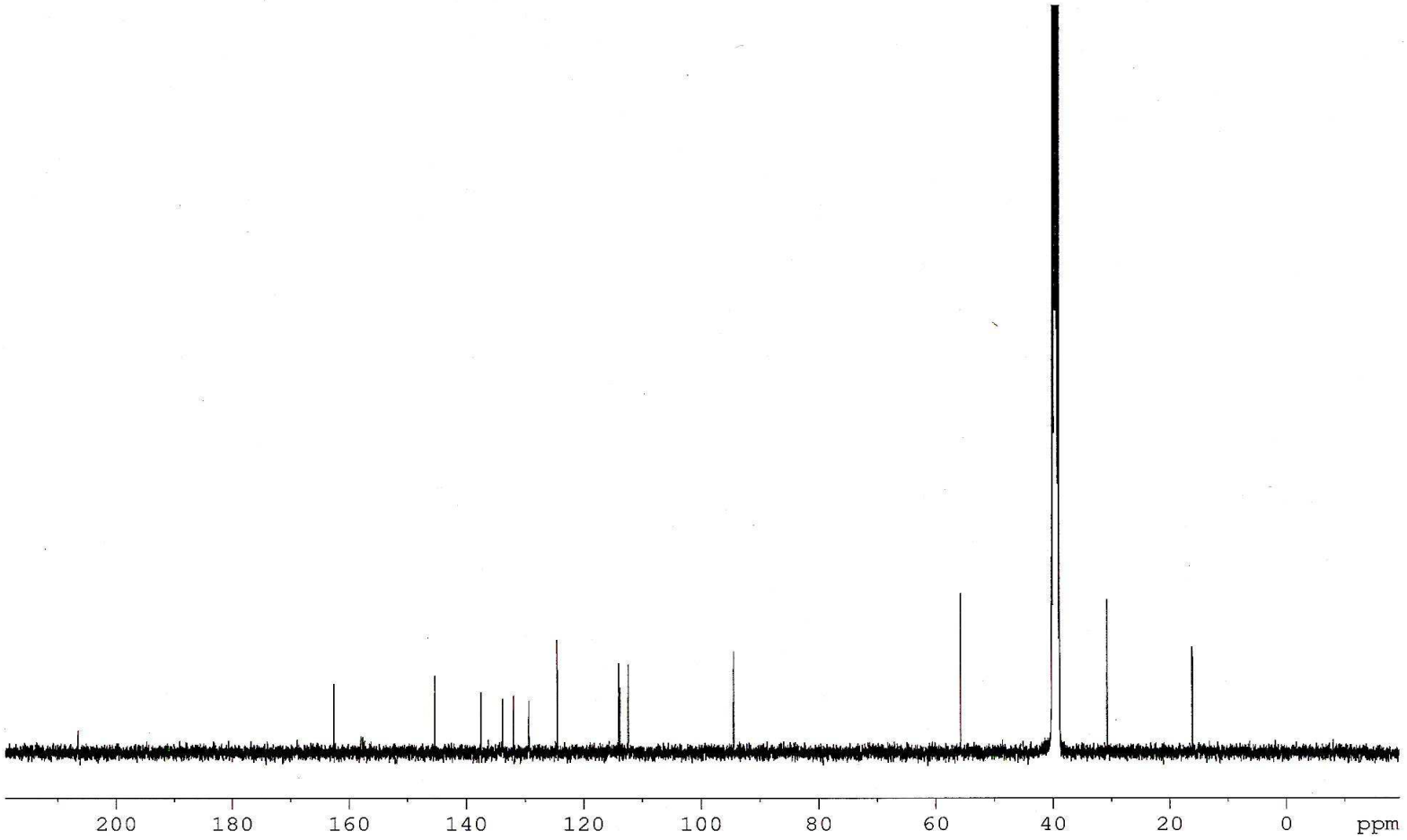

Figure A-45. ^{13}C-NMR spectrum of harmine-*N*-oxide (**94**) in DMSO-d_6.

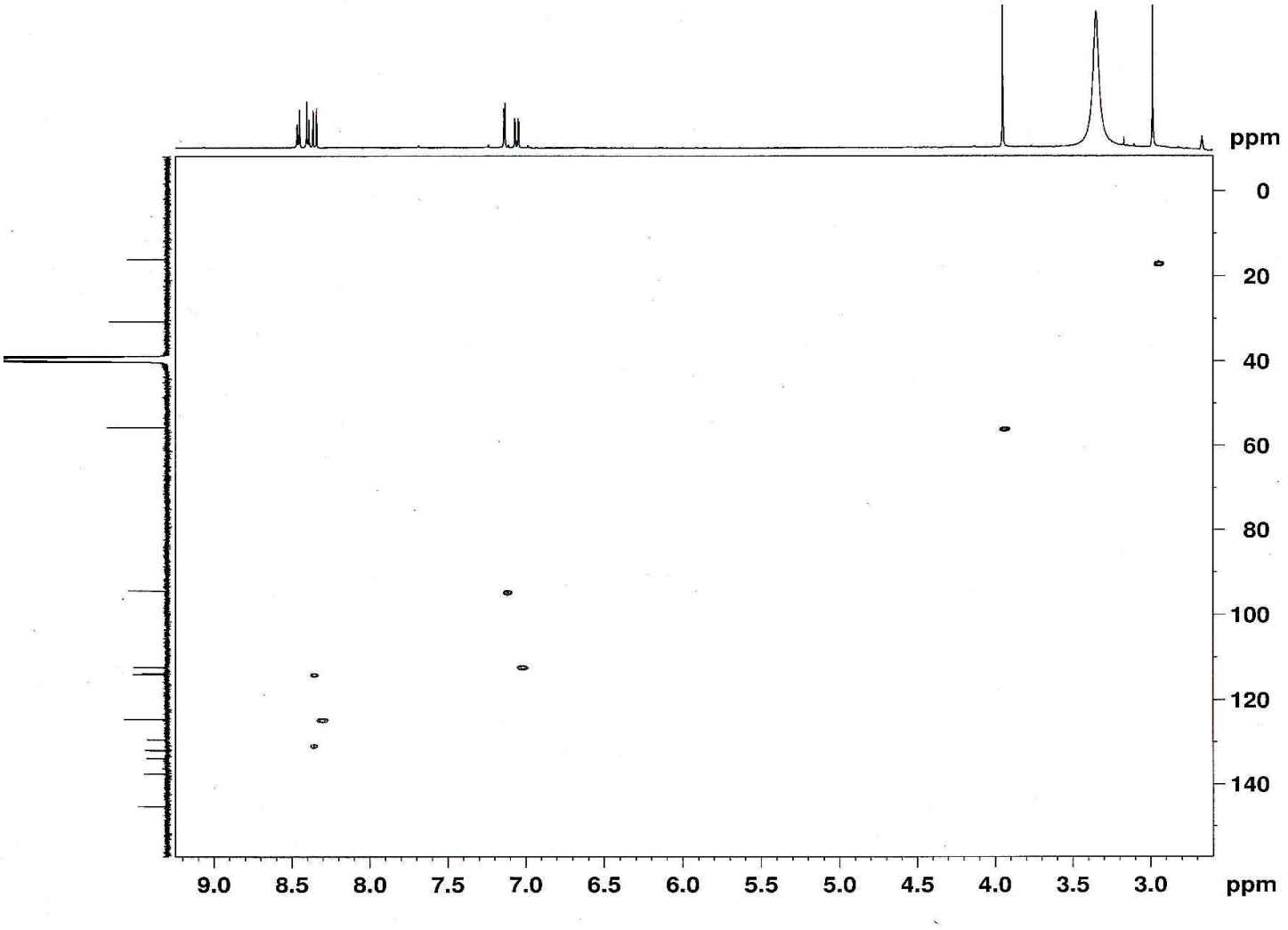

Figure A-46. HSQC spectrum of harmine-*N*-oxide (**94**) in DMSO-d_6.

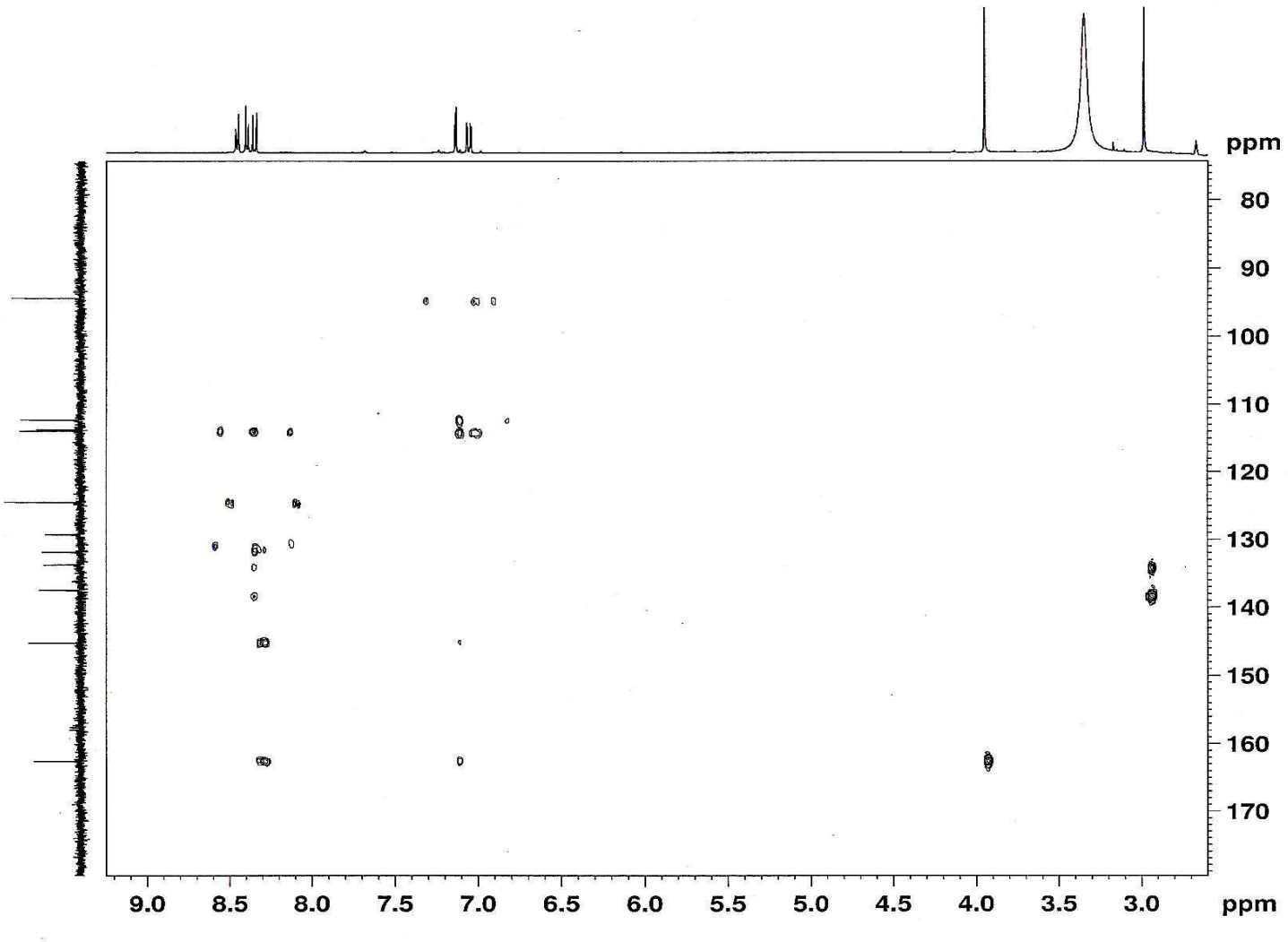

Figure A-47. HMBC spectrum of harmine-*N*-oxide (**94**) in DMSO-d_6.